REGULATION OF MICROTUBULE DYNAMICS BY *SACCHAROMYCES CEREVISIAE* PLUS-END TRACKING PROTEINS

A Dissertation

Presented to the Faculty of the Graduate School

of Cornell University

In Partial Fulfillment of the Requirements for the Degree of

Doctor of Philosophy

by

Kristina Anne Blake-Hodek

February 2010

REGULATION OF MICROTUBULE DYNAMICS BY *SACCHAROMYCES CEREVISIAE* PLUS-END TRACKING PROTEINS

Kristina Anne Blake-Hodek, Ph. D.

Cornell University 2010

Microtubule dynamics are regulated by a variety of proteins that bind to microtubule ends, and influence their polymerization properties. A number of these plus-end binding proteins have been identified and the interactions between these proteins are important for regulating microtubule dynamics. Stu2, Bik1, and Bim1 are three microtubule plus-end tracking proteins in *Saccharomyces cerevisiae* and each has been shown to influence microtubule assembly *in vivo*. I have found that Stu2, Bik1, and Bim1 interact both with themselves and each other in all pairwise combinations. Mapping of protein-protein interaction domains, competitive interaction assays, and physical characterization of protein complexes indicate that these proteins do not associate in a single complex but rather compete for binding to each other. Overall, these results suggest that the interactions among these proteins are dynamic and that different complexes of these proteins may perform distinct roles in the cell.

In order to further characterize these proteins, I purified Bim1 and Bik1. I show that *in vitro* Bim1 and Bik1 form homodimers that can interact with each other to form a tetramer, indicating the Bim1-Bik1 interaction is direct. Using purified GFP tagged versions of these proteins, I observed Bim1 to localize directly to the microtubule plus-end, however, Bik1 required Bim1 for efficient plus-end localization. I also examined the effects of Bim1 and Bik1 on

MT assembly and dynamics *in vitro*. I found that Bim1 has a stabilizing effect on microtubules resulting in an increase of polymer formation. This effect is primarily due to the suppression of microtubule catastrophes by Bim1, although Bim1 also increases microtubule growth rates and rescue frequencies. The ability of Bim1 to promote MT polymerization is likely due to a direct effect of Bim1 on MT plus-end structure as I found that Bim1 does not bind tubulin subunits. In contrast, Bik1 had a destabilizing effect on microtubules, increasing the frequency of catastrophes. This may be due to the formation of polymerization-incompetent tubulin oligomers as I observed Bik1 to promote oligomerization of tubulin subunits. Combining equal-molar amounts of Bim1 and Bik1 resulted in an effect on microtubule dynamics similar to Bim1 alone. These results indicate that Bim1 is able to suppress the catastrophe promoting activities of Bik1 and could be due to formation of a Bim1-Bik1 complex that disrupts Bik1-tubulin interactions. In agreement with this theory, Bik1 is known to bind both Bim1 and tubulin through the same domain. Overall, these results add to our knowledge of plus-end tracking proteins and the individual method each protein uses to influence MT dynamics.

BIOGRAPHICAL SKETCH

The author was born on September 14, 1976 in St. Paul Minnesota to Linda Blake and James Hodek. She grew up in Minnesota where she enjoyed many camping and canoeing trips. She graduated from Mounds View High School in 1995 where she found that she was very interested in the sciences. She continued her education at St. Olaf College in Northfield, MN graduating in 1999 with majors in Biology and Chemisty and a concentration in Molecular Biology. While at St. Olaf she particularly enjoyed her studies in the areas of ecology as well as developmental biology. She worked with Dr. Henry Kermott researching the "nest relief" song of the House Wren and also with Dr. Laurie Sammartano examining the effects of UV irradiation on *RAD51* deficient tetrahymena. She also had the amazing opportunity to study biology with Dr. Eric Cole in the famous Galapagos Islands.

After college she decided to obtain her PhD, and was accepted into the Field of Genetics and Development at Cornell University where she joined the laboratory of Dr. Tim Huffaker in the Spring of 2001. While pursing her PhD she found she enjoyed teaching, teaching the Genetics 281 laboratory numerous times, and served as the course coordinator in the summer of 2008. During her time in Ithaca, she also had two children with fellow graduate student Hans Salamanca-Granados. They were blessed with a son, Erik James Salamanca and a daughter, Isabella Sofia Salamanca. Upon completion of her PhD in August 2009, the author hopes to start her postdoctoral work in the laboratory of Mike Goldberg at Cornell University.

To my family.

ACKNOWLEDGMENTS

I would like to thank all of the professors that have helped my over my graduate career. First, my advisor, Tim Huffaker, who has been a great mentor over the years. He taught me how to design thoughtful experiments and analyze my data in meaningful ways. Most importantly, he helped me learn how to better present and organize my data for papers and presentations. Additionally, his constant support during my time off for my family was incredibly appreciated, words cannot express how thankful I am for his patience. I would also like to thank to my committee members, Eric Alani and Tony Bretscher for their enthusiasm for science and valuable advice. I am most grateful to Lynne Cassimeris for allowing me to conduct experiments in her laboratory and showing me the tricks of VE-DIC microscopy. I am also grateful to John Lis and Bik1 Tye for serving on my A-exam committee and Mike Goldberg and Mariana Wolfner for allowing me to do rotations in their laboratories. I would especially like to thank Debbie Nero for helping me to develop as a teacher and letting me teach genetics so many times.

I would also like to thank all of the members of the Huffaker laboratory. My labmates over the years: Beth Lalonde, Karena Kosco, Christine Brew, Hongwei Yin, Liru You, Mike Wolyniak, Eric Hwang, Xue Xia, Baoying Huang, Alex Amaro, Yin-Loon Lee, Gilda Shayan, Laurie Cook, Zane Bergman, Srich Murugesan, Lily Cao, and Patrick Wu have been wonderful friends and colleagues making the lab a great place to work in. I am especially thankful to Karena Kosco who introduced me to the lab and started me on my thesis project. I would also like to thank Gilda Shayan for

her tireless efforts in our two-hybrid screen. I am also grateful to the many friends I have met in Ithaca during my graduate career, who have made my time in Ithaca more enjoyable.

Finally, I would like to thank my family for their unceasing love and support throughout the years. This dissertation was only possible with their help and encouragement. I would especially like to thank my Dad for coming out to help Hans take care of Erik and Isa so I could spend these last few weeks concentrating on writing, I am eternally grateful. He also deserves many thanks for proofreading my thesis. I hope that someday I will be able to help my children the way he has helped me. I am most indebted to Hans, for all his help and support over the years, I couldn't have done it without you! To Erik and Isa, I would like to say thanks for your endless smiles and laughter and for bringing such joy to my life!

TABLE OF CONTENTS

LIST OF TABLES

LIST OF FIGURES

LIST OF ABBREVIATIONS

+TIP	Plus-end tracking protein
AA	Amino Acid
aMT	astral microtubule
ATP	adenosine triphosphate
CFP	cyan fluorescent protein
cMT	cytoplasmic microtubule
GDP	guanosine diphosphate
GFP	green fluorescent protein
GTP	guanosine triphosphate
HRP	horseradish peroxidase
FRAP	flouresence redistrabution after photobleaching
kMT	kinetochore microtubule
MAP	microtubule associated protein
MT(s)	microtubule(s)
MTOC	microtubule organizing center
nMT	nuclear microtubule
pMT	polar microtubule
RFP	red fluorescent protein
SD	yeast minimal media
SPB	spindle pole body
VE-DIC	video enhanced differential interference contrast
YPD	yeast rich media with dextrose

CHAPTER 1

GENERAL INTRODUCTION

Microtubule (MT) arrays are an integral component of the cellular cytoskeleton and essential for a variety of cellular processes such as chromosome segregation, membrane trafficking, and maintenance of cell shape. MTs are organized into polarized arrays in most cells, with MT minus-ends anchored at the microtubule organizing center (MTOC) and MT plus-ends radiating outwards into the cell where they alternate stochastically between states of polymerization and depolymerization, a process termed dynamic instability (Mitchison and Kirschner, 1984). This process is central to the biological function of MTs, allowing them to probe the cell for specific targets such as kinetochores and cortical sites, and for the rapid reorganization of MT arrays in response to cellular signaling events (Desai and Mitchison, 1997). The dynamics and interactions of MT plus-ends must be precisely regulated to achieve the correct configuration of MT arrays throughout the cell cycle. This is accomplished, in large part, by a group of MT binding proteins termed plus-end tracking proteins (+TIPs) for their ability to accumulate at and track MT plus-ends (Schuyler and Pellman, 2001; Akhmanova and Yap, 2008). Localization to the MT plus-end perfectly positions +TIPs to control MT dynamics and interactions. Present throughout eukaryotes, a variety of conserved motor and nonmotor +TIP families have been identified and many +TIPs are known to interact with one another (Akhmanova and Hoogenraad, 2005; Honnappa *et al*., 2006). These interactions are thought to be transient and the complex interplay of +TIPs throughout the cell cycle is believed to be

important in the regulation of microtubule dynamics and organization (Wolyniak *et al*., 2006; Niethammer *et al*., 2007). Although much work has been done on characterizing +TIPs, many questions remain about how +TIPS individually and in combination work to regulate MT dynamics.

The budding yeast, *Saccharomyces cerevisiae*, has a number of homologues to higher eukaryotic +TIPs, and with its relatively simple cytoskeleton, sequenced genome, and genetic malleability, it provides an excellent model system to study the effect of associated proteins on microtubule dynamics. This study focuses on characterizing three yeast microtubule-binding proteins, Stu2, Bik1, and Bim1, and their roles in regulating MT dynamics.

Microtubule Structure

The basic building block of a microtubule is a heterodimer of alpha and beta tubulin. α-tubulin and β-tubulin share ~50% identity at the amino acid level, are both ~55 kDa, and contain GTP binding sites (Burns, 1991). α-β heterodimers are arranged in a head-to-tail manner to form linear protofilaments that bundle to form the hollow cylindrical structure of a microtubule (Figure 1.1A). Single MTs *in vivo* are typically comprised of 13 protofilaments forming a tube approximately 25 nm in diameter (Tilney *et al*., 1973). MTs *in vitro* can have varying numbers of protofilaments depending on the assembly conditions (Chretien *et al*., 1996), but primarily have 13 protofilaments when nucleated from axonemes or centrosomes (Evans *et al*., 1985). The lateral associations of the 13 protofilaments are thought to form a B-type helix (Desai and Mitchison, 1997). In the B-type helix, the majority of lateral associations are between α-tubulin-α-tubulin subunits and β-tubulin-

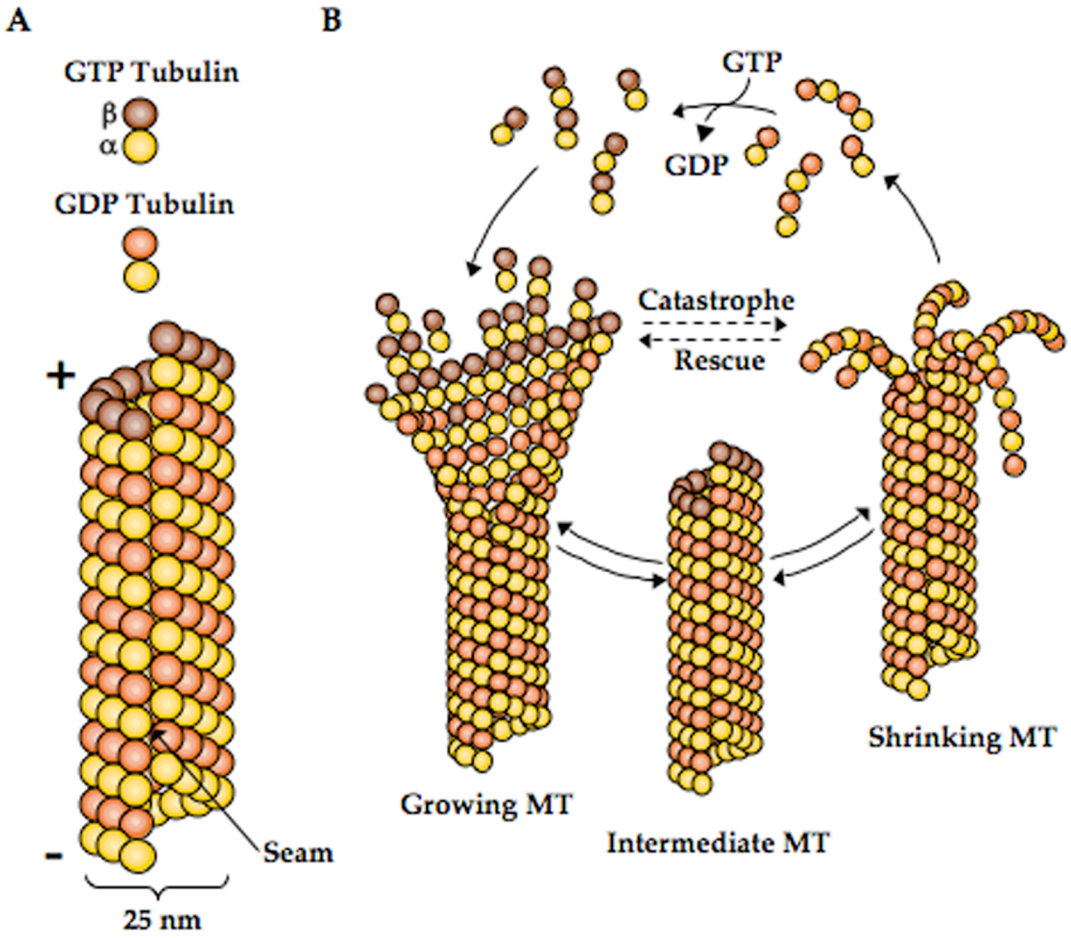

Figure 1.1 MT structure and dynamics. A. MTs are comprised of heterodimers of α and β-tubulin. B. MT dynamics are coupled to GTP hydrolysis. Figure modified from Akhmanova and Steinmetz (2008).

β-tubulin subunits, except for what is referred to as the "seam" of the MT, where alpha subunits contact beta subunits (Figure 1.1A) (Kikkawa *et al*., 1994). The MT seam is thought to be a "weak link" in the MT structure and possibly to contribute to MT disassembly. These lateral associations also lead to MT polarity, where the α subunits are at one end of the polymer and β subunits the other end. The β subunit end of the microtubule is referred to as the "plus end", and is the site of fast polymerization or growth. The α subunits comprise the "minus end" of a microtubule, which has a much slower polymerization rate (Walker *et al*., 1988). Polarity is key to the organization of most MT arrays and for the function of MT plus and minus end directed motors, which recognize MT polarity and move their cargo accordingly.

MT Dynamic Instability

As early as 1882, although not properly called MTs, the dynamic properties of MTs were known to biologists, as seen in Walther Flemming's illustrations of the mitotic spindle during mitosis (Kline-Smith and Walczak, 2004). In the 1950's polarized light microscopy allowed for the visualization of mitotic spindle dynamics in living cells (Inoue and Salmon, 1995; Rieder and Khodjakov, 2003). In 1972, purified tubulin was shown to reversibly self-polymerize *in vitro*, demonstrating the dynamic nature of MTs (Weisenberg, 1972). Various models for MT dynamics were hypothesized and in 1984, Mitchison and Kirschner put forward a model called MT dynamic instability. It stated that, although there is a bulk MT steady state, individual MTs can switch alternately from a state of polymerization to a state of depolymerization (Figure 1.1B) (Mitchison and Kirschner, 1984). This model

lead to a MT search and capture model to describe how dynamic MTs probe the cytoplasm in search of a specific target sites in the cell.

The dynamic instability of individual MTs was first visualized in the late 80s both *in vitro* (Walker *et al*., 1988; Horio and Hotani, 1986) and *in vivo* (Cassimeris *et al*., 1988; Sammak and Borisy, 1988; Schulze and Kirschner, 1988). Dynamic MTs were seen in states of growth or shrinkage with frequent transitions between each, but exactly how these transitions occur is still poorly understood. MTs can also exist in a paused state neither growing nor shrinking. The transition from growing or pausing to shrinkage is called a catastrophe, while the transition from shrinkage or pausing to growth is termed a rescue (Figure 1.1B) (Walker *et al*., 1988). The dynamic properties of MTs can be measured by plotting the growth of a microtubule over time, in a "life-history" plot (Figure 1.2) (Walker *et al*., 1988). From these plots four parameters of MT dynamics can be calculated: the rates of MT growth and shrinkage, as well as the frequencies of catastrophes and rescues. Studies of MTs *in vitro* revealed that the MT growth rate is dependent on tubulin concentration; the higher the tubulin concentration the faster the MT growth rate (Walker *et al*., 1988). Shrinkage rates, on the other hand, were found to be independent of tubulin concentration and it was shown that MTs depolymerize quite rapidly. Catastrophe frequencies were also found to be dependent on growth rates, and thus the free tubulin concentration (Drechsel *et al*., 1992). As the MT growth rate increases, fewer catastrophes are seen. Rescues are seen more frequently at higher tubulin concentrations, but there appears to be no correlation of rescues with shrinkage rates (Walker *et al*., 1988; Manna *et al*., 2008).

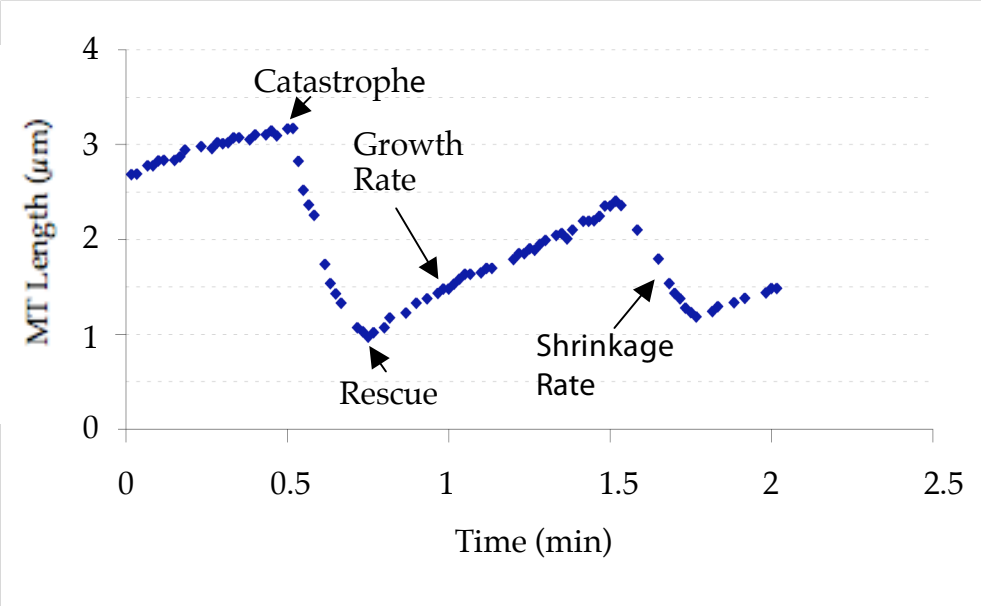

Figure 1.2 MT Life History Plot. Microtubule dynamics are defined by four parameters: the growth rate, shrinkage rate, catastrophe frequency (transitions from growth to shrinkage) and rescue frequency (transitions from shrinkage to growth). These parameters can be measured by plotting changes in MT length over time.

GTP hydrolysis is important for MT dynamics

Tubulin subunits are added to the MT growing end as GTP-tubulin; and MT dynamics are dependent on GTP hydrolysis (Hyman *et al*., 1992) (Figure 1.1B). Shortly after incorporation into the MT, the GTP within the β-tubulin subunit is hydrolyzed to GDP. This process results in the formation of a GTP-tubulin cap at the growing end of the MT, while the MT lattice is comprised of GDP-tubulin. GTP tubulin protofilaments are proposed to be straight (an alternative model is described below) and maintain strong contacts between neighboring protofilaments, while GDP-tubulin subunits have a curved conformation but are held in place in the straight MT by the GTP cap (Howard and Hyman, 2003). Therefore, when the GTP cap is lost, the MT becomes unstable and depolymerizes. Studies that physically severed MTs found cut MTs were unstable and rapidly depolymerized, consistent with the idea of a MT end stabilizing structure (Tran *et al*., 1997; Walker *et al*., 1989). As the MT depolymerizes, the individual GDP-tubulin protofilaments peel outwards in curved structures (Figure 1.1B) (Mandelkow *et al*., 1991). Then these curved protofilaments fall apart and the free GDP-tubulin resulting from this depolymerization can be exchanged for GTP-tubulin, which can again add onto the end of a growing MT (Desai and Mitchison, 1997). Recent work has indicated that the size of the GTP cap is dynamic and fluctuates anywhere from a few GTP tubulin subunits to several layers of GTP-tubulin or GDP-Pi tubulin (Schek *et al*., 2007; Howard and Hyman, 2009). Although the GTP model has been accepted for several decades, it was not until recently that evidence for the cap was shown to exist *in vivo*. A study by Dimitrov and colleagues visualized the GTP cap in cell extracts with an antibody that specifically recognized the conformation of GTP tubulin

(Dimitrov *et al*., 2008). Surprisingly, they also found that, in addition to tip recognition, the antibody also localized to spots randomly along the MT, which they refer to as "GTP remnants". Amazingly, these remnants could lead to rescues when a shrinking MT encountered a GTP remnant within the MT. The remnants appear to be an intrinsic part of MT polymerization, as they were also found in MTs polymerized from purified tubulin.

Incorporation of tubulin into the growing MT: two alternate models

Although the MT is a helical structure, MT growth does not occur in a helical manner. MT polymerization is thought to occur by the formation of a "sheet" of protofilament and heterodimer lateral interactions as shown through Cryo-EM of microtubules (Figure 1.1B) (Chretien *et al*., 1995). Closure of this sheet then forms the cylindrical structure of the MT, and Chrétien and colleagues hypothesized that when sheet closure catches up to the polymerizing end, a catastrophe could result. The number of tubulin subunits that can add onto the growing MT end at one time has recently been studied. Studies using optical tweezers have suggested that tubulin adds to the growing MT end in short oligomers of 3 or more tubulin subunits (Kerssemakers *et al*., 2006), while another study suggests assembly takes place via single tubulin subunits (Schek *et al*., 2007). Using this sensitive technique, Schek and colleagues found that MTs can undergo a short depolymerization event equivalent to a few layers of tubulin dimers, but that this is quickly reversed back to polymerization. As mentioned above, this suggests that the GTP-cap may consist of several layers of tubulin subunits.

The process of how tubulin dimers become stably incorporated into the MT is not fully understood. The conventional model (mentioned above) is the

allosteric model in which GTP-tubulin has a straight conformation while GDP-tubulin has a curved or kinked conformation (Wang and Nogales, 2005). In this model, GTP binding changes the conformation from curved GDP-tubulin to straight GTP-tubulin and this straightened heterodimer incorporates into the MT lattice more easily. In this case, it is the binding of GTP that causes the conformational change. The recent production of a GTP-tubulin conformation specific antibody mentioned above gives additional support to this model (Dimitrov *et al*., 2008). An alternative model is the lattice model in which GTP-tubulin and GDP-tubulin are both curved and GTP-tubulin is only straightened after incorporation into the MT (Buey *et al*., 2006). The GTP-tubulin is important as the GTP bound form allows for strong lateral contacts between the protofilaments of the growing MT sheet. Thus, the conformational straightening occurs after the heterodimer is incorporated into the lattice. Recent work showing that both the GTP and GDP bound conformations of gamma tubulin are curved gives strength to the lattice model (Rice *et al*., 2008). Howard and Hyman incorporate both models stating that the binding of GTP to tubulin causes a conformation change to a less kinked (but not fully straightened) GTP-tubulin dimer, which only becomes fully straightened after incorporation into the lattice (Howard and Hyman, 2009).

MT function and organization of MT arrays

MTs provide shape and polarity to the cell and are involved variety of cellular processes such as cell migration, membrane trafficking, and chromosome segregation. One of the central features of MTs is their dynamic ability to reorragnize themselves into different types of arrays (Figure 1.3) in order to carry out their roles in these processes. In most non-differentiated

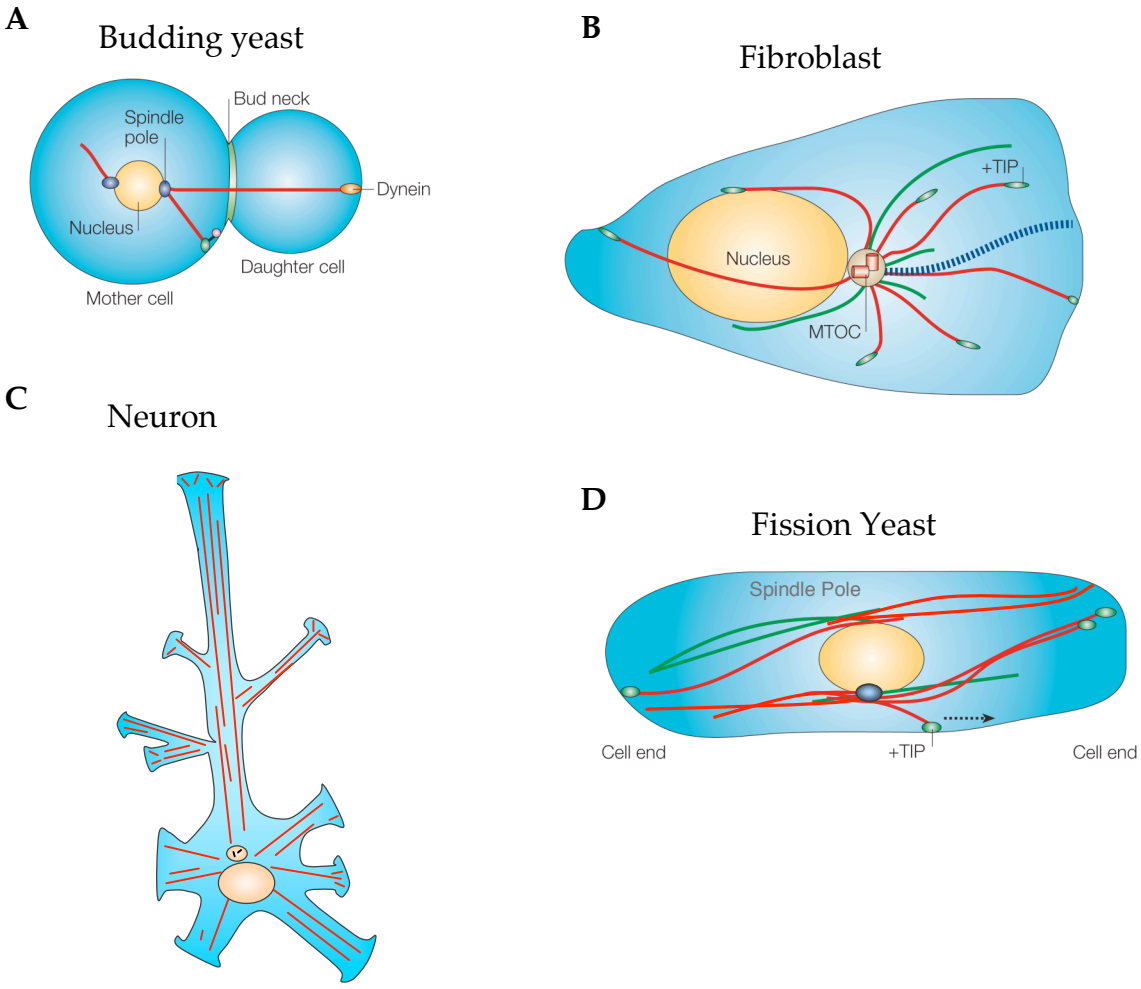

Figure 1.3 Organization of MT arrays in different cell types. A. astral MTs (aMTs) in budding yeast are nucleated from the spindle pole body and are important for spindle migration and orientation. B. MT array in fibroblast cell. MTs usually grow continually until they reach the cell edge where they grow and shrink dynamically. Growing MTs are shown in red, shrinking MTs are shown in green. A stable MT is shown as a dashed blue line C. MTs in a neuronal cell with branched axons. This requires the severing of MTs and their subsequent transport by motor proteins. D. aMTs in fission yeast are organized in bundles and are important for cell shape and polarity. Figure was adapted from Galjart 2005 and Baas *et al.*, 2005.

cells, MTs are organized into radial polarized arrays with MT minus-ends anchored at the microtubule-organizing center (MTOC) and MT plus-ends radiating outwards into the cell (Figure 1.3A and B). MTOCs are known as centrosomes in animal cells and are comprised of a pair of centrioles surrounded by a pericentriolar matrix. A trilaminar plaque embedded in the nuclear envelope called the spindle pole body (SPB) functions as the MTOC in yeast.

MTs are involved in fibroblast polarization and migration through formation of leading edge (Figure 1.3B). During migration, MTs plus-end arrays become highly concentrated at the leading edge and activate Rac, which in turn stimulates actin microfilament and lamellipodial growth (Hall, 2005). In many types of differentiated cells and fission yeast, MTs are arranged in non-centrosomal arrays (Figure 1.3C and D) (Bartolini and Gundersen, 2006; Luders and Stearns, 2007). In neurons, MT arrays are important for steering growth cones and for regulating axon elongation and axon branching (Lee *et al.*, 2004; Zhou *et al.*, 2004; Baas *et al.*, 2005). In fission yeast, MTs are organized along the length of the cell providing the cell with a liner shape (Figure 1.3D), and loss of MTs causes fission yeast to form bent or branched cells (Sawin and Snaith, 2004).

Additionally, MTs used as tracks by MT motors (discussed below) for the trafficking of molecules and vesicles throughout the cell interior and from the cell interior to the cell cortex. For example, MT motors can transport cargo to specific cell adhesion sites (Akhmanova *et al.*, 2009) and between the ER and the Golgi (Vaughan, 2005). The transport of selected cargos by MT motors to specific sites also induces cell polarity, as illustrated in fission yeast by the transport of specialized protein complexes to the cell tip (Bretscher, 2005).

Although MTs play roles in many cellular processes, they are probably best known for their role in chromosome segregation during mitosis or meiosis. As cells undergo division, the MT cytoskeleton undergoes a radical rearrangement where the MTOCs undergo duplication and MTs are nucleated from both MTOCs. These MTs are organized into a bipolar array, a structure known as the mitotic spindle (Figure 1.4). Spindles are comprised of different types of MTs; astral MTs (aMTs) which radiate outwards into the cytoplasm, and spindle MTs that are further classified into polar MTs (pMT) which interdigitate across the spindle, and kinetochore MTs (kMTs) which attach to the kinetochores of chromosomes (Figure 1.4). The ability of dynamic MTs to perform their cellular functions and rearrange into these different types of arrays relies on a variety of different MT binding proteins (discussed below).

Microtubule Associated Proteins

The dynamics, movements, and interactions of MTs must be precisely regulated for the cell to carry out the MT functions and arrays described above. This is accomplished through a group of proteins referred to as microtubule-associated proteins (MAPs). Indeed, although purified MTs can undergo dynamic switches from growth to shrinkage i*n vitro*, studies of MTs *in vivo* show much faster polymerization rates and higher frequencies of catastrophes and rescues, indicating MAPs influence MT assembly and disassembly in the cell (Cassimeris, 1993). Since their first discovery, many different classes of both motor and non-motor MAPs have been identified. Acting as MT stabilizers or destabilizers, MAPs can influence MT organization and dynamics in the cell through a variety of ways, including severing MTs, bundling MTs, sliding MTs, altering the growth and shrinkage rates, or the

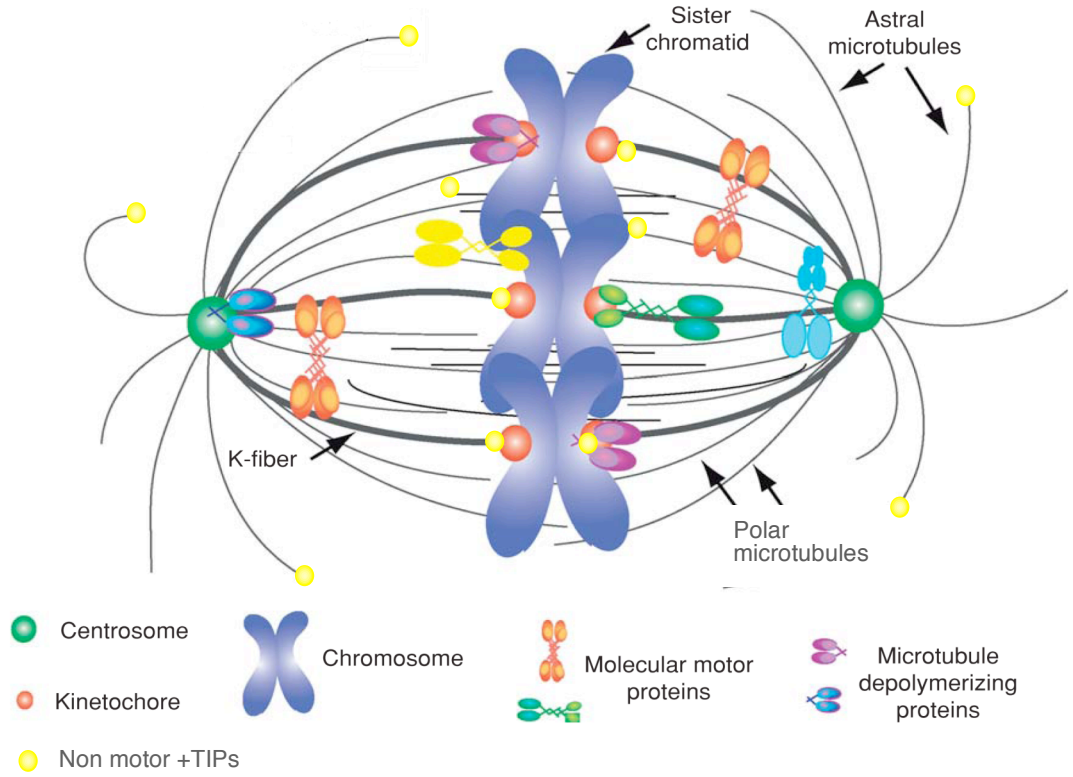

Figure 1.4 The Mitotic Spindle. During mitosis the MT skeleton rearranges into a bipolar array nucleating from the duplicated MTOCs. Molecular motors and non motor +TIPs are important for the formation and maintenance of this array. Both MT stabilizing and destabilizing proteins are necessary for this process. K-fibers, as bundles of kinetochore MTs. Figure is adapted from Walczak and Heald 2008.

frequency of catastrophes and rescue. The precise manner in which MAPs can alter MT turnover are varied; they can function by binding to tubulin subunits, to MT lattice, or specifically to MT ends. Several examples of MAP activity are illustrated in Figure 1.5, and will de discussed in further detail in the individual MAP sections below.

Classical MAPs

MAPs were first identified by their ability to copurify with MTs during purification cycles of MT assembly and disassembly of tubulin from brain tissue (Olmsted, 1986). These MAPs are often referred to as the "classical" MAPs and include MAP1, MAP2 and tau in neurons, as well as the ubiquitously expressed MAP4. These MAPs are highly enriched in neuronal cells and have been shown to stabilize MTs; binding along the MT lattice and strongly suppressing catastrophes and increasing rescues (Figure 1.5). MAP4 is known to be important in the formation of interphase MT arrays, and its ability to promote rescues acts opposingly to the destabilizing catastrophe activity of Op18 (Holmfeldt *et al*., 2009).

MT Severing Proteins

The MT severing proteins, katanin and spastin, are also important for the formation of MT arrays (Baas *et al*., 2005; Baas *et al*., 2006). Katanin is thought to form a hexameric ring complex that wraps around the MT and severs it. This can occur near the centrosome, which it is thought to be important in mitosis, or at various points along MTs which is important for formation of axonal branches (Figure 1.3C). In axons, katanin and spastin are proposed to sever MTs into shorter MTs which can then be transported along

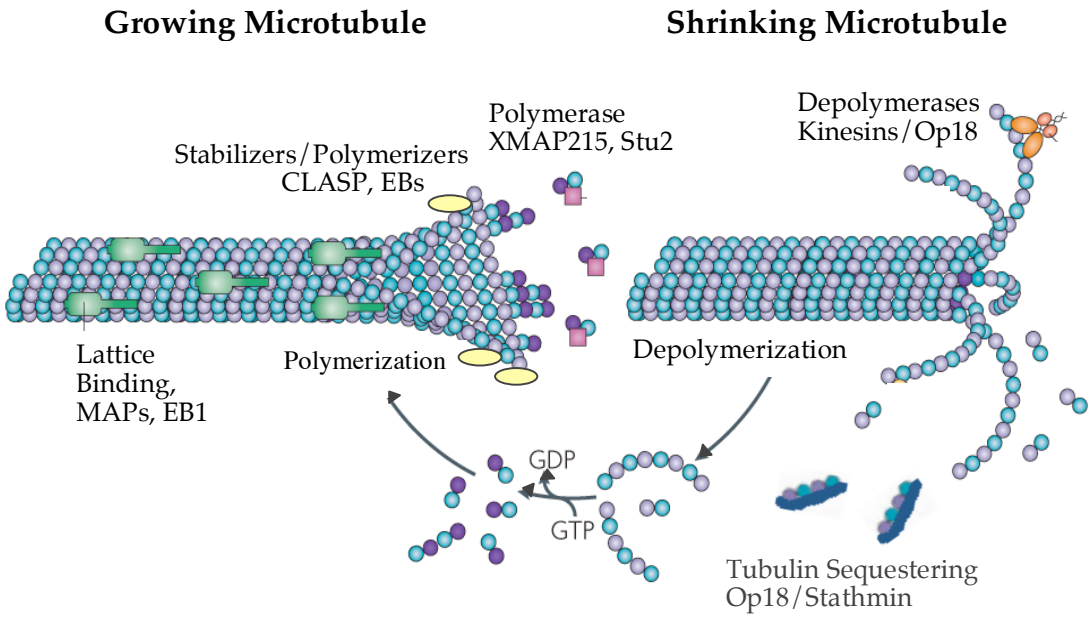

Figure 1.5 Various MAP activities. In order to stabilize MTs, some proteins such as the classical MAPs and EB family members, have been shown to localize along the MT lattice or seam. Several plus-end tracking protein (+TIP) families, such as the CLASP and EB families, have been shown to stabilize MTs and/or to promote growth by directly binding at the plus-end tip region. Another +TIP family, the XMAP215/Stu2 family, has been shown to promote growth by acting as a polymerase and recruiting tubulin dimers to the plus-end. Other MAPs or +TIPs, including Op18 and various kinesins, can act as depolymerizers either by binding directly to MTs and actively depolymerizing them, or by binding tubulin dimers and sequestering them from incorporation into the MT.

longer MTs by motor proteins in a process called "cut and run" (Baas *et al*., 2005).

Op18/Stathmin

The Oncoprotein 18 (Op18)/Stathmin family of MT destabilizing proteins are expressed in all cell types and are highly over-expressed several types of cancer cells (Hanash *et al*., 1988; Curmi *et al*., 2000; Price *et al*., 2000). Op18/Stathmin has been shown to increase MT catastrophes *in vitro* (Howell *et al*., 1999; Manna *et al*., 2006; Manna *et al*., 2009) and depletion of Op18/stathmin in Xenopus extracts and newt epithelial cells causes a decrease in MT catastrophes and increase in the amount of tubulin polymer (Howell *et al*., 1999; Belmont *et al*., 1996). Evidence suggests that Op18/Stathmin can induce MT catastrophes in two ways: (1) by acting directly at the MT ends to induce hydrolysis of GTP, therefore removing the stabilizing GTP and (2) by sequestering free tubulin dimers (Figure 1.5) (Howell *et al*., 1999; Manna *et al*., 2009; Larsson *et al*., 1999; Steinmetz *et al*., 2000). Op18/Stathmin has been shown to regulate a variety of MT processes such as centrosomal nucleation during interphase (Ringhoff and Cassimeris, 2009), MT flux (Manna *et al*., 2009), and axon maintenance (Holmfeldt *et al*., 2009).

Microtubule Plus-End Tracking Proteins

Plus-end tracking proteins (+TIPs) are a specialized class of MAPs that are named for their spectacular ability to specifically bind and track MT plus-ends (Figure 1.6) (Akhmanova *et al*., 2001; Akhmanova and Steinmetz, 2008). By binding MT plus-ends, these proteins are perfected positioned to influence MT plus-end structure, dynamics, and interactions. +TIPs include both motor

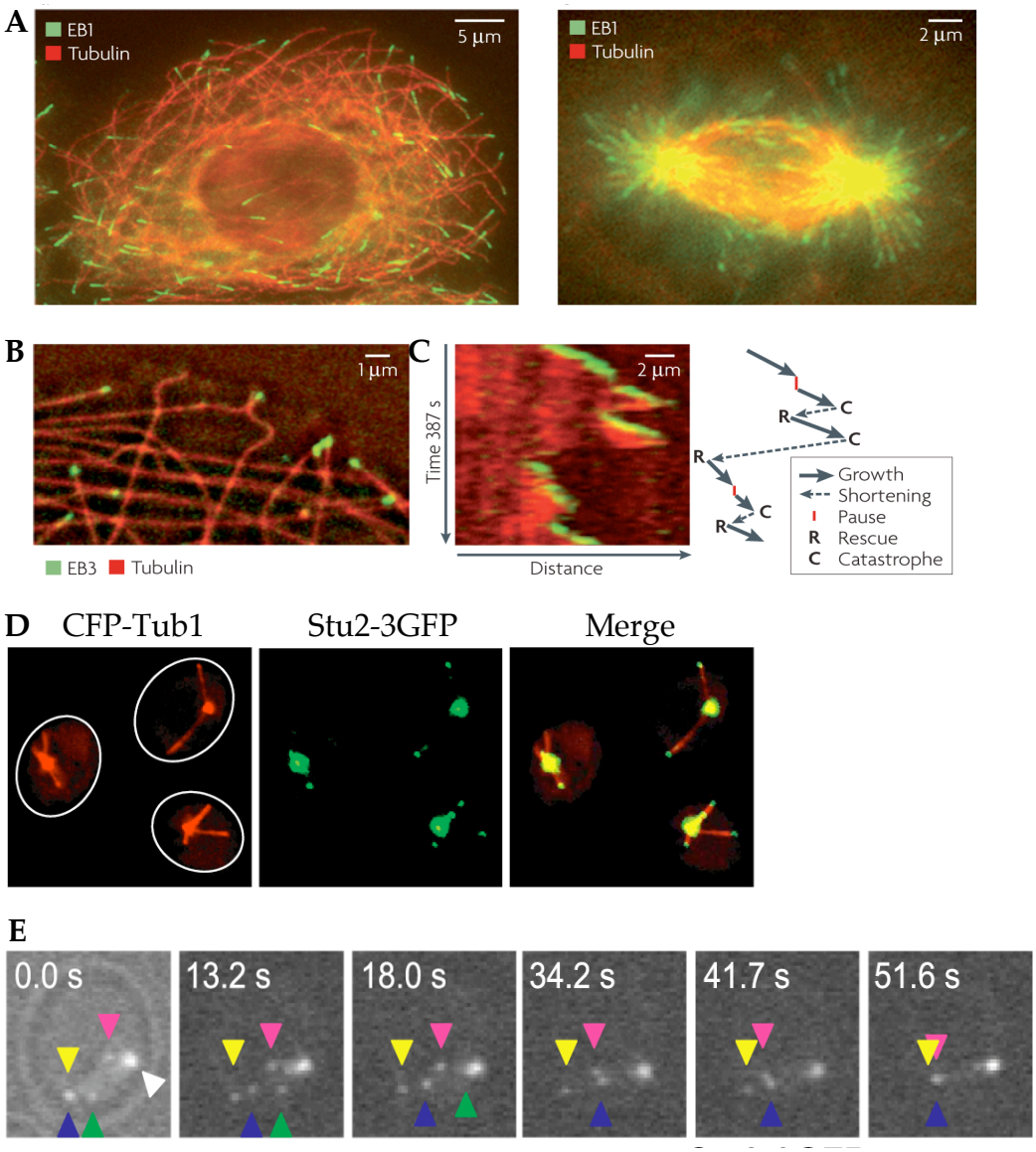

Figure 1.6 MT plus end tracking by mammalian and yeast +TIPs.
A. An interphase (left) and mitotic (right) mouse kidney epithelial cell stained for EB1 and β-tubulin. B. Close up image of EB1-GFP on the plus-ends of MTs, visualized with mCherry-α-tubulin, in a human lung fibroblast cell. C. Kymograph of EB1 plus-end tracking, which shows EB1 only tracks on growing MTs, disappearing from shrinking MTs and paused MTs, but quickly reassociates once MTs begin regrowing. D. Images of budding yeast cells expressing Stu2-3GFP and CFP-Tub1. E. Time-lapse images of Stu2-3GFP. White arrowhead indicates the spindle pole body; each colored arrowhead indicates the position of a particular GFP dot over time. The green arrowhead follows a shrinking MT, indicating that Stu2 can track on both growing and shrinking MTs. Times indicated are in seconds. Figure is adapted from Akhmanova and Steinmetz (2008) and Wolyniak *et al.*, (2006).

and non-motor proteins, and are defined as proteins which track MT plus-ends throughout the cytoplasm, proteins which track MTs in specific regions of the cell such as the leading edge, and proteins which transiently bind MT ends influencing their interactions or destabilizing them (Akhmanova and Steinmetz, 2008; Mimori-Kiyosue and Tsukita, 2003; Morrison, 2007).

Non-motor +TIPs

A large number of non-motor +TIPs families have been characterized and found to reside in evolutionarily conserved families. Four of the best conserved are the CLIP-170, CLASP/Orbit, EB1 and XMAP215/TOG protein families which extend from yeast to humans (Akhmanova and Hoogenraad, 2005; Akhmanova and Steinmetz, 2008; Galjart, 2005; Gard *et al*., 2004). Each of these protein families is described below.

The CLIP-170 family

CLIP-170 was the first identified plus-end tracking protein (Perez *et al*., 1999). Originally discovered as a protein that bound to MTs (Rickard and Kries 1990), it was found to mediate interactions between endocytic vesicles and MTs, hence the name cytoplasmic linker protein, CLIP (Pierre *et al*., 1992). CLIP-170 homologues (CLIP-170/CLIP-190/Bik1/Tip1) are found in a variety of organisms and localize to growing MT-plus ends, MTOCs, kinetochores, and the mitotic spindle (Perez *et al*., 1999; Berlin *et al*., 1990; Lin *et al*., 2001; Dujardin *et al*., 1998; Carvalho *et al*., 2004; Busch *et al*., 2004; Dzhindzhev *et al*., 2005; Tanenbaum *et al*., 2006). CLIPs track on all classes of MTs except MTs that lack the final tyrosine residue from the α-tubulin C-terminal tail (Badin-Larcon *et al*., 2004; Peris *et al*., 2006).

Structural characteristics of CLIP-170 The structure of CLIP-170 family members consist of a globular N-terminal MT binding domain (Mishima *et al*., 2007), followed by a long stretch of coiled-coil important for dimerization (Scheel *et al*., 1999) and ending in a C-terminus with two Zn-fingers and a terminal EEY/F motif which mediates protein interactions (Figure 1.7) (Honnappa *et al*., 2006; Pierre *et al*., 1992; Berlin *et al*., 1990; Miller *et al*., 2006; Weisbrich *et al*., 2007). The N terminal MT binding domain consists of 2 cytoskeleton associated protein glycine rich (CAP-Gly) domains that have been shown to mediate MT binding *in vitro* (Pierre *et al*., 1992; Gupta *et al*., 2009). CAP-Gly domains are found in several other proteins including the related +TIPs, CLIP-115 (De Zeeuw *et al*., 1997) and $p150^{Glued}$ (Lansbergen *et al*., 2004), Alf1, an α-tubulin chaperone (Feierbach *et al*., 1999), as well as CLIPR59, a lipid raft associated protein that may depolymerize MTs (Lallemand-Breitenbach *et al*., 2004). The C-terminus of CLIP-170 is known to be important for localization to kinetochores and for interactions with the CAP-Gly domain of $p150^{Glued}$ (Lin *et al*., 2001; Dujardin *et al*., 1998; Lansbergen *et al*., 2004). The C-terminal residues of CLIP-170s are an EEY/F motif, which is also found at the C-terminal tails of EB1 and α-tubulin (Honnappa *et al*., 2006; Miller *et al*., 2006). The budding yeast homologue, Bik1, is structurally very similar to mammalian CLIP-170 except that it only contains one N-terminal CAP-Gly domain and one C-terminal Zn finger and is much shorter in length (Figure 1.7) (Berlin *et al*., 1990).

CLIP-170 proteins control MT assembly and dynamics. CLIP-170 family members have been shown to promote both MT assembly and dynamics. In Drosophila, CLIP-190 is known to be involved in nucleation of non-

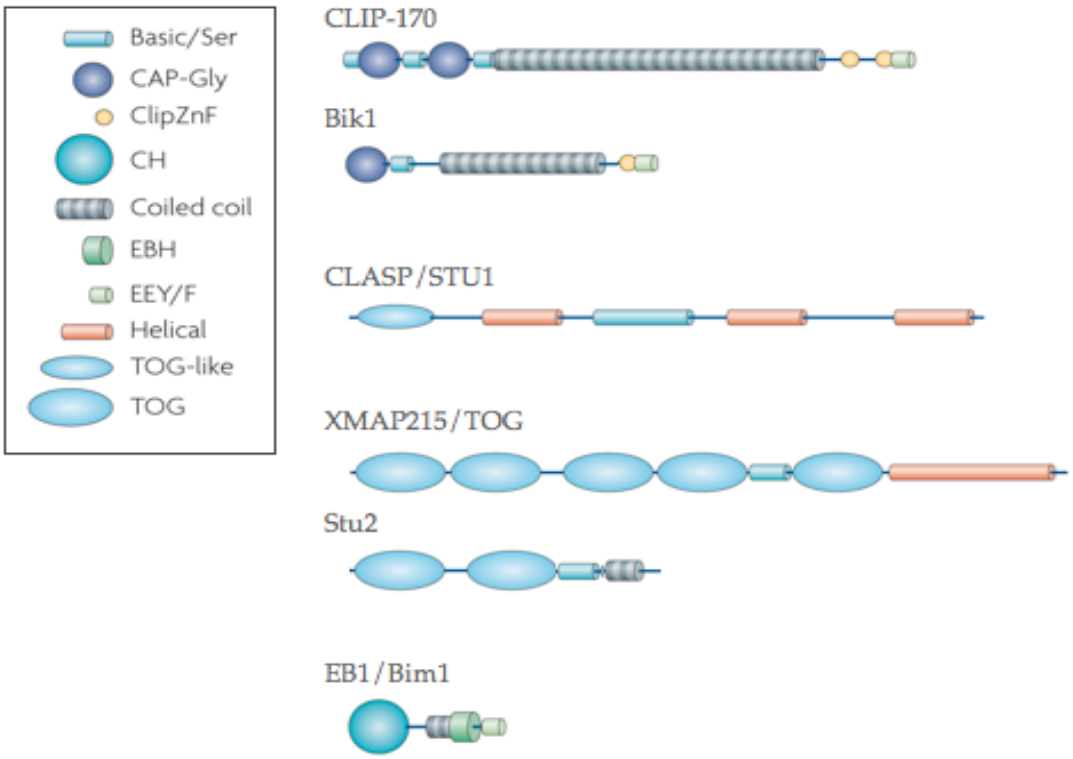

Figure 1.7 Illustration of +TIP structural domains. The prominent structural elements of the +TIP CLIP-170, CLASP, XMAP215, and EB1 protein families are indicated. Basic/Ser, Basic, Serine rich region; CAP-Gly, cytoskeletal associated protein glycine rich region; ClipZnF, zinc knuckle; CH, calponin homology; EBH, EB1 family homology domain; F, EEY/F acidic-aromatic motif; TOG, tumor overexpressed gene domain. Figure modified from Akhmanova and Steinmetz (2008).

centrosomal MT arrays (Rogers *et al*., 2008). Deletion of Bik1 in budding yeast is not lethal, but results in fewer and shorter aMTs and aberrant spindle structures, while Bik1 overexpression results in lethality with a loss of all microtubule structures (Berlin *et al*., 1990; Lin *et al*., 2001). Bik1 is also known to have a role in spindle formation and elongation, as it is involved in nucleation of spindle MTs (Tanaka *et al*., 2005; Tanaka, 2005; Tanaka *et al*., 2005) and is synthetically lethal with the spindle mid-zone protein, Ase1 (Pellman *et al*., 1995). These results indicate Bik1 may have a role in MT dynamics, and a recent study in our lab showed that a *bik1*Δ strain has reduced aMT dynamics throughout the cell cycle (Wolyniak *et al*., 2006). Bik1 is also involved in the dynein-dependent step of nuclear migration (Sheeman *et al*., 2003). Work in fission yeast, has also shown that the CLIP-170 homologue, Tip1, also controls MT dynamics. Tip1 works as an anti-catastrophe factor, as loss of Tip1 results in premature MT catastrophe at the cell cortex before MTs have reached the cell tip (Brunner and Nurse, 2000). Loss of CLIP-170 in mammalian cells also alters dynamics, and these cells show a decrease MT rescues at the cell cortex (Komarova *et al*., 2002). This function of CLIP-170 appears to be specific to interphase cells, as RNAi of CLIP-170 in mitotic cells had no affect on rescue frequency (Tanenbaum *et al*., 2006).

In vitro studies using the H2 microtubule binding region of CLIP-170 also show that CLIP-170 can stimulate rescues (Arnal *et al*., 2004). The H2 region has been shown to promote tubulin oligimerization and MT formation *in vitro* (Gupta *et al*., 2009; Arnal *et al*., 2004; Diamantopoulos *et al*., 1999; Slep and Vale, 2007) and can bind to tubulin dimers (Slep and Vale, 2007; Folker *et al*., 2005). Arnal and colleagues examined these oligomers by electron

microscopy and saw that they included curved filaments and rings. These oligomers were seen to associate with MT ends, and are proposed to incorporate into a MT, which promotes MT growth and increases the frequency of MT rescue (Arnal *et al*., 2004). However, it is unclear why curved protofilaments or rings would aid polymerization, as these are usually thought to be structures associated with depolymerization.

CLIP-170 cellular functions. The C-terminal region of CLIP-170 and Bik1 is important for kinetochore localization (Lin *et al*., 2001; Dujardin *et al*., 1998), and Bik1 has been shown to localize to kinetochores by ChIP (Lin *et al*., 2001; He *et al*., 2001). CLIP-170 is proposed to be important for the initial MT kinetochore capture, as RNAi of CLIP-170 leads to a defect in chromosome alignment (Dzhindzhev *et al*., 2005; Wieland *et al*., 2004). This does not appear to be the case in yeast, as Bik1 was not found to be necessary for initial chromosome capture (Tanaka *et al*., 2005). Rather, Bik1 has been proposed to play a role in the stability of kinetochore-MT attachments and chromosome segregation (Lin *et al*., 2001). The roles of both CLIP-170 and Bik1 at the kinetochore during mitosis appear to be overlap with another protein, as neither is essential for this process. Indeed, CLIP-170 null mice are viable and show only minor defects in chromosome alignment. However, CLIP-170 null mice are sterile and CLIP-170 has an essential role in spermatogenesis where it crosslinks and organizes MTs in the sperm manchette (Akhmanova *et al*., 2005). Additionally, Bik1 is synthetically lethal with the +TIP Bim1, and kinetochore MT dynamics are reduced in a Bim1 Bik1 double mutant (Wolyniak *et al.*, 2006).

Recent work has shown that CLIP-170 is involved in phagocytosis, as a MT stabilizer (Binker *et al*., 2007). Phagocytosis also involves actin polymerization and a recent study by Lewkowicz *et al.,* shows cooperation between the MT and actin networks in this process (Lewkowicz *et al*., 2008). They show that CLIP-170 interacts directly with the formin mDia, an actin nucleator, and can recruit mDia at the onset of phagocytosis to control actin polymerization.

As mentioned earlier, one function of MTs is to stimulate Rac1 activity and cell migration, and this process also involves CLIP-170. Rac1 activation is accomplished through IQGAP, a protein that directly interacts with CLIP-170. It has been proposed that IQGAP could be transported to the cortex on the plus-end of MTs through its interaction with CLIP-170. Alternatively, MTs and CLIP-170 could stabilize and activate IQGAP at the cortex, which then activates Rac1 (Fukata *et al*. 2002; Watanabe *et al*. 2004).

The CLASP family of proteins

CLIP-associating proteins (CLASPs) were first identified as binding partners of CLIPs, using yeast two –hybrid (Akhmanova *et al*., 2001). CLASP family members (CLASP/MAST/Orbit/Stu1) are characterized by having an N-terminal TOG-like domain, a central Ser, Arg, Pro rich region important for interactions with EB1 and MTs , and a C-terminus important for interactions with CLIP proteins, the Golgi complex, and the cell cortex (Figure 1.7) (Galjart, 2005). Unlike other +TIPs, CLASPs show a spatially regulated localization. In the cell body they can be seen to track MT plus-ends, however, within the leading edge they decorate along the MT lattice for a short distance (Akhmanova *et al*., 2001; Wittmann and Waterman-Storer, 2005). This lattice

localization is thought to stabilize MTs, and CLASPs can further promote MT stability by attaching MTs to the cell cortex (Lansbergen and Akhmanova, 2006; Lansbergen *et al*., 2006). Studies on the Drosophila homolog MAST/Orbit have shown that CLASPs stabilize MTs by increasing MT pausing (Sousa *et al*., 2007). CLASPs are also important for increasing MT density within the leading edge by promoting rescues in cooperation with EB1 (Mimori-Kiyosue *et al*., 2005). These results indicate that CLASPs may be important for cell migration, and CLASP2 has been shown to be necessary for directed cell migration during wound healing (Drabek *et al*., 2006).

Interestingly, CLASPs have also been shown to nucleate a noncentrosomal array of MTs from the golgi complex, by coating MT seeds (Efimov *et al*., 2007). These MTs are directed into the leading edge and may form a set of "pioneer" MTs that are important for the stabilization of the leading edge and directionality of movement, or they may serve as tracks for the transport of vesicles from the golgi to the leading edge.

In mitosis, CLASP and Orbit have been shown to be important for incorporation of tubulin subunits at the MT plus end for MT flux (Maiato *et al*., 2005). MT flux is the poleward movement of the MT lattice in spindle MTs; in which tubulin subunits are added at the plus end of MTs and removed at the MT minus end, while the MT length remains constant (Rogers *et al*., 2005). Flux is important for chromosome movement and fixing incorrect chromosome spindle attachments (Cassimeris and Morabito, 2004; Ganem *et al*., 2005). The addition of tubulin subunits by Orbit at the plus end is balanced by the kinesin Klp10A depolymerization at minus end (Laycock *et al*., 2006). Loss of CLASP or Orbit polymerization at the plus end leads to spindle collapse (Maiato *et al*., 2005; Maiato *et al*., 2003). In budding yeast,

MTs do not flux, however Stu1 is also important for the maintenance of a bipolar spindle as loss of Stu1 leads to spindle collapse (Yin *et al*., 2002). This may be due to the tension by attached kMTs, which collapses the spindle in the absence of a polymerizing activity by Stu1 at kMT, as seen for CLASP/Orbit. In agreement with this theory, Stu1 localizes to kinetochores and double depletion of Stu1 and kinetochore components relieves the spindle collapse of a *stu1-5* mutant (Amaro, 2010). However, these double mutant spindles do not elongate with the same kinetics as wild type or single kinetochore mutant spindles indicating that Stu1 also plays a role in elongation and stability during anaphase. This is in agreement with previous results showing that Stu1 localizes to the spindle midzone where it is involved in stabilization and elongation (Yin *et al*., 2002).

The XMAP215/TOG/Msps/Stu2 family of proteins

Protein structure. The XMAP215/TOG family is characterized by having a series of TOG repeats in the N-terminus. Homologs in higher eukaryotes have 5 such repeats, while Stu2, the budding yeast family member, has 2 (Figure 1.7) (Ohkura *et al*., 2001). TOG domains are comprised of a series of HEAT repeats, which are important for tubulin binding (Al-Bassam 2006, Brouchard 2008, Kessemaker 2007) (Kerssemakers *et al*., 2006; Al-Bassam *et al*., 2006; Brouhard *et al*., 2008). The crystal structure of a TOG domain from Zyg-9, the *Caenorhabditis elegans* family member, Stu2, and the MiniSpindles (Msps) from Drosophila were recently solved and revealed a flat paddle-shaped structure (Slep and Vale, 2007; Al-Bassam *et al*., 2007). The C-terminal halves of these proteins are less well conserved, but are known to contain MT binding domains (Wang and Huffaker, 1997; Nakaseko *et al*., 2001; Popov *et al*., 2001).

Additionally, Stu2 is known to form homodimers while homologues from higher eukaryotes are monomers (Al-Bassam *et al*., 2006; Cassimeris *et al*., 2001; van Breugel *et al*., 2003).

Regulation of MT dynamics. The effects of the XMAP215/TOG family have been studied extensively both *in vivo* and *in vitro*. Many studies have found that XMAP215 family members can promote MT growth and directly increase the MT growth *in vitro* (Popov and Karsenti, 2003). Two models currently exist to explain the activity of these proteins. The first model is a template model where XMAP215 can serve as a template for tubulin oligomers and deliver preassembled protofilaments to the MT plus-end (Kerssemakers *et al*., 2006; Slep and Vale, 2007). In this model XMAP215 can bind several tubulin dimers at one time through its multiple TOG domains. In the second model, XMAP215 or Stu2 binds a single tubulin dimer and facilitates repeated rounds of tubulin heterodimer additions as it surfs the MT plus end (Figure 1.5) (Al-Bassam *et al*., 2006; Brouhard *et al*., 2008). In support of this second model, both XMAP215 and Stu2 were shown to bind tubulin dimers in a 1:1 stochiometry.

Intriguingly, this family of proteins can also have MT depolymerizing activity as well (van Breugel *et al*., 2003; Vasquez *et al*., 1994; Shirasu-Hiza *et al*., 2003; Holmfeldt *et al*., 2004). The presence of MT stabilizing and destabilizing activity within the same proteins may not be as surprising as at sounds. Rather, it suggests that these proteins can act as catalysts in MT assembly, accelerating the addition or removal of tubulin dimers (Howard and Hyman, 2007; Asbury, 2008). In agreement with this idea, *in vivo* studies have shown that depletion of Msps and Stu2 results in an increase in MT

pausing. This indicates that these proteins increase overall dynamics, promoting both catastrophes and rescues and acting as anti-pause factors (Kosco *et al*., 2001; Brittle and Ohkura, 2005).

Cellular Functions. XMAP215 has been shown to promote the growth of interphase MT arrays in Xenopus egg extracts, and this activity opposes the MT depolymerase XKCM1, a kinesin-13 family member (see below) (Tournebize *et al*., 2000). The antagonistic activities of these two proteins were also seen *in vitro*, and addition of these two proteins resulted in MTs that polymerize quickly and are highly dynamic (Kinoshita *et al*., 2001). This led to a model where XMAP215 and XKCM1 control dynamics throughout the cell cycle (Kinoshita *et al*., 2002). In this model, XMAP215 is more dominant in interphase for the formation of the long MT array, while a decrease in XMAP215 activity at mitosis allows for XKCM1 destabilization of MTs and the formation of the mitotic spindle. However, this may not be the case in mammalian cells as neither loss of TOG or MCAK (the mammalian XKCM1 homolog) has a major effect on interphase arrays. Rather, interphase arrays may be mainly controlled by the antagonistic activities of Op18 and MAP4 (see below) (Holmfeldt *et al*., 2009).

Although depletion of TOG does not have an effect on interphase arrays, it does leads to multipolar spindles in mitosis. This phenotype is believed to have resulted from a loss of MT focusing at spindle poles and is suppressed by codepletion of MCAK (Cassimeris and Morabito, 2004; Holmfeldt *et al*., 2004; Gergely *et al*., 2003). In budding yeast, Stu2 is required for spindle elongation, and this activity is opposed by the depolymerizing kinesin-8, Kip3, which is an ortholog of the kinesin-13 mentioned above (Severin *et al*., 2001). These

results indicate the conservation and importance of the antagonistic relationship between stabilizing XMAP215/Stu2 family members and depolymerizing kinesins.

Most XMAP215/Stu2 family members can localize to centrosomes and spindle pole bodies independently of MTs (Cassimeris and Morabito, 2004; Chen *et al*., 1998; Matthews *et al*., 1998; Graf *et al*., 2000). This localization is also important for MT nucleation and MT anchoring in yeast and higher eukaryotes in addition to the MT focusing activity at spindle poles mentioned above (Graf *et al*., 2000; Lee *et al*., 2001; Popov *et al*., 2002; Usui *et al*., 2003).

XMAP215/Stu2 family members are known to localize to kinetochores in a variety of organisms (Cassimeris and Morabito, 2004; Graf *et al*., 2000; Aoki *et al*., 2006). In budding yeast, Stu2 has been shown by ChIP to localize to kinetochores independently of MTs (He *et al*., 2001). Loss of Stu2 results in improper metaphase chromosome alignment, and this may be due to the reduced kMT dynamics in *stu2* mutants and a role for Stu2 in kinetochore-MT attachment (He *et al*., 2001; Kosco *et al*., 2001). An elegant study by Tanaka and colleagues showed that Stu2 is involved in kinetochore capture and that the release of Stu2 from the kinetochore can stimulate rescues on depolymerizing kMTs in order to prevent loss of kinetochore-MT side attachment (Tanaka *et al*., 2005). In fission yeast, the kinetochore localization of Dis1, is thought to facilitate kinetochore-MT attachments (Aoki *et al*., 2006; Garcia *et al*., 2001). However, in mammalian cells, TOG is not required for kinetochore-MT attachments, but rather the MT polymerization activity of TOG is important for generating the high density of MTs in the spindle which is proposed to be important for chromosome oscillations (Cassimeris *et al*., 2009).

The EB1 family of proteins

EB protein structure. EB proteins have an N-terminal calponin homology (CH) domain responsible for MT binding (Hayashi and Ikura, 2003), followed by a flexible linker region, and a C-terminus containing coiled-coil and EB homolog domains important for dimerization (Figure 1.7) (Honnappa *et al*., 2006; Slep *et al*., 2005). EB proteins end in a flexible acidic tail with a final acidic-aromatic motif (EEY/F) similar to α-tubulin and CLIP-170 (Honnappa 2006). The EB homology domains and terminal EEY/F sequence are important for interactions with a variety of other +TIPs and for their localization to the MT plus end (see below) (Lansbergen and Akhmanova, 2006; Vaughan, 2005; Bieling *et al*., 2008; Dixit *et al*., 2009). In mammalian cells, there are three EB proteins, EB1, EB2, and EB3, which share the same general structure outlined above. EB1 and EB3 localize to plus-ends and control dynamics while EB2 does not appear to have a major role in this process. However, there is at least partial redundancy in their function as EB2 is able to localize to plus-ends and required for viability in the absence of EB1 or EB3 (Komarova *et al*., 2009). Budding and fission yeast each have one EB family member, Bim1 and Mal3 respectively, and these are most similar to EB1.

EBs promote MT dynamics and stability. The effect of EB family members on MT dynamics is varied and depends on the system studied. *In vivo*, studies in Drosophila, mouse fibroblasts and budding yeast show that EB proteins have an anti-pausing effect by promoting catastrophes and rescues (Wolyniak *et al*., 2006; Rogers *et al*., 2002; Kita *et al*., 2006), while studies in Xenopus, fission yeast and CHO cells indicate that EB proteins suppress MT catastrophes (Komarova *et al*., 2009; Tirnauer *et al*., 2002b; Busch and Brunner, 2004).

In contrast to their *in vivo* phenotypes, fission yeast mal3 and mammalian EB3 increase catastrophes and rescues *in vitro* (Komarova *et al*., 2009; Bieling *et al*., 2007; Vitre *et al*., 2008). However, another study found mammalian EB1 to suppress catastrophes, in agreement with its *in vivo* phenotype (Manna *et al*., 2008). The central role of EB proteins in the recruitment of a wide variety of other +TIPs (discussed below) may be responsible for the complexity of results seen between EBs family members. EBs may be responsible for recruiting or blocking access of different +TIPs to the MT depending on the organism or cell type studied.

Despite their differences in affecting catastrophe frequencies, EB family members are generally thought to promote MT growth and assembly (Rogers *et al*., 2008; Komarova *et al*., 2009; Tirnauer *et al*., 2002b; Busch and Brunner, 2004; Tirnauer *et al*., 2002a). Structural studies indicate EB proteins may promote MT growth by binding both the MT plus-end structure and lattice, enhancing the lateral associations between protofilaments (Figure 1.5) (Vitre *et al*., 2008; Sandblad *et al*., 2006; des Georges *et al*., 2008), and Mal3 has been shown to specifically bind the MT seam which is thought to stabilize the MT (Sandblad *et al*., 2006).

EB cellular functions. EB proteins are known to be involved in a variety of cellular processes. Like the XMAP215 family, EB family members are also centrosomal components and important for MT assembly and anchorage (Rehberg and Graf, 2002; Louie *et al*., 2004). In Drosophila, EBs are involved in acentrosomal MT nucleation and Mal3 has been shown to be involved in initiating MT assembly (Rogers *et al*., 2008; Busch and Brunner, 2004). Additionally, loss of Bim1 or Mal3 results in fewer astral MTs in yeast

(Tirnauer *et al*., 1999; Beinhauer *et al*., 1997). In mammalian cells, EB1 is targeted to the centromere by the centrosomal protein, FOP, and the interaction between EB1 and $p150^{Glued}$ is important for MT anchorage at the centrosome and the formation of the interphase MT array (Askham *et al*., 2002; Yan *et al*., 2006).

EB1 and its interaction with another +TIP, APC, has also been shown to be important for kinetochore capture by MTs and maintenance of kinetochore-MT attachment (Nakamura *et al*., 2001). EB1 also has an important role MT mediated cell migration, interacting with many proteins at the leading edge to influence MT dynamics and attachments. EB1 and APC work with mDia to stabilize MT at the leading edge (Wen *et al*., 2004), and as mentioned above EB1 and CLASP interactions are thought to be important for the promotion of rescues in this region (Mimori-Kiyosue *et al*., 2005). Additionally, EB proteins are involved in the attachments of MTs to the actin network and cell cortex (Lansbergen and Akhmanova, 2006). In yeast, Bim1, is important in mediating the interaction between aMTs and the actin cytoskeleton, which is important for nuclear migration during mitosis (Yin *et al*., 2000; Hwang *et al*., 2003).

The MT polymerization and stabilization of activities of EBs are also important in the spindle. In yeast, Bim1 is known to promote polymerization of nuclear MTs (Tanaka *et al*., 2005) and Bim1 MT polymerization is also important for maintaining the length of the pMTs which interdigitate across the spindle and are important spindle stability (Gardner *et al*., 2008b).

Molecular Motor +TIPs

Two different classes of MT motors have been identified, kinesins and dynein. Dynein was identified as a minus directed motor (Vale *et al*., 1992), while the large kinesin family consists of both plus and minus directed motors as well as kinesins which have no motor activity (Lawrence *et al*., 2004). Motors use the energy of ATP binding and hydrolysis for their roles in several cellular processes including cargo transport on MT tracks (Gross, 2004), generation of force between MTs and the cell cortex (Wu *et al*., 2006), organization interphase MT arrays (Moore 2006), as well as being essential for spindle assembly and elongation (Figure 1.4) (Walczak and Heald, 2008). Several motor families are described below, with a focus on their MT depolymerizing activity. The ability of motors to crosslink and slide MTs in spindle function is also described briefly, but for a complete review see Walczak and Heald, 2008.

Kinesin-13s are class of MT destabilizers found in higher eukaryotes, but are not present in budding yeast (Lawrence *et al*., 2004). The best-characterized members of the kinesin-13 family include Xenopus XKCM1, mammalian MCAK, and drosophila Klp59C and klp10A (Kinoshita *et al*., 2001; Desai *et al*., 1999; Hunter *et al*., 2003; Rogers *et al*., 2004). These kinesins do not have motor activity but rather diffuse one-dimensionally along the MT lattice to find MT ends (Hunter *et al*., 2003; Helenius *et al*., 2006). However, the motor domain is responsible for the MT depolymerizing activity, and these proteins can depolymerize both plus and minus MT ends. Kinesin-13 family members destabilize MTs by binding to tubulin subunits at the end of the MT and causing tubulin subunits to bend, physically transforming the plus-end

structure into one of depolymerization (Figure 1.5) (Desai *et al*., 1999). Depolymerizing MT protofilaments are seen to form bent curls around the motor (Moores and Milligan, 2006). Studies on MCAK propose that up to 14 MCAK dimers assemble at the end of a microtubule to form a processive depolymerizing complex (Hunter *et al*., 2003). Kinesin-13 family members have been shown to from rings or spirals around MT *in vitro*, suggesting that a kinesin ring may move with the depolymerizing MT coupling a cargo such as a kinetochore to the depolymerizing MT. This process is analogous to the Dash/Dam complex in yeast (Tan *et al*., 2006). However, it is unclear if these kinesin-13 rings form *in vivo*.

Kinesin-13 activity is responsible for general interphase MT array maintenance (Walczak and Mitchison, 1996; Mennella *et al*., 2005; Kinoshita *et al*., 2006). The depolymerizing activity of XKCM1 has been shown to be antagonistic to the MT stabilizing activity of XMAP215 (discussed above) and the interplay of these proteins is important for interphase MT arrays (Tournebize *et al*., 2000). Kinesin-13 motors are also known to localize to the mitotic spindle and are involved in formation and maintenance of the spindle as well as chromosome congression, MT flux, and correction of incorrect chromosome-MT attachments (Kline-Smith and Walczak, 2004; Rogers *et al*., 2004; Moores and Milligan, 2006; Lan *et al*., 2004). Depletion of MCAK and kinesin-13 family members in various systems result in monopolar spindles indicating that formation of the MT spindle requires both stabilizing and destabilizing factors (Kline-Smith *et al*., 2004). Most cells have more than one kinesin-13 family member and their activities are specific, acting at opposite ends of the spindle. Some kinesin-13 proteins localize to the centrosome and depolymerize MT minus ends, contributing to MT flux, while others act at the

kinetochore to depolymerize MT plus-ends and segregate chromosomes during anaphase (Rogers *et al*., 2004; Mennella *et al*., 2005).

Kinesin-8. The kinesin-8 family is related to the kinesin-13 family, and there is probably some functional overlap between the two families (Moore and Wordeman, 2004). Kinesin-8 family members have been shown to be MT depolymerases, and depletion of kinesin 8 results in extremely long and stable MTs in a variety of organisms (Stumpff and Wordeman, 2007). Like kinesin-13 family members, the ATP dependent depolymerase activity of kinesin-8 can be stimulated by both MTs and free tubulin. However, unlike the kinesin-13 family, kinesin-8 proteins posses a functional plus-end directed motor and only depolymerize MT plus ends. This activity is length dependent as kinesin-8 proteins depolymerize longer MTs faster than shorter MTs (Varga *et al*., 2006). Recent studies in mammalian cells show kinesin 8 proteins cause catastrophes and then control and slow MT shrinkage rates, which suppresses chromosome oscillations and contributes to chromosome congression (Stumpff *et al*., 2008; Mayr *et al*., 2007; Gardner *et al*., 2008c). This function may be specific to mammalian cells, as budding yeast Kip3, does not appear to be involved in chromosome congression (Tytell and Sorger, 2006). However, the depolymerase activity of Kip3 is needed for proper spindle positioning (Gupta *et al*., 2009) and elongation (Tytell and Sorger, 2006) where it opposes the activity of Stu2, as mentioned above (Severin *et al*., 2001). Like kinesin-13s, kinesin-8s are also known to be important for spindle bipolarity (Cottingham *et al*., 1999; Goshima and Vale, 2003) and have been shown to couple kinetochores to the depolymerizing MTs during anaphase (Mayr *et al*., 2007; Grissom *et al*., 2009).

Kinesin-14. Kinesin-14 family members are minus-end directed motors (Endow *et al*., 1990; McDonald *et al*., 1990) and, like the above mentioned kinesin families, also possess a MT depolymerase activity (Sproul *et al*., 2005; Endow *et al*., 1994). However, the activity of kinesin-14s is distinct from kinesin-8 and 13, as the ATPase depolymerizing activity is only stimulated in the presence of MTs and not by free tubulin dimers, nor do kinesin-14s bind tubulin dimers (Hunter *et al*., 2003; Sproul *et al*., 2005). Biochemical analysis of the budding yeast kinesin-14, Kar3, led Spoul and colleagues to suggest a model in which Kar3 stays coupled to the MTs ends, and depolymerizes MT plus ends by removing a single tubulin dimer with each ATP hydrolysis coupled powerstroke (Sproul *et al*., 2005). Kar3 uses its plus-end depolymerase activity during mating to position the nucleus for karyogamy, coupling the depolymerizing MT to the cell cortex and dragging the nucleus into the schmoo tip (Maddox *et al*., 2003). Kar3 has also been shown to be responsible for poleward chromosome transport along MTs after lateral capture (Tanaka *et al*., 2005). Interestingly, Kar3 associates with two different light chains; Vik1 in the nucleus during mitosis and Cik1 in the cytoplasm for vegetative growth (Sproul *et al*., 2005; Manning *et al*., 1999; Allingham *et al*., 2007). Structural work has shown that Vik1 (and presumably Cik1) is a modified kinesin that lacks ATPase activity itself, but aids Kar3 in its powerstroke movement (Allingham *et al*., 2007). Kinesin-14 family members can crosslink MTs, and it has been proposed that they can slide both parallel and anti-parallel MTs. MT sliding is important for spindle organization and elongation (Goshima *et al*., 2005; Cai *et al*., 2009; Braun *et al*., 2009).

Kinesin-5. Although not considered to be +TIPs, the kinesin-5 family has been included in this section with the other kinesin motors, and they play an important role in the organization of the spindle and have recently been shown to have depolymerase activity. Kinesin-5 motors are plus-end directed motors that self-interact to form homotetramers. These homotetramers localize to and crosslink antiparallel polar MTs (pMTs) in the spindle midzone. This crosslinking allows the plus-end motor activity of these kinesins to slide antiparallel pMTs past one another and provides a force to elongate the spindle (Walczak and Heald, 2008; Kapitein *et al*., 2005). The poleward sliding of MTs also contributes to MT flux in the spindle (Mitchison *et al*., 2005; Brust-Mascher *et al*., 2009). The budding yeast kinesin-5 members, Cin8 and Kip1, have recently been shown to promote MT disassembly of both kinetochore and astral MTs (Gardner *et al*., 2008a). The depolymerization of longer kinetochore MTs by Cin8 and Kip1 was found to be important for chromosome congression.

Dynein. Dynein is a well conserved minus-end directed motor that is involved in a multitude of MT mediated processes including flagellar movement (Riedel-Kruse *et al*., 2007), cargo transport (Vallee *et al*., 2004), chromosome capture and congression (Schmidt *et al*., 2005), spindle organization (Goshima *et al*., 2005), nuclear migration (Heil-Chapdelaine *et al*., 2000; O'Connell and Wang, 2000; Nguyen-Ngoc *et al*., 2007), and spindle elongation (Hildebrandt and Hoyt, 2000). Similar to the above kinesins, dynein has also been shown to have a MT destabilizing activity (Carminati and Stearns, 1997). Dynein works in conjunction with the conserved multi-subunit dynactin complex, which is responsible for dynein activation (Kahana

et al., 1998; King *et al*., 2000; King and Schroer, 2000; Kardon *et al*., 2009). Dynein is anchored to the cortex by Num1, and once anchored, the dynactin-activated minus-end directed motor allows for the sliding of MTs around the cell cortex, which provides a force for nuclear movement and spindle elongation (Walczak and Heald, 2008; Hildebrandt and Hoyt, 2000; Bloom, 2001).

Mechanisms of Plus-end Tracking

Several mechanisms have been proposed for the accumulation of +TIP proteins at MT plus-ends. These include: (1) intrinsic binding to the plus-end structure, (2) intrinsic binding followed by MT "surfing" (3) intrinsic binding followed by MT "treadmilling" (4) transport to the plus-end by a plus-end kinesin directed kinesin, (5) binding to another +TIP, in a process termed "hitchhiking", and (6) copolymerizing with tubulin subunits. In treadmilling, the +TIP has an affinity for the plus-end structure and binds to the growing plus-end. As the MT grows, the +TIP remains stationary, and subsequently dissociates from the MT lattice. This dissociation is proposed to occur by a lower affinity of the +TIP for MT lattice versus the plus-end structure, or by phosphorylation of the +TIP. MT "surfing" is when the associated +TIP moves with the polymerizing MT plus end (Carvalho *et al*., 2003).

Intrinsic plus-end localization has been shown for several +TIP proteins (Figure 1.8A). Fluorescently tagged purified versions of EB1, Mal3, XMAP215, and Stu2 were shown to directly bind MT plus-ends *in vitro* (Al-Bassam *et al*., 2006; Brouhard *et al*., 2008; Dixit *et al*., 2009; Bieling *et al*., 2007; Bieling *et al*., 2008). XMAP215 +TIP tracking involves "surfing" with the growing or shrinking MT plus-end (Brouhard *et al*., 2008). However, plus-end tracking

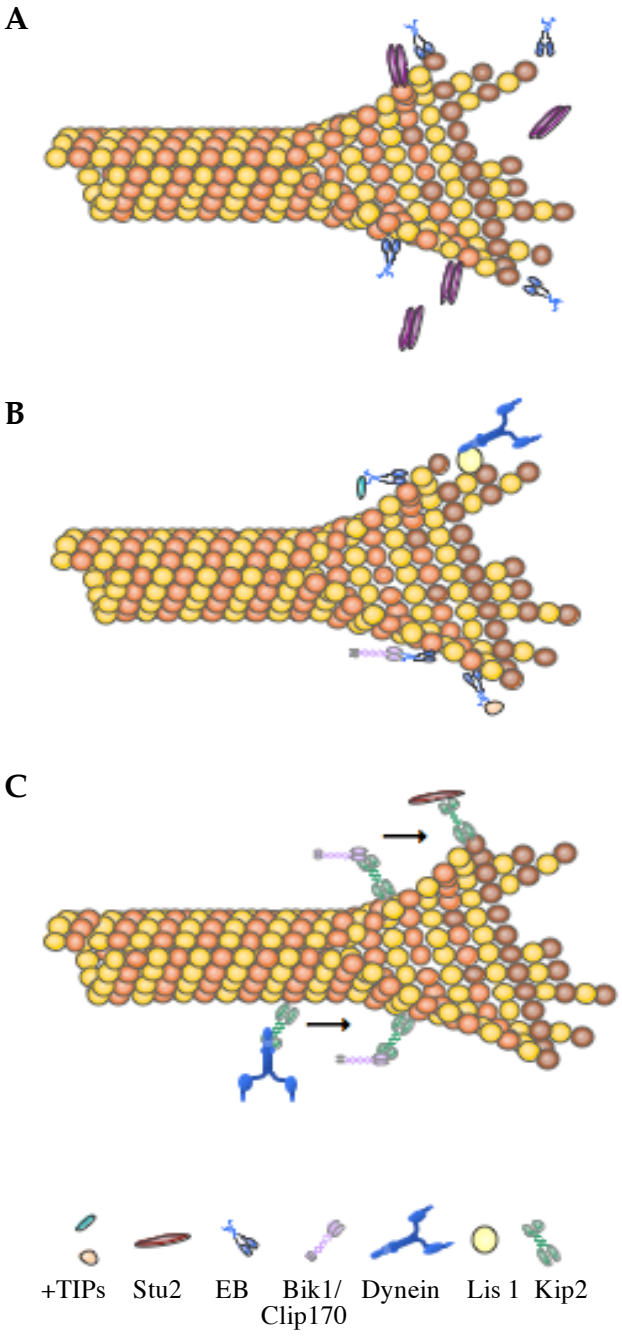

Figure 1.8 Plus-end Tracking Mechanisms. A. Some +TIP proteins, including EB1 family members and Stu2, have an intrinsic affinity for the MT plus end. B. A large number of +TIPs localize to the MT plus tip by "hitchhiking" on EB proteins. Dynein also "hitchhikes' on Lis1 and Bik1 for plus-end localization. C. Many proteins, including Bik1 and dynein, are transported to the plus-end by plus end directed kinesins

does not involve surfing or treadmilling for EBs or for CLIP-170, which is dependent on EB1 for plus-end binding (see below). Rather EBs and CLIP-170 proteins show rapid turnover at plus-ends, rapidly associating and dissociating with the MT plus-tips (Bieling *et al*., 2007; Bieling *et al*., 2008; Dragestein *et al*., 2008). The dwell times of EB and CLIP-170 have been calculated and are very short with individual molecules binding to the MT plus-tip for only 0.05 (EB) and 0.2 (CLIP-170) seconds (Bieling *et al*., 2008).

A variety of proteins have been shown to "hitchhike" on EB proteins, indicating that EB may be a master regulator of MT dynamics (Figure 1.8B) (Lansbergen and Akhmanova, 2006; Vaughan, 2005). The C-terminus of EB1 (EB1c) interacts with a variety of unrelated +TIPs including APC, MCAK, STIM1, MACF, CLIP-170, and CLASPS (Akhmanova and Steinmetz, 2008; Morrison, 2007) and is important or essential for the plus-end accumulation of these factors. The molecular mechanism of EB dependent CLIP-170 accumulation at MT plus ends involves interactions between the CLIP-170 CAP-Gly domains and the C-terminal EEY/F motifs of EB1 and alpha-tubulin (Honnappa *et al*., 2006; Mishima *et al*., 2007; Weisbrich *et al*., 2007; Bieling *et al*., 2008; Dixit *et al*., 2009), and interactions with both EB1 and alpha tubulin are necessary for efficient CLIP-170 plus-end tracking (Peris *et al*., 2006; Bieling *et al*., 2008). The interaction of EB1c with APC1, STIM1, CLASP, MCAK, and MACF does not involve the terminal EEY/F motif, but rather the hydrophobic cavity and tail within the EB1 homology domain (Honnappa *et al*., 2006; Slep and Vale, 2007; Honnappa *et al*., 2009). A conserved short polypeptide motif, Ser-x-Ile-Pro (SxIP), is present in each of these +TIPs interacts with the EB homology domain and is important for plus-end accumulation (Honnappa *et al*., 2009). Dynein is also a +TIP hitchhiker, dependent on the +TIPs Lis1 and

Bik1 for its plus-end localization (Sheeman *et al*., 2003; Lee *et al*., 2003).

Transport to the plus-end by kinesin motors has been shown for several +TIPs (Figure 1.8C) (Carvalho *et al*., 2003). In yeast, the majority of Tip1 and Bik1 (CLIP170 homologs) plus-end accumulation is dependent on transport by a plus-end directed kinesin motor (Carvalho *et al*., 2004; Busch and Brunner, 2004). This is quite different than the requirement of EB1 for mammalian CLIP-170, as described above. However, in fission yeast proper kinesin plus-end accumulation is in turn dependent on the EB1 homolog, Mal3, again highlighting the central role of EB proteins in plus-end tracking (Busch and Brunner, 2004; Browning *et al*., 2003). In addition to the plus-end targeting of dynein by Bik1 and Lis1, transport by the kinesin Kip2 is also important for dynein plus-end localization (Caudron *et al*., 2008).

Regulation of +TIPS

Autoinhibition- Full-length CLIP-170 is proposed to be autoinhibited by intramolecular N and C-terminal interactions that interfere with its ability to bind other proteins or MTs. Using scanning force microscopy and electron microscopy CLIP-170 was visualized as a long thin flexible molecule that could circularize (Scheel *et al*., 1999; Lansbergen *et al*., 2004). This is proposed to occur through interactions of the CAP-Gly domain with the C-terminal Zn knuckle and EEY/F domain (Figure 1.7) (Lansbergen *et al*., 2004; Goodson *et al*., 2003). Once CLIP-170 is bound to a MT or another protein such as EB1 or $p150^{glued}$ the molecule is "opened up" and can interact with other partners. Phosphorylation of CLIP-170 is speculated to interfere with these intramolecular interactions and can open the molecule (Lansbergen *et al*.,

2004). This type of autoinhibition may be present in Bik1 as well, as the N and C terminus of Bik1 interact (Wolyniak *et al*., 2006).

EB1 has also been shown to be autoinhibited by interactions of its C-terminal tail with the N-terminal MT binding domains (Hayashi *et al*., 2005). Binding of p150glued, another CAP-Gly containing protein, to the C-terminus of EB1 or deletion of the EB1 C-terminus strongly enhances EB1 binding and activity at MT ends (Manna *et al*., 2008; Hayashi *et al*., 2005). Autoinhibition may be used in the cell to regulate the MT binding and polymerization dynamics of these proteins.

Phosphorylation As with many other processes in the cell, a primary method of MAP regulation is phosphorylation. An example of this includes the interactions between EB1 and many of its binding partners. As mentioned above the Ser-x-Ile-Pro (SxIP) domain of several +TIPs is important for EB1 mediated MT plus-end association. When this region is phosphorylated, it disrupts the interactions of these proteins with EB1 and thus controls their MT association (Honnappa *et al*., 2009). Another example of phosphorylation regulation is by mTOR. mTOR is known to phosphorylate CLIP-170 and $p150^{glued}$ homologues (Choi *et al*., 2000; Vaughan *et al*., 2002). Inhibition of mTOR results in a loss of MT dynamics, indicating that phosphorylation activates CLIP-170 and $p150^{glued}$. Additionally, phosphorylation of Op18/Stamathin has been shown to interfere with its ability to sequester tubulin dimers, thus suppressing its catastrophe promoting activities (Manna *et al*., 2009).

Experimental Purpose

With its relatively simple cytoskeleton, the budding yeast *Saccharomyces cerevisiae* is an ideal model system to study +TIPs and elucidate their roles in modulating MT function. MT arrays in yeast are exclusively involved in events leading to chromosome segregation, reducing the complexity of +TIP involvement with other MT functions such as organelle transport or cell shape (Huffaker *et al*., 1988; Palmer *et al*., 1992). Additionally, yeast has a small and completely sequenced genome with few duplicated genes; +TIP families are represented by a single gene, which simplifies their analysis. The budding yeast +TIPs Stu2, Bim1 and Bik1 are highly conserved with their mammalian counterparts, and like many other processes conserved from yeast to mammalian cells, the basic processes involved in MT regulation should be similar. This study further characterizes the +TIP proteins Stu2, Bik1, and Bim1 in order to better understand how +TIPs work to regulate MT dynamics.

I found that these three proteins interact both with themselves and each other in all pairwise combinations. Mapping of protein-protein interaction domains, competitive interaction assays, and physical characterization of protein complexes indicate that these proteins do not associate in a single complex but rather compete for binding to each other. This suggests that the interactions among these proteins are dynamic and that different complexes of these proteins may perform distinct roles in the cell.

Depletion of Stu2, Bim1, and Bik1 results in a decrease in MT dynamics and an increase MT pausing (Tirnauer *et al.* 1999; Kosco *et al.* 2002; Wolyniak *et al.* 2006). However, the phenotypes seen in during *in vivo* depletion studies do not necessarily reflect the intrinsic biochemical activity of the depleted protein (this topic is explored in further detail in Chapter Three). As described earlier,

and illustrated in Figure 1.5, +TIPs can work to regulate MT polymerization and depolymerization dynamics in several ways. In order to understand how these +TIPs control MT dynamics, it is important to have a clear understanding of the activity of each protein and how this activity is changed or modified in the presence of other +TIPs. To this end, I purified Bim1 and Bik1 to further characterize these proteins and determine their activities on MT dynamics individually and in combination *in vitro*.

In vitro, I observed Bim1 to localize directly to the microtubule plus-end, however, Bik1 required Bim1 for efficient plus-end localization. Bim1 can promote MT assembly, and this effect is primarily due to the suppression of microtubule catastrophes by Bim1, although Bim1 also increases microtubule growth rates and rescue frequency. The ability of Bim1 to promote MT polymerization is likely due to a direct effect of Bim1 on MT plus-end structure as I found that Bim1 does not bind tubulin subunits. In contrast, Bik1 destabilized MTs. This may be due to the formation of polymerization-incompetent tubulin oligomers as I observed Bik1 to promote oligomerization of tubulin subunits. Combining equal-molar amounts of Bim1 and Bik1 resulted in an effect on microtubule dynamics similar to Bim1 alone. These results indicate that Bim1 is able to suppress the catastrophe promoting activities of Bik1 and could be due to formation of a Bim1-Bik1 complex that disrupts Bik1-tubulin interactions. In agreement with this theory, Bik1 is known to bind both Bim1 and tubulin through the same domain. Overall, this study adds to our knowledge of plus-end tracking proteins, their interactions, and the individual method each protein uses to influence MT polymerization.

CHAPTER TWO

Characterization of interactions between the +TIPs, Stu2, Bim1 and Bik1

INTRODUCTION

Importantly, most +TIPs have the ability to physically associate with a number of other +TIPs, creating a complex web of interactions that are summarized in Figure 2.1. These interactions play important roles in integrating +TIP activities at the MT plus end. The regulation of MT dynamics by the +TIP network is likely to involve a combination of destabilizing and stabilizing factors where these proteins work cooperatively, independently, or antagonistically to regulate MT dynamics. Indeed, both antagonistic and cooperative relationships have been found between a variety of +TIPs (as described in Chapter 1, for review see (Holmfeldt *et al*., 2009; Howard and Hyman, 2007). +TIPs interactions are also important for localization to the plus-end, with a variety of +TIPs being dependent on EB1 proteins for their efficient plus-end accumulation (Figure 1.7)

The budding yeast +TIP Stu2 is a major promoter of MT dynamics in yeast. In order to identify Stu2 interactors that might regulate Stu2 activity or other +TIPs that regulate MTs dynamics, our laboratory performed a two-hybrid screen using Stu2 as bait (Chen, 1998). This screen identified Stu2 itself, and the +TIPs Bik1 and Bim1. Bim1 and Bik1 are also known to be important for MT function and dynamics, as described in Chapter One. Further two-hybrid testing revealed that Bik1 and Bim1 interact with each other and can also self-interact (Wolyniak *et al*., 2006). In addition to their

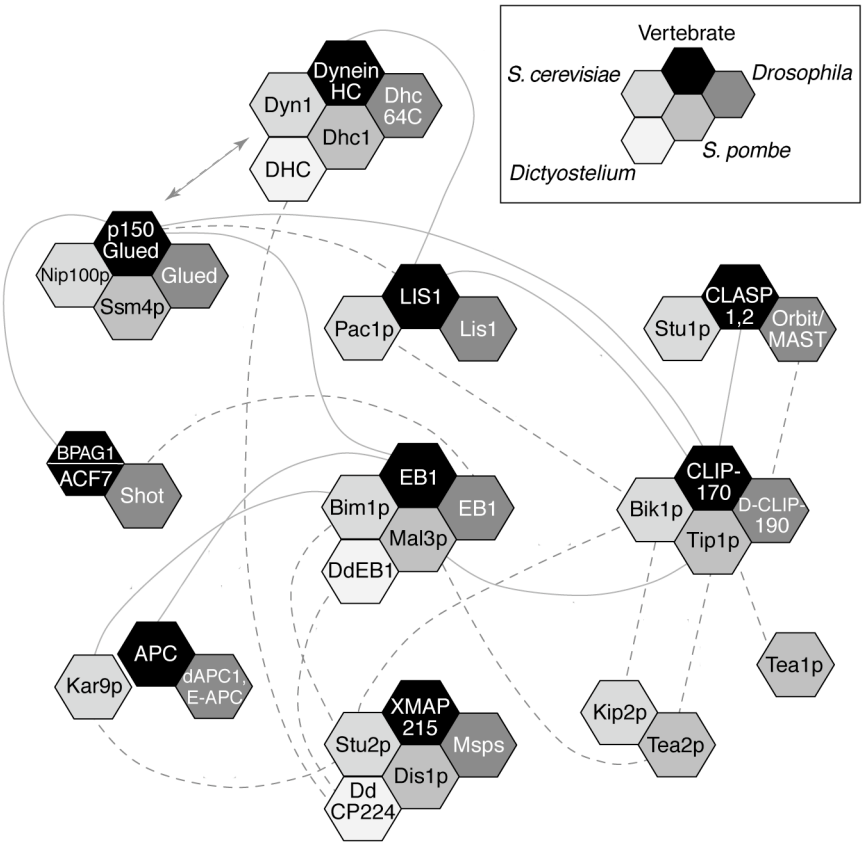

Figure 2.1 A Map of +TIP Interactions. The interactions between +TIP families from *S. cerevisiae, S. pombe*, *Dictyostelium, Drosophila*, and vertebrates are shown here. Straight lines indicate that these interactions have been shown directly while dashed lines indicate two-hybrid or coimmunoprecipitation. A double-headed arrow indicates the interactions between dynein and the dynactin complex. Figure is modified from Akhmanova and Hoogenraad 2005.

physical interactions, Stu2, Bik1 and Bim1 are also synthetically lethal in all pairwise combinations (Kosco *et al*., 2001). **T**he following study focuses on further characterizing the nature of the interactions between the budding yeast +TIPs Bim1, Bik1, and Stu2.

MATERIALS AND METHODS

Yeast Strains

The yeast strains used in this study are listed in Table 2.1. The PCR-based gene deletion and modification method was used for deletion and epitope-tagging of chromosomal yeast genes (Longtine *et al*., 1998). The *BIM1-3GFP* fusion was created at the endogenous *BIM1* locus. A portion of BIM1, encoding the C-terminal 178 amino acids, was cloned into PB1960 (Lin *et al*., 2001), containing three tandem copies of GFP, to create pKAB41. pKAB41 was then linearized within *BIM1* with PstI and transformed into yeast. Correct integrations were identified by PCR of genomic DNA and Western blotting.

Fluorescence Microscopy

All images were obtained with a 100x objective. Visualization of GFP- and CFP-conjugated proteins in live cells was done using a Zeiss Axioplan 2 Imaging microscope (Thornwood, NY) and Openlab software (Improvision, Lexington, MA). Time-lapse images of Stu2-3GFP and Bim1-3GFP were captured with a spinning disk confocal imaging system (UltraVIEW, Perkin-Elmer, Wellesley, MA).

Table 2.1 Yeast strains

Strain	Genotype
CUY25	*MAT*a *ade2 his3-Δ200 leu2-3,112 ura3-52*
CUY1247	*MAT*α *STU2-GFP::HIS3MX6 his3-Δ200 leu2-3,112 ura3-52*
CUY1316	*MAT*a P_{GAL1}*-HA-BIM::HIS3 his3-Δ200 leu2-3,112 lys2-801 ura3-52*
CUY1763	*MAT*a *ade2-101 his3-Δ200 leu2-3,112 ura3-52 (YCp BIK1-3HA LEU2)*
CUY1764	*MAT*a *ade2-101 his3-Δ200 leu2-3,112 ura3-52 (YCp BIK1-3HA LEU2; YCp BIK1-3Myc URA3)*
CUY1765	*MAT*α *STU2-GFP::HIS3MX6 his3-Δ200 leu2-3,112 ura3-52 (YCp STU2-3HA LEU2)*
CUY1766	*MAT*a P_{GAL1}*-HA-BIM::HIS3 his3-Δ200 leu2-3,112 lys2-801 ura3-52 (YCp BIM1-3Myc URA3)*
CUY1767	*MAT*α *BIM1-3GFP::TRP1 his3-Δ200 leu2-3,112 trp1-1 ura3-52*
CUY1768	*MAT*a *BIM1-3GFP::TRP1 URA3::CFP-TUB1::ura3-52 his3-Δ200 leu2 lys2-801 trp1*
CUY1804	pKAK162 (P_{ADH1}*-GAL4* $_{AD}$*-STU2*$^{657\text{-}888}$ *LEU2*) and pKAB6 (P_{ADH1}*-GAL4* $_{BD}$ *-BIM1*$^{145\text{-}345}$ P_{MET25}*-BIK1 TRP1*) in Y190
CUY1805	pKAK162 (P_{ADH1}*-GAL4* $_{AD}$ *-STU2*$^{657\text{-}888}$ *LEU2*) and pKAB3 (P_{ADH1}*-GAL4* $_{BD}$ *-BIM1*$^{145\text{-}345}$ P_{MET25}*-STU2 TRP1*) in Y190
CUY1807	pXC233 (P_{ADH1}*-GAL4* $_{AD}$ *-BIK1*$^{199\text{-}440}$ *LEU2*) and pKAB1 (P_{ADH1}*-GAL4* $_{BD}$ *-STU2*$^{657\text{-}888}$ P_{MET25}*-BIM1 TRP1*) in Y190
CUY1808	pXC233 (P_{ADH1}*-GAL4* $_{AD}$ *-BIK1*$^{199\text{-}440}$ *LEU2*) and pKAB4 (P_{ADH1}*-GAL4* $_{BD}$ *-STU2*$^{657\text{-}888}$ P_{MET25}*-BIK1 TRP1*) in Y190
CUY1810	pKAK100 (P_{ADH1}*-GAL4* $_{AD}$ *-BIK1 LEU2*) and pKAB3 (P_{ADH1}*-GAL4* $_{BD}$ *-BIM1*$^{145\text{-}345}$ P_{MET25}*-STU2 TRP1*) in Y190
CUY1811	pKAK100 (P_{ADH1}*-GAL4* $_{AD}$ *-BIK1 LEU2*) and pKAB6 (P_{ADH1}*-GAL4* $_{BD}$ *-BIM1*$^{145\text{-}345}$ P_{MET25}*-BIK1 TRP1*) in Y190
Y151	*MAT*a *PGAL1-lacZ gal4 gal80 his3-Δ200 leu2-3,112 ura3-52 ade2-101 trp1-94*
Y190	*MAT*a *URA3::PGAL1-lacZ LYS2::PGAL1-HIS3 gal4 gal80 his3 leu2-3,112 ura3-52 ade2-101 trp1-901 cyhr*

Two-Hybrid Assays

Two-hybrid assays were performed as described by Durfee *et al.,* (Durfee *et al*., 1993). Yeast strains Y190 and Y151 and the plasmids pAS2 (YEp: $_{PADH1}$*GAL4AD-HA LEU2*) and pACTII (YEp: $_{PADH1}$*GAL4BD-HA TRP1 CYH2*) were obtained from Steve Elledge (Harvard Medical School, Boston, MA). Deletions of *BIK1* and *BIM1* were created in the strain Y151. *GAL4AD* and *GAL4BD* fusions to full-length or truncated *BIK1*, *BIM1,* or *STU2* genes were made in pAS2 and pACTII, respectively. These were then cotransformed into Y190, Y151, or PJ69α. β-galactosidase activity was determined by the filter assay and scored for blue color by visual inspection. Interactions in the PJ69α background were only tested using the His and Ade reporters as the filter-lift assay for B-galactosidase does not work properly in this strain (James *et al*., 1996).

Three-Hybrid Assays

For the three-hybrid experiments, pBridge (Clontech, Palo Alto, CA) was used in conjunction with pACTII constructs. pBridge allows for the expression of a *GAL4BD* fusion from the *ADH1* promoter and another gene from *MET25* promoter. β-galactosidase activity was quantitated by a liquid assay (Clontech protocol PT3024-1). Cells were grown in SD medium lacking leucine and tryptophan and supplemented with the appropriate amount of methionine to an OD_{600} of 0.5– 0.9. Cells, 1.5 ml, were pelleted, washed with buffer 1 (100 mM HEPES, 154 mM sodium chloride, 4.5 mM l-aspartate, 1% BSA, 0.05% Tween 20), and concentrated by resuspending in 300 μL of buffer 1. Cells, 100 μL, were then frozen in liquid nitrogen and thawed at 37°C; this was repeated four times. Chlorophenol red-β-d-galactopyranoside (0.7 ml,

2.23 mM, CPRG; Roche Diagnostics, Indianapolis, IN) in buffer 1 was added to the cells. After development of red color, the reaction was stopped by adding 3 mM $ZnCl_2$. Cells were spun down, and the absorbance of the supernatant at 578 nm was read. β-galactosidase units equal $(1000 \times OD_{578})/(T \times V \times OD_{600})$, where T is elapsed time (in min) until development of red color and V is the volume of cells used (0.1 ml) times the concentration factor (5).

Immunoprecipitation Experiments

Immunoprecipitations were done as described previously (Chen *et al*., 1998). For strains in which *BIM1-HA* is expressed from *GAL1* promoter, cells were grown in galactose-containing medium for 4 h before preparing extracts. Stu2 antibody was described previously (Kosco *et al*., 2001). Bik1 antibody was made in rabbits using a Bik1 polypeptide containing amino acids 130-426. The rat monoclonal anti-yeast-tubulin antibody, YOL1/34 is from Accurate Chemical and Scientific (Westbury, NY). Mouse monoclonal antibodies HA11 and 9E10 that recognize the HA and myc epitopes, respectively, are from Berkeley Antibody Company (Berkeley, CA). HRP-conjugated goat anti-rabbit and HRP-conjugated goat anti-mouse were purchased from Bio-Rad Laboratories (Hercules, CA).

Protein Purification and In Vitro Binding Assays

BIM1 and *BIK1* were cloned into pET-GST-TEV (Moseley *et al*., 2004) and transformed into BL21 DE3 *Escherichia coli* cells (Stratagene, La Jolla, CA). The cells were induced with 1 mM IPTG for a hour at 25 ˚C. The GST fusion proteins were then purified on glutathione-Sepharose beads (Amersham Biosciences, Piscataway, NJ) in PBS. Soluble Bim1 was generated by treating

the GST-Bim1 beads with TEV protease (Invitrogen, Carlsbad, CA), which cleaved between GST and Bim1. Bim1 was then purified from the His-tagged TEV protease by passage over Talon Resin (BD Biosciences Clontech, Mountain View, CA). A fragment of *STU2* encoding the C-terminal 385 amino acids (Stu2-ΔC) was previously cloned as a 6x-His fusion in pWP86 (Kosco *et al*., 2001). pWP86 was transformed into BL21 DE3, induced with IPTG, purified onto Talon Resin (BD Biosciences Clontech), and eluted with imidazole. Binding assays were performed as described (Bauer *et al*., 1996). Rabbit polyclonal Bim1 antibody was a gift from Rita Miller (University of Rochester, Rochester, NY).

RESULTS

Bim1 tracks on the plus-ends of growing and shrinking MTs

Stu2, Bik1, and Bim1 are observed in the cytoplasm as one to several dots per cell often near the cell cortex (Lin *et al*., 2001; Kosco *et al*., 2001; Tirnauer *et al*., 1999). This localization suggests that these proteins reside at the plus ends of cytoplasmic microtubules. In the case of Stu2 and Bik1, this has been demonstrated directly in live cells double-labeled for microtubules and Stu2 or Bik1 (Wolyniak *et al*., 2006; Carvalho *et al*., 2004). To demonstrate the plus-end localization of Bim1 on cytoplasmic microtubules, I tagged Bim1 with three tandem copies of GFP and expressed them in cells along with CFP-Tub1 (α-tubulin). The Bim1 dots consistently colocalized with the distal ends of cytoplasmic microtubules at all stages of the cell cycle (Figure 2.2A). Time-lapse imaging of Bim1-3GFP demonstrated that Bim1 bound the plus ends of both growing and shrinking microtubules (Figure 2.2B). Similar results have been reported for Stu2 and Bik1 (Wolyniak *et al*., 2006; Carvalho *et al*., 2004).

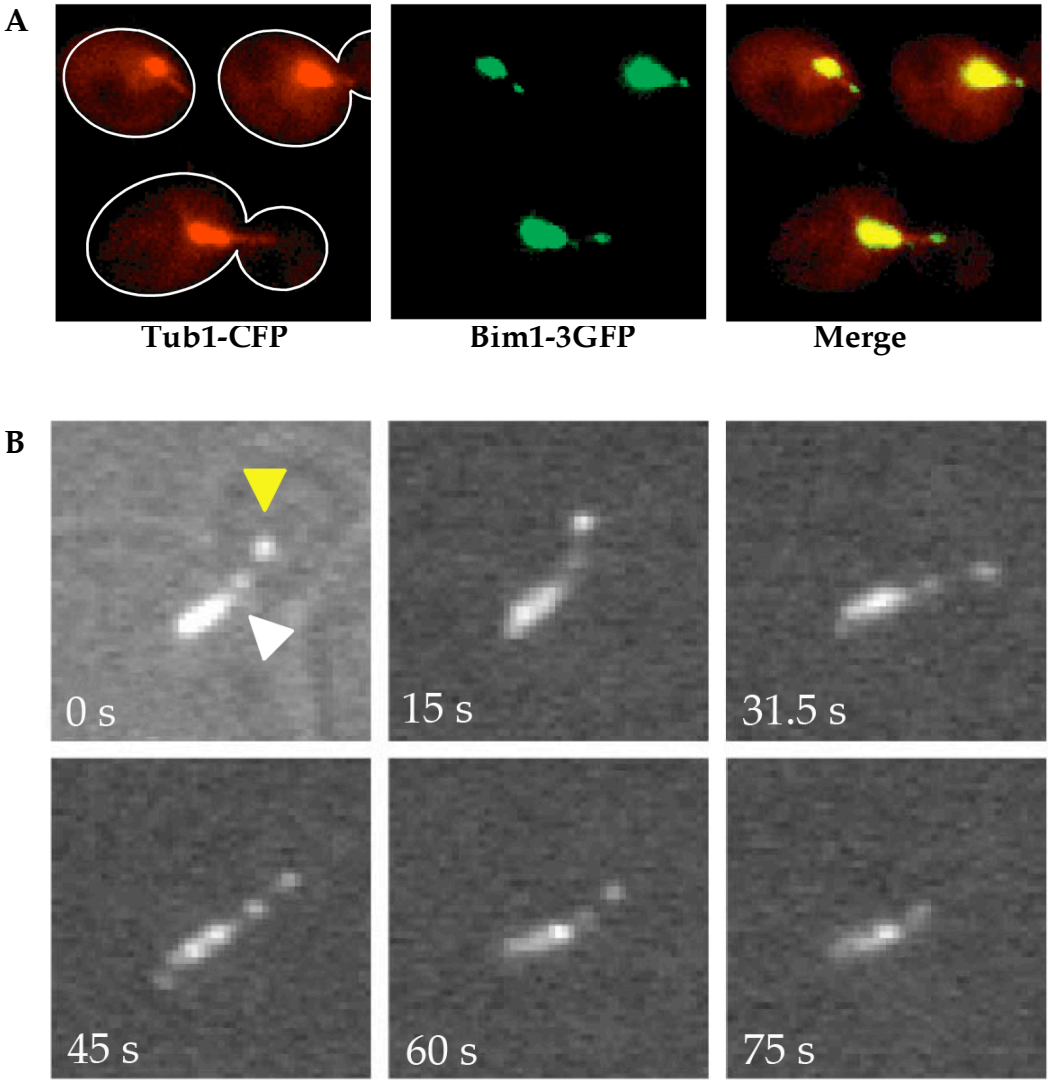

Figure 2.2 Bim1 tracks on the plus ends of growing and shrinking aMTs. A. Images of live cells expressing CFP-Tub1 and Bim1-3GFP (CUY1768). Bim1-3GFP is expressed from the endogenous *BIM1* promoter. B. Time-lapse images of Bim1-3GFP (CUY1767). Times indicated are in seconds. The cell shown has a preanaphase spindle with an aMT reaching into the bud. The yellow arrowhead indicates the position of a particular Bim1-3GFP dot tracking on growing, then shrinking aMT over time. The white arrowhead indicates the spindle pole body the aMT is nucleated from.

Stu2, Bik1, and Bim1 Interact in All Pairwise Combinations

Previously, our laboratory performed a two-hybrid screen using Stu2 as bait and identified Stu2, Bik1, and Bim1 (Chen *et al*., 1998). We also found that Bik1 and Bim1 interact in the two-hybrid assay (Wolyniak *et al*., 2006). To confirm the two-hybrid interactions, I performed coimmunoprecipitation assays. Antibodies specific for Stu2, Bik1, or Bim1-HA were used to immunoprecipitate these proteins from yeast cell extracts (Bim1-HA is expressed from the *GAL1* promoter). In each case, the other two proteins coimmunoprecipitated with the target protein (Figure 2.3A). The Stu2-Bim1 interaction appears to be less prominent based on the weaker Stu2 signal in the Bim1-HA precipitation and the weaker Bim1-HA signal in the Stu2 precipitation. In addition, the Stu2-Bim1 interaction was not detected in cells expressing Bim1 from its endogenous promoter, although the Bik1-Bim1 interaction was clearly observed in these cells. There was no detectable tubulin in any of the immunoprecipitates indicating that these interactions are not mediated by microtubule subunits. Thus, I can detect interactions of Stu2, Bik1, and Bim1 *in vivo* in all pairwise combinations.

Having established that Stu2, Bik1, and Bim1 interact *in vivo*, I next investigated whether these proteins could associate directly *in vitro*. Full length Bik1 and Bim1 were fused to GST, expressed in *E. coli*, and immobilized on glutathione-Sepharose resin. Purified, soluble full-length Bim1 and a C-terminal fragment of Stu2 (Stu2-C) that contains the Bik1- and Bim1-binding domain (see below) were tested for their association with these immobilized proteins (Figure 2.3B). GST-Bik1 bound to both Bim1 (lane 6) and Stu2 (lane 9), whereas GST alone was unable to associate with either Bim1 (lane 5) or Stu2 (lane 7). However, I could not demonstrate an association between GST-

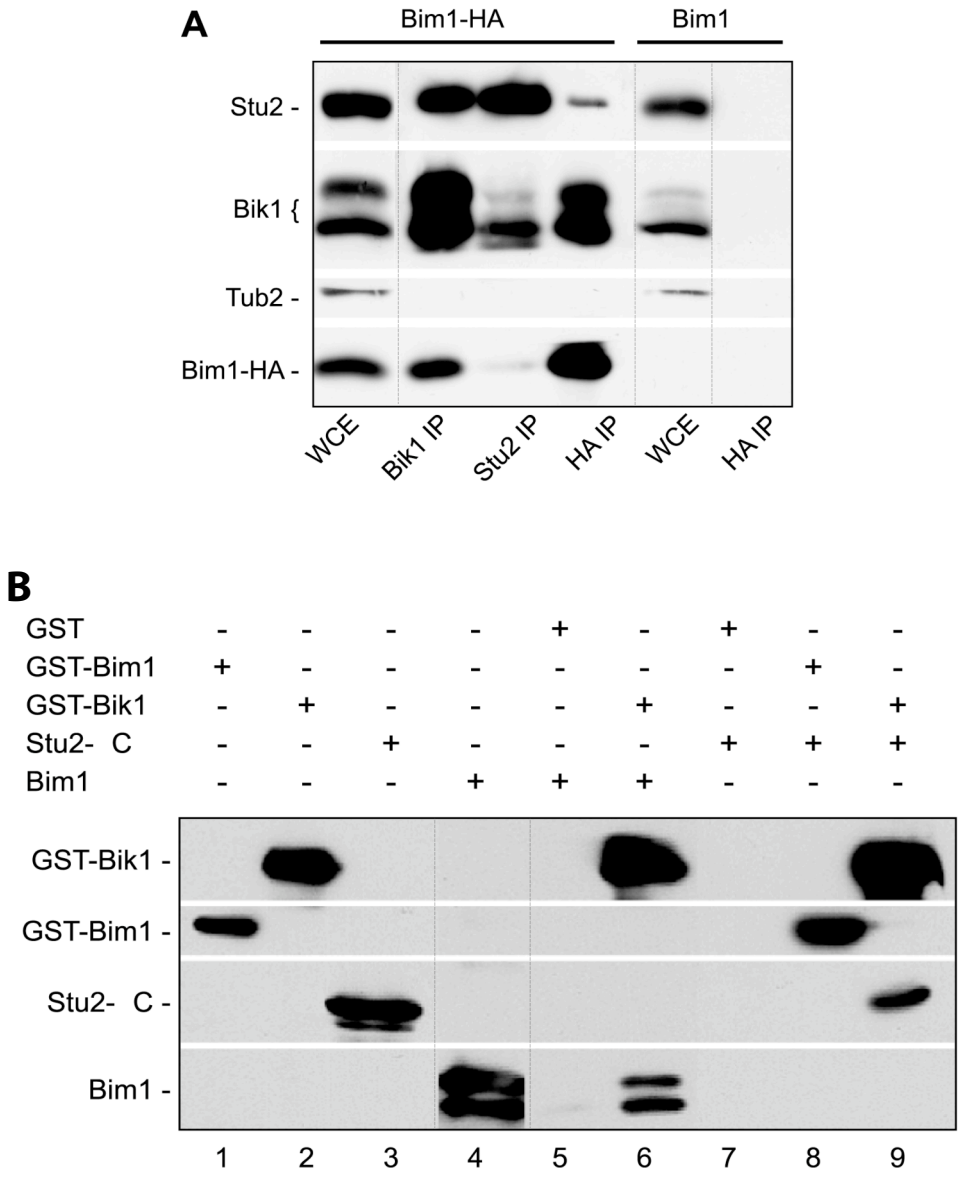

Figure 2.3. Stu2, Bim1 , and Bik1 interact in all pairwise combinations in vivo and in vitro. A. Stu2, Bik1, and Bim1 associate with each other in vivo. Protein extracts from a strain expressing Bim1-HA (CUY1316) or a control strain (CUY25) were immunoprecipitated with antibodies that recognize Stu2, Bik1, or HA (indicated as IP at bottom). Immunoprecipitates were subjected to SDS-PAGE followed by Western blotting with the antibodies indicated at left. WCE, whole cell extract. B. Binding assays in vitro. GST-Bik1, GST-Bim1, or GST alone were immobilized on beads and incubated with Stu2-C or Bim1 as indicated. Bound protein was detected by Western blotting after SDS-PAGE.

Bim1 and Stu2 (lane 8).

Stu2, Bik1, and Bim1 are not dependent upon each other for MT localization

As previously mentioned, several +TIP proteins do not localize to the MT plus-tip on their own, but rather require binding to another +TIP for localization, a process known as "hitchhiking" (Carvalho *et al*., 2003). Since Stu2, Bik1, and Bim1 all interact with each other, the possibility exists that these proteins are dependent on each other for plus-end localization. To address this question I created 3GFP fusions of each protein, and examined their aMT plus-end localization in the absence of one of the other proteins. Stu2-3GFP and Bim1-3GFP both localized to aMTs in a Bik1 deletion strain. Similarly, Stu2-3GFP and Bik1-3GFP both localized to aMTs in a Bim1 deletion strain. Since Stu2 is an essential gene, I used a conditional Stu2 depletion allele $stu2^{CU}$ (Kosco *et al*., 2001). Both Bim1-3GFP and Bik1-3GFP were able to localize to plus-ends in the absence of Stu2. Thus, the Stu2, Bik1, and Bim1 interactions are not required for plus-end localization.

Stu2, Bim1 and Bik1 self-associate

The identification of Stu2 itself in the two-hybrid screen using Stu2 as the bait, suggested that Stu2 self-associates. Similarly, our lab has found that both Bik1 and Bim1 self-associate in the two-hybrid assay (Wolyniak *et al*., 2006). I further investigated these self-interactions using coimmunoprecipitation. To assay the Stu2 self- interaction, I created a strain that expresses both Stu2-HA and Stu2-GFP. When anti-HA antibody was used to immunoprecipitate Stu2-HA, the Stu2-GFP was precipitated along with it (Figure 2.4). I assayed the Bik1 and Bim1 self-interactions by creating strains that express both Bik1-HA

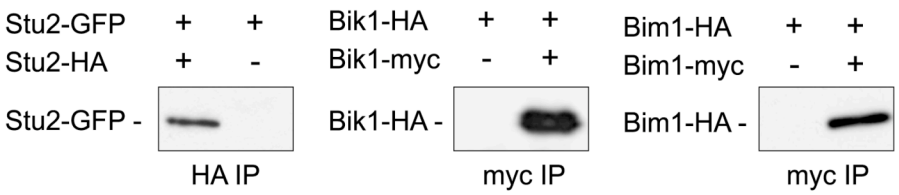

Figure 2.4 Stu2, Bik1, and Bim1 associate with themselves *in vivo*. Strains expressing two tagged forms of Stu2, Bik1, or Bim1 (CUY1765, CUY1764, or CUY1766) were precipitated using antibody to one tag and blotted with antibody to the other tag. Control strains are CUY1247, CUY1763, and CUY1316.

and Bik1-myc or Bim1-HA and Bim1-myc, respectively. In both cases, immunoprecipitations using anti-myc antibody pulled down the HA-tagged version of these proteins (Figure 2.4). These results demonstrate that Stu2, Bik1, and Bim1 self-associate *in vivo*. My results for Stu2 agree with the results of Van Brugel *et al.,* (2003) indicating that Stu2 self-interacts and exists as a homodimer in both yeast whole cell extract and as a purified protein *in vitro*. The self-interactions of Bim1 and Bik1 will be examined in further detail in Chapter Three.

Identification of Stu2, Bik1, and Bim1 Interaction Domains

To investigate the domains of Stu2 that are sufficient for self-interaction and Bim1 and Bik1 interaction, I created a series of N- and C-terminal truncations of Stu2 to be used in the two-hybrid assay (Figure 2.5). The region of Stu2 required to interact with itself is contained within a 190 amino acid segment (612-801) that also includes a portion of its microtubule-binding domain (amino acids 558-657) (Wang and Huffaker, 1997). The C-terminal 34 amino acids of Stu2 (amino acids 855-888) are sufficient for interaction with both Bim1 and Bik1. The fact that this domain of Stu2 does not overlap its microtubule- binding domain provides further evidence that these interactions are not mediated by microtubules.

In a similar manner, our lab has also determined that the N-terminal 189 amino acids of Bik1, which contain its microtubule- binding domain (Lin *et al.,* 2001), are sufficient for interaction with Bim1 (Wolniak *et al.,* 2006). The C-terminal 242 amino acids of Bik1 (amino acids 199-440), which contain its coiled-coil and metal-binding motif, are sufficient for an interaction with Stu2. A somewhat longer C-terminal fragment of Bik1 (amino acids 123- 440) is

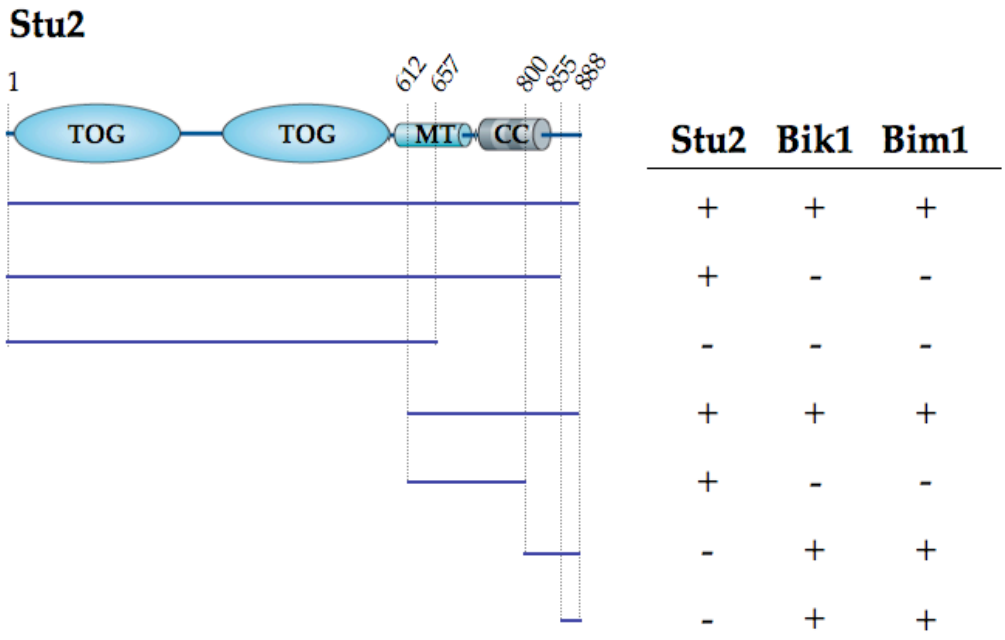

Figure 2.5 Mapping protein-protein interaction domains in Stu2. Two-hybrid interactions were tested between the fragments of Stu2 diagrammed in the drawings at the left, and full-length Stu2, Bik1, and Bim1. Interactions were determined using a colony filter β-galactosidase color assay and scored for blue color. (+), positive interaction; (-), negative interaction. Protein structural features are indicated: CC, predicted coiled-coil region; MT, microtubule-binding domain; TOG, Tumor overexpressed gene domain.

required for interaction with itself. Finally, the C-terminal 200 amino acids of Bim1 (amino acids 145-345) interact with Stu2, Bik1, and itself (Wolyniak *et al.*, 2006).

Stu2, Bik1, and Bim1 Compete for Binding to Each Other

Given that Stu2, Bik1, and Bim1 interact in all pairwise combinations, it seemed appropriate to investigate the nature of these interactions. There are three distinct possibilities: 1) The interactions could be independent. For example, if Stu2 binds Bik1 and Bim1 independently, the binding of Bik1 to Stu2 would not affect the binding of Bim1 to Stu2 and vice versa. 2) The interactions could be dependent. For example, Stu2 may interact directly only with Bik1 which in turn binds Bim1, thus bridging the interaction between Stu2 and Bim1. 3) The interactions could be competitive. For example, Bik1 and Bim1 may compete for binding to Stu2. The following work examines these possibilities and was done in collaboration with Karena Kosco, a former graduate student in our lab.

To determine whether the Stu2-Bik1, or Stu2-Bim1 interaction is bridged through Bim1 or Bik1, respectively, we performed two-hybrid assays in *bim1*Δ and *bik1*Δ strains. *STU2* is an essential gene so we were not able to test the Bik1-Bim1 interaction in a *stu2*Δ strain (Wang and Huffaker, 1997). We found that deletion of *BIK1* does not diminish the Stu2-Bim1 interaction, and deletion of *BIM1* does not diminish the Bik1-Stu2 interaction. Because Kar9 is known to interact with both Stu2 (Miller *et al.*, 2000) and Bim1 (Korinek *et al.*, 2000; Lee *et al.*, 2000), we also tested whether deletion of Kar9 affected the Stu2-Bim1, Stu2-Bik1, or Bik1-Bim1 interaction; it did not in any of these cases. Thus, we found no evidence for interdependence among the Stu2/Bik1/Bim1

interactions.

To test for competition in binding, we used a three-hybrid system. In this system, in addition to the expression of the bait and prey constructs, a third gene is placed under the control of the conditional *MET25* promoter and fused to a nuclear localization sequence. If overexpression of the third protein competes with the two-hybrid interaction, then an inhibitory effect should be observed on reporter gene expression. In these experiments, the overexpression of Bim1 and Bik1 in the absence of methionine was lethal, so a concentration of 5 or 7.5 μg/ml methionine was used, respectively. In the presence of 150 μg/ml methionine only low levels of Stu2, Bim1, or Bik1 are expressed, whereas in cells grown in 5 or 7.5 μg/ml methionine, the levels of Stu2, Bim1, or Bik1 are much greater (Figure 2.6A). Strikingly, overexpression of Bim1 reduced the Stu2-Bik1 interaction to 14% of that obtained with low levels of Bim1 (Figure 2.6B, Table 2.2). This is comparable to the reduction observed in control cells overexpressing Bik1. The Bik1$^{199-440}$ fragment expressed in these cells does not bind Bim1 (Wolyniak *et al*., 2006) so this result indicates that Bik1 and Bim1 compete for binding to Stu2. Similarly, overexpression of Bik1 reduced the Stu2-Bim1 interaction to 7%. In addition, overexpression of Stu2 reduced the Bim1-Bik1 interaction by about half, an effect similar to that observed in control cells overexpressing Bik1.

Mutational Analysis of Stu2

Based on the three-hybrid competition assays presented above, these proteins do not appear to be in a tertiary complex. This suggests that discrete Stu2-Bim1 or Stu2-Bik1 heterodimers may perform different functions in the cell to regulate MT dynamics. In order to try to determine the importance of

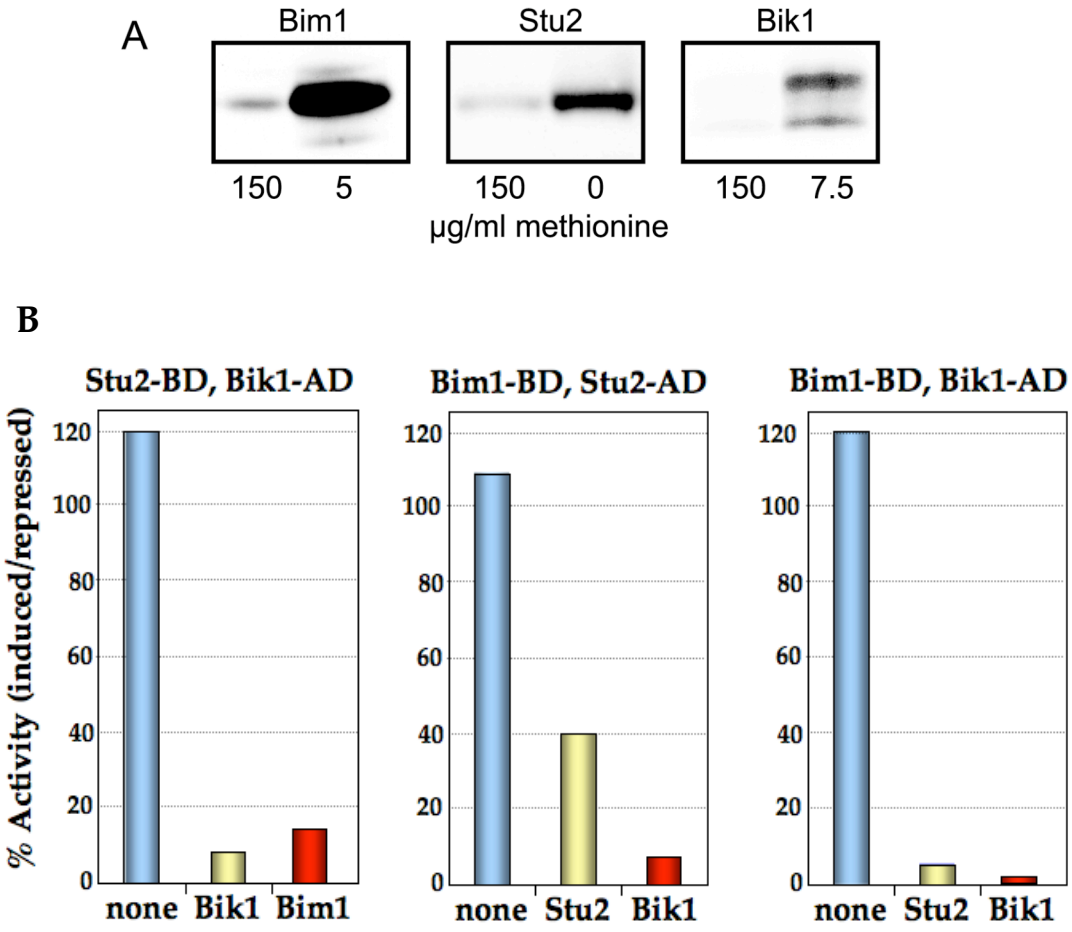

Figure 2.6. Stu2, Bik1, and Bim1 compete for binding to each other. Strains were grown on 150 µg/ml methionine to repress expression from *pMET25*, and 0 µg/ml methionine to induce expression of *pMET25-STU2*, 5 µg/ml methionine to induce expression of *pMET25-BIM1*, or 7.5 µg/ml methionine to induce expression of *pMET25-BIK1*. A. Yeast extracts were subjected to SDS-PAGE followed by Western blotting using anti-HA antibody to detect Bim1, Stu2, or Bik1 (each is fused to an NLS and the HA tag). B. Each strain contains a protein fused to the Gal4-binding domain (BD), a protein fused to the Gal4 activation domain (AD), and a protein that is overexpressed (OE) from the *MET25* promoter (except for controls indicated as none). The percent activity for each strain equals 100% activity in low methionine (induction)/activity in high methionine (repression) and was calculated from averages of three independent experiments.

Table 2.2 Three-Hybrid Assay β-galactosidase Activity

			β-galactosidase activity		
BD	AD	OE	high Met	low Met	% Activity
$Stu2^{657-888}$	$Bik1^{199-440}$	none	149.6 ± 9.2	179.8 ± 7.6	120
		Bik1	28.5 ± 2.0	2.3 ± 0.2	8
		Bim1	106.1 ± 7.3	14.9 ± 9.2	14
$Bim1^{145-344}$	$Stu2^{657-888}$	none	221.7 ± 17.7	240.0 ± 11.7	108
		Stu2	131.8 ± 6.6	53.3 ± 4.5	40
		Bik1	141.4 ± 6.1	10.6 ± 0.9	7
$Bim1^{145-344}$	$Bik1^{1-440}$	none	615.0 ± 18.3	705.0 ± 57.9	115
		Bik1	12.3 ± 0.6	4.8 ± 0.4	39
		Stu2	463.7 ± 30.4	212.7 ± 5.9	46

Levels shown for β-galactosidase activity are averages from three experiments. The percent activity for each strain equals 100% activity in low methionine (induction)/activity in high methionine (repression).

these interactions, we performed a mutagenesis of Stu2 to identify alleles of Stu2 that specifically fail to interact with either Bik1 or Bim1, but not both at the same time. The following work was done in collaboration with Gilda Shayan, an undergraduate in our lab. As stated earlier, the C-terminal 33 AAs of Stu2 are required for interaction with Bik1 and Bim1, while the region 612-800 AA containing the CC region is required for Stu2 self-interaction. The C-terminus of Stu2 is highly charged, indicating that charge-charge interactions are likely to be important in Stu2 protein interactions.

Therefore, we created 8 different mutant alleles in the C-terminus of Stu2 by PCR mutagenesis, changing charged residues to alanines (Figure 2.7). The yeast 2-hybrid system was used to screen the Stu2 alleles and identify those which specifically blocked interact with Bim1 or Bik1. The eight mutant alleles of Stu2 were cloned behind the Gal4 activation domain and tested against Gal4 binding domain fusions of Kar9, Spc72, Bim1, and Bik1. Kar9 has been shown to bind the C-terminus of Stu2 (612-888 AA) and is involved in spindle orientation. Spc72 is a SPB protein that, like Bim1 and Bik1, has been shown to interact with the last 33 AA of Stu2 (Usui *et al*., 2003). Stu2 itself, Kar9, and Spc72 served as specificity controls in this experiment; alleles that fail to interact with Bik1 or Bim1 should still interact with Stu2, Spc72, and Kar9. Importantly, this screen could then also identify alleles of Stu2 that specifically fail to interact with Stu2 itself, or Kar9 and Spc72.

The Gal4 AD and BD fusions were cotransformed into the yeast two-hybrid strain Y190 and screened for interaction. Two mutant alleles, Stu2-6 and Stu2-8, failed to interact with Bik1 but still interacted with Bim1 (Table 2.3). However, Stu2-6 and Stu2-8 also failed to interact with Stu2 and Kar9. All 8 mutant Stu2 alleles still interacted with Bim1 and Spc72. We retested

Figure 2.7 Creation of Stu2 Mutant Alleles. 8 mutant *stu2* alleles, each indicated by a different color, were created by changing the charged residues in each grouping to alanine.

these interactions by repeating the 2-hybrid assay in diploid (Y190/Y187) cells. Diploid cells gave identical interaction results to the Y190 haploid. In the course of these experiments we noticed that both the haploid and diploid yeast showed reduced growth (smaller colonies and slower growth in liquid culture) when harboring the Gal4 fusion plasmids. This is likely due to the overexpression of these fusion proteins from the high copy 2μm vectors, as the overexpression of Bim1, Stu2 and Bik1 has been shown to be lethal (Berlin *et al*., 1990; Tirnauer *et al*., 1999; Kosco, 2002). To try to compensate for this, I cloned these proteins into low copy *CEN* two-hybrid vectors. However, the majority of the previously categorized two-hybrid interactions disappeared using these vectors. This is likely due to the fact that these are weak interactions, (as can be seen by the Miller units obtained using the CPRG liquid assay, Table 2.2) possibly due to the dynamic and transient binding of these proteins in the cell.

Due to the strain viability concerns in the Y190 background as well as somewhat imprecise nature of two-hybrid interaction tests themselves, we decided to also test the Stu2 alleles in a different yeast two-hybrid strain background, PJ69α (James *et al*., 1996). We hoped the PJ69α background might better tolerate the overexpression of the proteins. After cotransformation, the PJ69α strain also showed reduced viability, although not to the extent of Y190. However, the interaction results obtained in this background were significantly different from those in Y190 (Table 2.4). In contrast to the above results, neither wildtype Stu2, nor one of the 8 mutant *stu2* alleles interacted with Bik1 or Spc72. Additionally, although they showed weak or no interaction with Kar9 in Y190, all 8 alleles interacted with Kar9 in PJ69α. In agreement with the Y190 results, Bim1 interacted with all 8 alleles

Table 2.3 Two Hybrid Interactions of Stu2 Alanine mutants in Y190

BD/AD	Stu2	Stu2-1	Stu2-2	Stu2-3	Stu2-4	Stu2-5	Stu2-6	Stu2-7	Stu2-8
Stu2	+	+	+	+	+	+	-	+/-	-
Bik1	+	+	+	+	+	+	-	+	-
$Bim1^{9-344}$	+	+	+	+	+	+	+	+	+
Kar9	+/-	+/-	+/-	+/-	+/-	+/-	-	-	-
Spc72	+	+	+	+	+	+	+	+	+
pACTII	-	-	-	-	-	-	-	-	-
Diploids of Y190/Y87 produced the same results as shown above									

Table 2.4 Two Hybrid Interactions of Stu2 Alanine mutants in PJ69α

BD/AD	Stu2	Stu2-1	Stu2-2	Stu2-3	Stu2-4	Stu2-5	Stu2-6	Stu2-7	Stu2-8
Stu2	+	+	+	+	+	+	-	+/-	+
Bik1	-	-	-	-	-	-	-	-	-
$Bim1^{9-344}$	+	+	+	+	+	+	+	+	+
Kar9	+	+	+	+	+	+	+	+	+
Spc72	-	-	-	-	-	-	-	-	-
pACTII	-	-	-	-	-	-	-	-	-
Diploids of Y190/PJ69α produced the same results as shown above									

and Stu2 still failed to interact with Stu2-6, however, the Stu2-8 interaction was positive in this test. To further examine these conflicting results, we made a diploid strain by mating the PJ69α and Y190 strains. The PJ69α/Y190 diploid gave the same results as the PJ69α haploid.

DISCUSSION

Similar to Stu2 and Bik1, Bim1 is a plus-end tracking protein

Bik1 and Stu2 have been shown to track along the plus ends of both growing and shrinking microtubules (Wolyniak *et al*., 2006; Carvalho and Pellman, 2004). Here I show that Bim1 also tracks along growing and shrinking microtubules. These abilities of Bik1 and Bim1 in yeast are distinct from those of their mammalian counterparts, CLIP-170 and EB1, that track along the ends of only growing microtubules (Perez *et al*., 1999; Mimori-Kiyosue *et al*., 2000). The ability to bind shrinking MTs may be important for controlling the shrinkage rate or influencing rescue frequency.

Mechanisms of plus-end tracking

I also found that these proteins are not interdependent upon each other for the majority of their aMT plus-end localization. This is in agreement with work on Bik1 that shows the majority of Bik1 plus-end accumulation is dependent upon transport by the kinesin Kip2 (Carvalho *et al*., 2004). Additionally, Stu2 and the Bim1 homologs, mal3 and EB1, have been shown to localize to MTs *in vitro* independently of other plus-tips (van Breugel *et al*., 2003; Dixit *et al*., 2009; Bieling *et al*., 2007). However, I did not examine if these interactions are important for kinetochore localization, as Stu2 and Bik1 are

both known to bind kinetochores (He *et al*., 2001). Additionally, since a small amount of Bik1 is seen on aMTs in the absence of Kip2, this localization may be dependent on Stu2 or Bim1.

Interactions between Stu2, Bim1, and Bik1

Like many +TIPs Stu2, Bik1, and Bim1 display a mutual affinity (Akhmanova and Hoogenraad, 2005; Akhmanova *et al*., 2005). Two-hybrid, coimmunoprecipitation, and *in vitro* binding assays indicate that Bik1 interacts directly with both Stu2 and Bim1. The evidence for a Stu2-Bim1 interaction is not as strong. Stu2 and Bim1 do interact in the two-hybrid assay and by coimmunoprecipitation when Bim1 is expressed from the *GAL1* promoter. However, Bim1 is overexpressed in both of these assays, and we do not observe coimmunoprecipitation of Stu2 and Bim1 when Bim1 is expressed at endogenous levels. These results indicate that Stu2 and Bim1 have the ability to interact but this interaction is limited in the cell. One possibility is that these proteins interact only at the plus-ends of cytoplasmic microtubules where a small fraction of the total Stu2 and Bim1 is located. In addition, we do not observe binding of Stu2 and Bim1 *in vitro*, which might suggest that Stu2 and Bim1 are linked by another protein in the cell. Bik1 and Kar9 are known to bind both Stu2 and Bim1, but neither of these is essential for the Stu2-Bim1 two-hybrid interaction. Alternatively, Stu2 and Bim1 may interact directly in the cell, but this interaction requires posttranslational modifications that do not occur in *E. coli*. Stu2 and Bim1 have been found to functionally interact only in G1 stage of the cell cycle (Wolyniak *et al.* 2006). This suggests that this interaction is regulated by the cell cycle, a process that could involve post-translational modifications of either protein.

Stu2, Bim1, and Bik1 interactions are not mediated by MTs

Stu2, Bik1, and Bim1 can associate with microtubules directly, but three lines of evidence indicate that their interactions do not require microtubule binding. 1) Tubulin does not coimmunoprecipitate with any of these proteins. 2) the *in vitro* binding studies, which confirm the Stu2-Bik1 and Bik1-Bim1 interactions, were done in the absence of tubulin. 3) The region of Stu2 that mediates the Bim1 and Bik1 interactions does not contain the microtubule-binding domain (Figure 2.5). The tubulin binding domain of Stu2 resides in the HEAT repeat domains (Al-Bassam *et al*., 2006) and the MT binding domain in the amino acids 558-657 (Wang and Huffaker, 1997). The regions of Bik1 and Bim1 that bind Stu2 also do not contain the MT binding domains for these proteins (Wolyniak *et al*., 2006). The MT binding region of Bik1 lies within the CAP-Gly domain (Lin *et al*., 2001), and that of Bim1 resides in the N-terminal CH domain defined in the EB1 homologue RP1 (Juwana *et al*., 1999). Thus, the only interaction region containing a microtubule-binding domain is $Bik1^{1-189}$, which interacts with Bim1 (Wolyniak *et al*., 2006).

Interactions between Stu2, Bim1, and Bik1 are dynamic

Although Stu2, Bik1, and Bim1 can interact in all pairwise combinations, our results argue against the notion that these proteins associate in a single heterotrimeric complex. First, three-hybrid experiments indicate that Stu2, Bik1, and Bim1 compete for binding to each other. Specifically, the C-terminal 34 amino acids of Stu2 are sufficient to bind both Bik1 and Bim1, but cannot bind both simultaneously. Second, deletion of *BIK1* or *BIM1* does not disrupt the Stu2-Bim1 or Stu2-Bik1 interaction, respectively, as might be expected for a multi-protein complex. These findings suggest that cells contain distinct Stu2-

Bik1, Stu2-Bim1, and Bik1-Bim1 complexes that may play unique roles in regulating microtubule function.

The interactions between many +TIPs are thought to be transient and the complex interplay of the +TIPs network is believed to be important in regulation of microtubule dynamics and organization (Morrison, 2007; Cassimeris, 1999). +TIP interactions may be influenced by changes in the cellular environment, which cue discrete proteins networks to reorganize the MT cytoskeleton. An example of this occurs when interphase cells transition to mitosis; MTs become more dynamic and the cytoskeleton undergoes a significant remodeling to form the mitotic spindle. A recent study by Niethammer *et al*., (2007) examined the interactions between multiple +TIPs and found their interactions to alter throughout the cell cycle to regulate MT dynamics.

Identification of Stu2 separation of function alleles

The screen for alleles of Stu2 which are specifically deficient in Bim1 or Bik1 binding did identify 2 alleles of possible interest, Stu2-6 and Stu2-8 which failed to interact with Bik1 but retained their interaction with Bim1. However, these alleles also failed to interact with Stu2 (Stu2-6 in both strains used and Stu2-8 in the Y190 background). The identification of Stu2-6 and Stu2-8 as interfering with the Stu2 self-interaction is somewhat surprising since the neither of these mutations is in the region required for Stu2 interaction. These alleles may be misfolded, however, this is unlikely as these mutants still interact with both Bim1 and Spc72. Rather, these results indicate that regions outside the minimal (612-801) Stu2-Stu2 interaction domain can influence this interaction. Additionally, no alleles were found that disrupted the Stu2-Bim1

interaction.

Repeating this screen using an alternate mutagenesis strategy, like random PCR mutagenesis, may yield more successful results. Stu2 may not be the best candidate for mutagenesis due the α-helical nature of the protein in this region. Alternatively, Bim1 and Bik1 could be mutagenized and screened for separation of interaction alleles.

This screen was complicated by the fact that the two-hybrid 2μm plasmids used caused reduced strain viability. Additionally, the two different two-hybrid strain backgrounds used gave conflicting results, the Stu2-Bik1 and Stu2-Spc72 interactions were completely lost in the PJ69α background. This may be due to the nature of the PJ69α strain, as it was designed to reduce false positives and may not detect weaker or transient protein-protein interactions. Since no alleles were found that specifically disrupted any Stu2 interactions this project was not pursued further. However, the Stu2-6 and Stu2-8 are interesting candidates and should be integrated into yeast to determine if they have any mutant phenotypes and to confirm their two-hybrid interactions by coimmunoprecipitation.

CHAPTER THREE

Regulation of Microtubule Dynamics by the Plus-end Tracking Proteins Bim1 and Bik1

INTRODUCTION

The results presented in the previous chapter indicate that the interactions between Stu2, Bim1, and Bik1 are transient and occur in pairwise combinations rather than a large +TIP complex at the MT plus end. In order to examine the functional significance of these interactions, our lab created double mutant combinations of these three proteins (Wolyniak *et al.*, 2006). This study found that Bim1 and Stu2 work cooperatively to regulate aMT dynamics in G1, but that this partnership dissolves once cells enter mitosis. Bik1 worked independently of both Stu2 and Bim1 to control aMT dynamics throughout the cell cycle. In mitosis, FRAP was used to assess kMT dynamics. Here, individual loss of Bim1 or Bik1 had little effect on kMT dynamics, but loss of both showed a reduction in dynamics indicating these proteins are redundant for promoting spindle dynamics. Stu2 was the primary promoter of kMT dynamics with a possible supportive interaction by Bik1 or Bim1. These results were somewhat surprising given the physical interactions between these proteins. One explanation for this may be redundancy, as loss of one +TIP interaction may simply be replaced by another +TIP or +TIP combination, which can perform the same role. This may be one reason why cells have such a variety of MT stabilizers and destabilizers. Such redundancy is seen in the case of motors, as the budding yeast has several molecular

motors that perform essential roles but no single motor is needed for survival (Hildebrandt and Hoyt, 2000).

Many questions remain about the individual activities of +TIPs and their interactions with each other in the regulation of MT dynamics. *In vivo* depletion/deletion analyses of +TIPs are powerful tools to assess the function of +TIPs, however, their interpretation is complicated for several reasons. First, as mentioned above, there may be redundancy between the depleted +TIP and other +TIPs still present in the cell, which may mask the activity of the protein in question. Second, any effects seen may be the result of the unchecked activities of the remaining +TIPs and not due to loss of the depleted protein. Finally, as +TIPs can be responsible for the recruitment of other proteins to the MT, any effects seen on dynamics may be due to loss of another "hitchhiking" protein and not the +TIP being investigated. Clearly, any model of the regulation of MT plus-end dynamics will require knowledge of the intrinsic biochemical activity of each +TIP. Therefore, to better understand how +TIPs individually and in combination work to regulate MT dynamics, I purified the budding yeast plus +TIPs, Bim1 and Bik1 to directly examine their effects on MT dynamics *in vitro* and the results are presented below.

MATERIALS AND METHODS

Reaction Buffers

The following reaction buffers were used: Buffer A (20 mM Tris, 500 mM KCl, 20 mM Immidazole, pH 8.5); Buffer B (20 mM Tris, 1 M KCl, 20 mM Immidazole pH 8.5); Buffer D (20 mM Tris, 200 mM KCl, 5 mM BME pH 8.0); SGF Buffer (25 mM Tris, 180 mM KCl, 1 mM $MgCl_2$, 1 mM EGTA, pH 7.5);

BRB80K (80 mM Pipes, 100 mM KCl, 1 mM $MgCl_2$, 1 mM EGTA, 5 mM BME pH 6.8); PBS (4.3 mM Na_2HPO_4, 1.47 mM KH_2PO_4, 137 mM NaCl, 2.7 mM KCl, pH 7.4); and PEM (100 mM Pipes, 1 mM EGTA, 1 mM $MgCl_2$, pH 6.8).

Bim1 and Bik1 protein purification

Bik1 and Bim1 were purified from insect cells using a baculovirus expression system. Recombinant baculovirus was made with pFastBacHT, where Bik1 or Bim1 were cloned downstream of a 6xHis tag and TEV protease cleavage sequence (Invitrogen, Carlsbad, CA). 200 mls SF9 insect cells (10^6 cells/ml) were infected with 2 ml of recombinant baculovirus (~10^8 pfu/ml) and harvested after ~65 hours. Cell were lysed by resuspension of cells (10 ml / 5 g cell pellet) in 50 mM Tris, 300 mM KCl, 5% glycerol, 10 mM immidazole, 1% NP40, pH 8.5 supplemented with EDTA-free complete protease inhibitor tablets (Roche, Switzerland) kept on ice for 20 min. The extracts were cleared by centrifugation for 20 min at 17,000 g (4˚C). Cleared extracts were incubated with NiNTA resin (250 μL bed volume) (Qiagen, Valencia, CA) for 1 hr at 4 ˚C. The resin was washed for 10 min at 4˚C with 15 ml of Buffer A, followed by Buffer B, Buffer A, and then Buffer D. The resin was then packed into a handmade column in Buffer D. The column was made by cutting the bulb top off of a 3.5 ml plastic transfer pipette (LPS, Rochester, NY), and placing a filter, which was removed from an empty spin column (BioRad, Hercules, CA) and cut to size, tightly into the bottom ridge of the pipette (Figure 3.1). A stop device was added to control the flow. The 6xHis fusion proteins were eluted with 1 ml Buffer D plus 150 mM immidazole and collected in 2-3 drop elutions. The elutions were checked by Bradford and SDS-PAGE followed by

Figure 3.1 Homemade column for small scale purification. Proteins were purified in batch form, and then placed in the column for the last wash and elution.

Coomassie staining to see which fractions contained the protein (usually the 2nd- 4th fractions) and elutions containing the majority of the protein pooled. The 6xHis tags were removed from the eluted proteins with AcTEV protease (Invitrogen) supplemented with EDTA-free complete protease inhibitors (Roche, Switzerland) for 3-5 hours at 16 ˚C. This was performed in SlidaLyzer dialysis cassettes (Pierce, Rockford, IL) against Buffer D to remove the immidazole. The cleaved mixture was again passed over NiNTA resin (100 μL bed volume) to remove AcTEV, the 6xHis tag, and any contaminants. Resin was separated from the cleaved Bim1 and Bik1 by passage over an empty spin column. The cleaved Bik1 and Bim1 were then dialyzed O/N at 4˚C using SlidaLyzer cassettes (Pierce, Rockford, IL) into SGF buffer or BRB80K. After dialysis, proteins were spun for 20 min at 20,000 g (4˚C) to remove aggregates. Protein concentrations were determined by Bradford (using a BSA standard) and visual comparison of purified proteins to a BSA standard on Coomassie stained gel. Proteins were snap frozen in liquid nitrogen and stored at -80˚C. Before use, proteins were precleared (Beckman Coulter TLA100.3, 55 krpm for 6 min at 4˚C).

Bim1-GFP and Bik1-GFP protein purification

Bik1-GFP or Bim1-GFP were cloned downstream of a GST tag and TEV protease cleavage sequence in pET-GST-TEV (Moseley *et al.*, 2004) and transformed into BL21 DE3 *Escherichia coli* cells (Stratagene, La Jolla, CA). 1 L of *E. coli* was grown to an OD of ~0.5 at 16 ˚C, and induced with 0.2 mM IPTG for 5 hours. Cells were harvested by centrifugation at 3500 rpm for 20 min at 4 ˚C in a Beckman Coulter J6B rotor. Cell pellets were washed with 200 ml PBS, centrifuged as above, then frozen at -80 ˚C. Pellets were resuspended in 20 ml

of PBS and complete protease inhibitor tablets (Roche) and incubated for ~45 min on ice with 1 mg/ml lysozyme (Sigma, St. Louis, MO). Cells were lysed by sonication using a Sonifier 350 (Kraus Lab), output setting 3, duty cycle 30% with 3-4 30 sec bursts, and 1 min cooling on ice in between. Lysis was confirmed by microscopy. Cell lysates were cleared by centrifugation at 17,000 g for 20 min at 4 ˚C, and the supernatant incubated with glutathione-sepharose beads (300 μL bed volume) (GE Healthcare, Piscataway, NJ) for 1 hr at 4˚C. Beads were washed 3x with PBS and 3x with BRB80K (15 ml, 10 min, 4˚C). Bim1-GFP and Bik1-GFP fusion proteins were cleaved from the glutathione resin using AcTEV protease (Invitrogen) in BRB80K (200-300 μL) supplemented with protease inhibitors (Roche) O/N at 4 ˚C. The resin was separated from the cleaved Bim1-GFP and Bik1-GFP by passage over an empty spin column (BioRad). Aggregate removal, protein concentration determination, protein storage, and preclearing were done as with insect cell purified proteins.

Tubulin

Porcine brain tubulin was purified as previously described (Vasquez *et al*., 1994) and used for VE-DIC assays. Lyophilized bovine brain tubulin and rhodamine-labled bovine brain tubulin were purchased from Cytoskeleton (Boulder, CO) and used for all other assays.

Yeast Extracts

250 mls of CUY28 (*MATalpha, his3Δ200, leu2-3,112, lys2-801, trp1-1, ura3-52*) were grown in yeast peptone dextrose (YPD) media (USbiological, Swampscott, MA) to log phase, washed with SGF buffer, and resuspended to

~500 μL with protease inhibitor tablets and PMSF (Alexis Biochemicals, Switzerland). Cells were rapidly frozen in liquid nitrogen and extracts made by grinding (Sorger *et al*., 1994). Extract yields were 10-15 mg/ml, as determined by Bradford assay using a BSA standard. Extracts were stored at -80˚C. Before use, yeast extracts were precleared (Beckman Coulter TLA100.3, 55 krpm for 6 at 4˚C).

Gel Filtration

Gel filtration was performed using a GE Healthcare Superose 6 10/300 GL column (Bretcher lab) and AKTA FPLC machine (Kraus Lab). The column was equilibrated and run in SGF buffer at a flow rate of 0.2 ml/min. Yeast whole cell extract (~3 mg) or equimolar amounts (5 μM in 500 μL) of precleared purified Bik1, Bim1, or tubulin were run over the column. For protein binding experiments, the proteins were incubated together for 10 min at 4 ˚C to allow complexes to form before loading. Elution was monitored by absorbance at 280 nm and 0.3 ml fractions collected and analyzed by SDS-PAGE and Coomassie staining or Western blotting for yeast whole cell extracts using an anti-Bim1 or anti-Bik1 antibody (Wolyniak *et al*., 2006). A secondary goat anti-rabbit HRP conjugated antibody was used (BioRad, Hercules, CA). The void volume of the column was determined using Blue Dextran (Sigma). To determine the Stokes radii of proteins and protein complexes, the column was calibrated using the following proteins (Sigma): Cytochrome C (1 nm), Carbonic Anhydrase (2.38 nm), BSA (3.55 nm), Alcohol Dehydrogenase (4.6 nm), Beta Amylase (4.8 nm), Apoferritin (6.1 nm), and Thyroglobulin (8.5 nm). Stokes radii were determined as averages of the Porath and Laurent-Kilander methods.

Sucrose Gradient Sedimentation

Sucrose gradients were performed as described in (van Breugel *et al.*, 2003) with slight modifications. Linear 5-20% sucrose gradients were made in SGF buffer using a Haakebuchler autodensity flow II C gradient pourer (Brown Lab). Yeast whole cell extract (90 μL of 5mg/ml) or equimolar amounts (12 μM in 90 μL) of precleared purified Bik1, Bim1, or tubulin were spun through the gradients in a TLS-55 rotor (Beckman Coulter) at 4 ˚C for 4 hours at 55 krpm. For protein binding experiments, the proteins were incubated together for 10 min at 4 ˚C to allow complexes to form before loading. After centrifugation, 19 equal fractions were taken from the top of each gradient, and analyzed as described for gel filtration fractions. To determine the S values for each protein and protein complex, each experiment contained a gradient loaded with standards (Sigma) of known S values: Cytochrome C (1.9S), Carbonic Anhydrase (2.89S), BSA (4.6S), Alcohol dehydrogenase (7.4S), Beta-Amylase (8.9S), and Catalase (11.3S).

MT cosedimentation assay

Taxol stabilized microtubules were made by incubating 2 μM taxol (Cytoskeleton) with tubulin in BRB80K plus 1 mM GTP (Sigma) at 37 ˚C for 15 min. Microtubules were separated from unpolymerized tubulin by centrifugation (Beckman Coulter TLA100.3, 25˚C for 30 min at 45 krpm). Microtubules were resuspended in BRB80K plus 2 μM taxol and 1 mM GTP. Increasing amounts of microtubules were incubated with 40 μM precleared Bim1 or Bik1 for 5-10 minutes at 25 ˚C. Bound protein was separated from unbound protein by centrifugation (Beckman Coulter TLA100.3, 25˚C for 30 min at 45 krpm). Supernatants were separated from pellets and equal

amounts analyzed by SDS-PAGE and Western blotting using DMY1, an anti-alpha tubulin antibody (Sigma) and anti-Bim1 or anti-Bik1 antibodies (Wolyniak *et al.*, 2006). Secondary goat anti-rabbit or goat anti-mouse HRP conjugated antibodies were used (BioRad, Hercules, CA). To determine the percent of bound protein, supernatant and pellet band intensities were quantified using Image J (NIH, Bethesda, MD).

Fluorescence imaging of localization to MTs

A 15 μM 1:20 mixture of rhodamine-labeled to unlabeled tubulin dimers was incubated with sea urchin axonemes fragments in BRB80K (37 ˚C for 15 min) to form microtubules. Microtubules were then incubated with precleared GFP (30 nM), GFP-Bim1 (10 nM), GFP-Bik1 (100 nM) or GFP-Bik1 (30 nM) plus Bim1 (10 nM) at 25˚C for 5 minutes. Mixtures were then fixed by incubation with 0.7% glutaraldehyde for 3 min, quenched with 0.1% sodium borohydride for 3 min, and diluted 1:50 before microscopy analysis. Images were acquired on a Axioplan 2 imaging microscope (Zeiss, Thornwood, NY) using Openlab software (Improvision, Lexington, MA). Rhodamine-labeled microtubules were imaged using a 100 msec exposure in the TRITC channel and GFP proteins using a 200 msec exposure in the GFP channel. Images were processed using Image J. The peak intensities of GFP, GFP-Bim1 or GFP-Bik1 along microtubules were determined using the line scan function of Image J. No signal was noted for GFP alone on microtubules. Microtubules were divided into 10 equal-length sections (van Breugel *et al.*, 2003) to determine the relative locations of the GFP-Bim1 or GFP-Bik1 dots along the microtubule. GFP-Bim1 or GFP-Bik1 dots were often seen at the ends of axonemes, including axonemes with no visible microtubules. These signals often

overlapped the ends of several microtubules and thus were not included in the analysis. A total of 114 microtubules were analyzed for GFP-Bim1 and 105 microtubules for GFP-Bik1 plus Bim1.

Microtubule assembly and VE-DIC

Microtubule dynamics assays were performed with microtubules nucleated from sea urchin axoneme fragments and visualized by video-enhanced differential interference contrast (VE-DIC) microscopy as previously described (Walker *et al*., 1988; Howell *et al*., 1999; Vasquez *et al*., 1997). Briefly, ~10 μl flow chambers were made using double-stick tape to mount coverslips on glass slides. Sea urchin axonemes fragments were then perfused into the chamber and allowed to adhere to the coverslip for 5 min as in Vasquez *et al*., 1994. Chambers were then perfused with 50 μl PEM plus 0.5% NP40 to remove unbound axonemes. To block nonspecific protein binding to the glass surfaces, 2 mg/ml casein was perfused into the chamber and incubated for 2 min then washed out with 50 μL PEM plus 0.5% NP40. Porcine brain tubulin samples with or without Bim1 and/or Bik1 in BRB80K and 1 mM GTP were then perfused into the chamber (Vasquez *et al*., 1994). Samples contained 8.6-14.4 μM tubulin and 0.1-1 μM Bim1 and/or Bik1. Each chamber was then warmed on the microscope stage to 35° C to initiate microtubule assembly. Video microscopy was done as previously described (Vasquez *et al*., 1997). Images were converted from super VHS to digital using iDVD (Apple, Cupertino, CA) and imported at a rate of 1 frame/sec as individual png files or Quicktime movies. Images were then imported into Image J for analysis.

MT Tracking and Analysis of Dynamics

Using the Image J measurement tool, the X-Y coordinates were determined for a microtubule at its fixed axoneme end (X^a, Y^a) and its growing end (X^b, Y^b) for each time point. The total microtubule length at each time point was then calculated to be C, where $C^2 = (X^a - X^b)^2 + (Y^a - Y^b)^2$. Microtubule lengths were then plotted over time to give a "life-history" plot of each microtubule. From these plots, growth and shrinkage rates were calculated from the slopes by a least squares regression analysis. To determine the average microtubule length for each sample, microtubule lengths were measured at 7-8 minutes. These lengths were multiplied by the average number of microtubules per axoneme to give the total microtubule length per axoneme. Variations around mean values are given as standard deviations. Comparisons of statistical significance were by a two-tailed unpaired *t* test allowing for unequal variance (Microsoft Excel).

Transition frequencies were calculated as described previously (Walker *et al*., 1988; Toso *et al*., 1993). Catastrophe (the switch from growth to shortening) frequencies were calculated by dividing the number of catastrophes observed by the sum of the total time spent in elongation. Rescue (the switch from shortening to growth) frequencies were calculated by dividing the number of rescues observed by the sum of the total time spent in shortening. Standard deviations for transition frequencies were determined from the catastrophe or rescue frequency divided by the square root of the number of transitions observed (Walker *et al*., 1988). This calculation assumes a Poisson distribution of growth or shortening times.

To examine the relationship between microtubule growth rate and catastrophe frequency, we binned individual microtubules according to their

growth rates into 0.2μm/min intervals and calculated the catastrophe frequency for each binned group. Then the average catastrophe frequency was plotted vs average growth rate for each binned group. This analysis was performed for three conditions: tubulin alone, tubulin plus Bim1, and tubulin plus Bik1. For tubulin alone, we binned microtubule growth rates from experiments using 8.6, 11.5, 13, and 14.4 μM tubulin. For tubulin plus Bim1, we binned microtubule growth rates from experiments using 11.5 μM tubulin with 0.1, 0.5, and 1 μM Bim1. For tubulin plus Bik1, we binned microtubule growth rates from experiments using 11.5 μM and 14.4 μM tubulin with 0.1, 0.5, and 1 μM Bik1.

RESULTS

Purified Bik1 and Bim1 form homodimers that associate to form a tetrameric complex

To investigate the biochemical activities of Bik1 and Bim1, I expressed 6His-tagged versions of Bik1 and Bim1 in SF9 cells using a baculovirus expression system and purified the proteins on Ni-NTA resin. Following removal of the 6His tag, both proteins migrated on SDS-PAGE at their expected MWs (38 kD for Bim1 and 51 kD for Bik1) and were >90% pure (Figure 3.2). I have previously shown that Bim1 and Bik1 self-associate *in vivo* (Chapter 2) and yeast 2-hybrid analysis indicates that, similar to their mammalian homologs, the coiled-coil regions of each protein mediate this self-interaction (Wolyniak *et al*., 2006). To determine the quaternary structure of the recombinant Bik1 and Bim1 proteins, I calculated the molecular weight

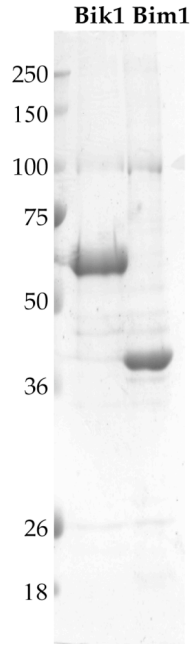

Figure 3.2 Purifcation of Bik1 and Bim1. Coomassie-stained SDS-PAGE gels of ~5 μg of Bik1 (left lane) and Bim1 (right lane) purified from insect cells.

of each protein from its Stokes radius and sedimentation coefficient (*S*) (Siegel and Monty, 1966). The Stokes radius was obtained by gel filtration using a Superose 6 column (Figure 3.3; Table 3.1) and the *S* value was obtained by centrifugation through a 5-20% sucrose gradient (Figure 3.4; Table 3.1). Purified Bim1 was calculated to have a molecular weight of 69.9 kD, which is close to the predicted molecular weight of 76.7 kD for a Bim1 homodimer. Purified Bik1 was calculated to have a molecular weight of 95 kD, close to the predicted molecular weight of 102.2 kD for a Bik1 homodimer. Thus, purified Bim1 and Bik1 appear to exist as homodimers in solution. The large Stokes radii determined for Bim1 and Bik1 indicate these proteins have elongated rod-like shapes. I determined the Perrin shape parameter for each protein (Bloom *et al*., 1988), and used the polynomial inversion procedure to calculate an axial ratio for each protein, assuming a prolate ellipsoid (Harding and Colfen, 1995). Bim1 was found to have an axial ratio of 13.4, while Bik1 had an axial ratio of 23.2. The large axial ratio for Bik1 is in agreement with the large axial ratio of 45 found for CLIP-170 (Pierre *et al*., 1992).

To compare the physical properties of recombinant Bim1 and Bik1 with the endogenous proteins, yeast extracts were run on the same gel filtration column and sucrose gradient, and the fractions analyzed by Western blotting (Figures 3.3 and 3.4). The calculated molecular weights of 98.8 kD for Bim1 and 117.7 kD for Bik1 from these analyses are consistent with these proteins forming homodimers *in vivo* (Table 3.1). Previous work found Bim1 in a ~250 kD complex in yeast extracts, although it may have existed as a homodimers within this larger complex (Lee *et al*., 2001). The discrepancy between this

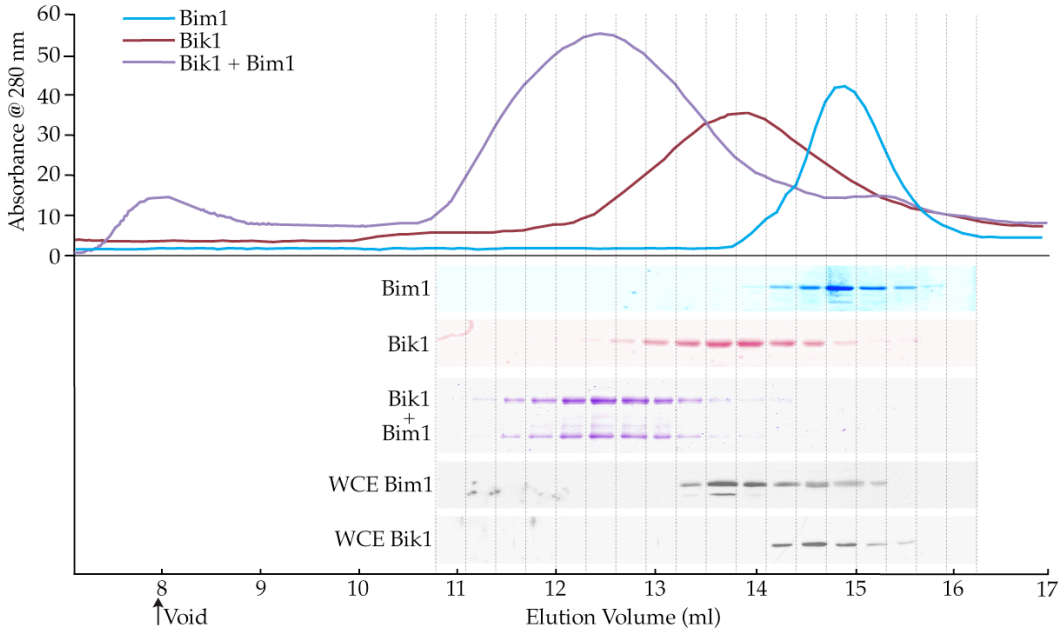

Figure 3.3 Size-exclusion chromatography of purified proteins and yeast whole cell extract (WCE). Chromatograms and Coomassie-stained SDS-PAGE gels are shown for eluted fractions of purified Bim1 (blue), Bik1 (red), or an equal-molar mixture of the two proteins (purple). SDS-PAGE and Western blotting was performed on yeast WCE fractions using an anti-Bim1 or anti-Bik1 antibody as indicated. An arrow indicates the column void volume.

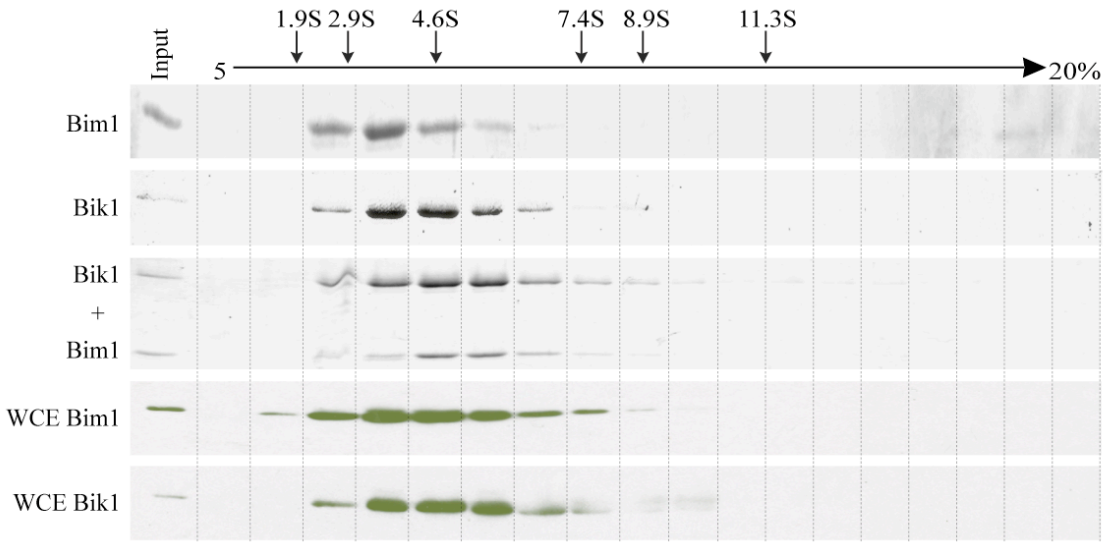

Figure 3.4 Sucrose gradient sedimentation of purified proteins and yeast WCE. Protein was loaded onto a 5-20% sucrose gradient and fractions collected after centrifugation. Fractions were analyzed by SDS-PAGE and Coomassie-staining for purified Bim1, Bik1, or an equimolar mixture of the two proteins. For yeast WCE, fractions were analyzed by SDS-PAGE and Western blotting, using a Bim1 or Bik1 antibody as indicated. Arrows indicate the positions of markers with known S values in the gradient.

Table 3.1. Physical properties of Bim1 and Bik1

Protein	Source	Stokes radius (nm)	S value	Calculated MW	Predicted MW
Bim1	pure	5.2	3.3	69.9	76.7 (dimer)
Bim1	WCE	5.6	4.2	98.8	
Bik1	pure	6.5	3.5	95.0	102.2 (dimer)
Bik1	WCE	6.5	4.3	117.7	
Bik1+Bim1	pure	8.2	5.0	168.3	178.9 (tetramer)
Tubulin	pure	4.1	5.5	96.4	110.7 (dimer)

WCE, whole cell yeast extract

result and our result is unclear and may be due to differences in the methods of extract preparation.

As Bim1 and Bik1 have been shown to interact *in vivo* and *in vitro* (Figure 2.3), I next determined the size of a Bim1-Bik1 complex. Bim1 and Bik1 were mixed in equal molar amounts and then analyzed by gel filtration and sucrose gradient sedimentation. In both conditions, the majority of Bim1 and Bik1 co-migrated as a larger complex than either Bim1 or Bik1 alone (Figures 3.3 and 3.4). The molecular weight of the complex was calculated to be 168.3 kD, close to the predicted MW of 178.9 kD for two molecules of both Bim1 and Bik1 (Table 3.1). Thus, Bim1 and Bik1 homodimers associate in solution to form a tetrameric complex.

Bim1 and Bik1 binding to tubulin subunits

I looked for the formation of Bim1-tubulin and Bik1-tubulin complexes by mixing tubulin dimers with equal molar amounts with Bim1 and Bik1, respectively. The mixtures were then analyzed by gel filtration. In the Bim1-tubulin mixture, each protein eluted at the same position as it did alone, indicating that Bim1 does not bind tubulin dimers (Figure 3.5A). In the Bik1-tubulin mixture, Bik1 eluted at the same position as it did alone (Figure 3.5B). About half of the tubulin elutes at the same volume as tubulin alone, however, a substantial fraction of the tubulin elutes earlier as a broad peak, which overlaps the Bik1 peak. It seems unlikely that this tubulin is forming a stable complex with Bik1, because the Bik1 peak does not shift and tubulin in the broad peak is not concentrated in the Bik1-containing fractions. Additionally,

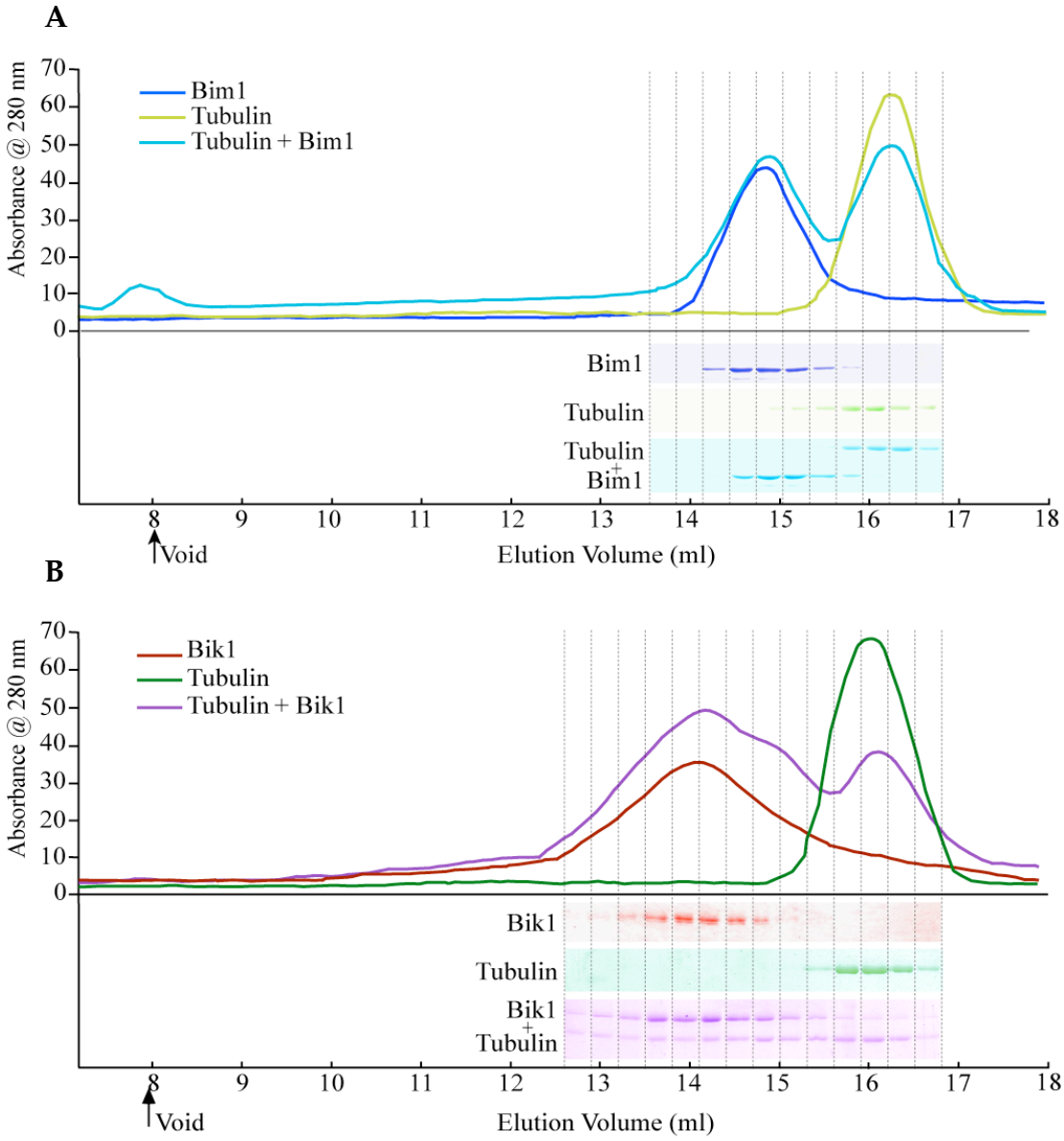

Figure 3.5 Bim1 and Bik1 do not bind tubulin heterodimers. Size-exclusion chromatography was used to assess binding of Bim1 and Bik1 to tubulin. Chromatogram and Coomassie-stained SDS-PAGE gels are shown for eluted fractions (0.3 mls) of (A) Bim1 (blue), tubulin heterodimers (green), or an equimolar mixture of the two proteins (turquoise) and (B) Bik1 (red), tubulin heterodimers (green), or an equimolar mixture of the two proteins (purple).

the calculated Stokes radius for Bik1 in the presence of tubulin is 6.3 nm, which is similar to the Stokes radius of 6.5 nm calculated for purified Bik1 alone (Table 3.1). An alternative explanation is that Bik1 stimulates the aggregation or oligomerization of tubulin subunits into larger molecular weight complexes. However, a Bik1-tubulin complex could simply be unstable during gel filtration, so I further analyzed the Bik1 tubulin mixture by sucrose gradient sedimentation to attempt to differentiate between these possibilities (Figure 3.6).

Sucrose sedimentation revealed no significant Bik1-tubulin binding, but I again saw tubulin oligomers form in the presence of Bik1 (Figure 3.6). Bik1 remains concentrated in the same fractions when mixed with tubulin as when individually run over the gradient. A sedimentation coefficient of 4.0 *S* was determined for Bik1 in the presence of tubulin, and combination with the calculated Stokes radius of 6.3 nm from gel fitration (Figure 3.5B) results in a molecular weight of 106.9 kDa for Bik1, indicating Bik1 remains as a homodimer in the presence of tubulin.

By gel filtration chromatography, tubulin eluted as a single peak, with a Stokes radius of 4.1 nm (Figure 3.5, Table 3.1). Sucrose gradient sedimentation of tubulin alone resulted in a sedimentation coefficient of 5.5 *S* for tubulin (Figure 3.6; Table 3.1). Combined with the Stokes radius from gel filtration, these values result in a calculated molecular weight of 96.4 kDa for a tubulin dimer, close to the expected weight of 110.7 kDa (Table 3.1).

Bim1 and Bik1 copelleting with MTs

I next measured the abilities of Bim1 or Bik1 to bind assembled microtubules using cosedimentation assays. In these assays Bim1 or Bik1 was

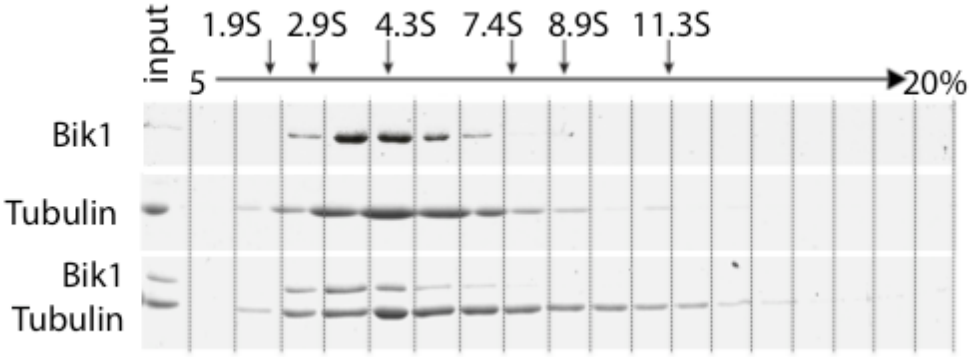

Figure 3.6 Sucrose gradient sedimentation of Bik1 and tubulin. Protein was loaded onto a 5-20% sucrose gradient and fractions collected after centrifugation. Fractions were analyzed by SDS-PAGE and Coomassie-staining for purified Bik1, tubulin, or an equimolar mixture of the two proteins. Arrows indicate the positions of markers with known S values in the gradient.

incubated with variable amounts of taxol-stabilized microtubules. Microtubule bound protein was separated from unbound protein by centrifugation and the supernatant and pellet analyzed by Western blotting. Bim1 bound to microtubules with an apparent dissociation constant, Kd, of 0.5 μM (Figure 3.7A), which is consistent with values found for other EB proteins (Manna *et al*., 2008; Tirnauer *et al*., 2002a; Berrueta *et al*., 1998). In contrast, only a small amount of Bik1, ~25%, copelleted with microtubules even at much higher tubulin concentrations (Figure 3.7B). This is in agreement with results for full-length CLIP-170, where only ~30% of the protein copelleted with MTs (Lansbergen *et al*., 2004).

Bim1 and Bik1 localization on MTs

In order to examine the localization of Bim1 and Bik1 along microtubules, I purified Bim1-GFP and Bik1-GFP. Each of these was incubated with microtubules that had been nucleated from axonemes and then visualized by fluorescence microscopy. Bim1-GFP appeared as dots along microtubules with an average of 2.9 dots per microtubule (n=114 MTs) (Figure 3.8A). 73% of these dots were located at the microtubule plus ends; the remainder was uniformly distributed along the lengths of the microtubules. In contrast, I only observed a faint Bik1-GFP staining along microtubules and axonemes (Figure 3.8B).

Since Bim1 and Bik1 interact (Figure 2.3), I examined the localization of Bik1-GFP in the presence of Bim1 to see if Bim1 could target Bik1-GFP to MTs. Indeed, when Bik1-GFP was mixed with unlabeled Bim1, Bik1-GFP dots wer

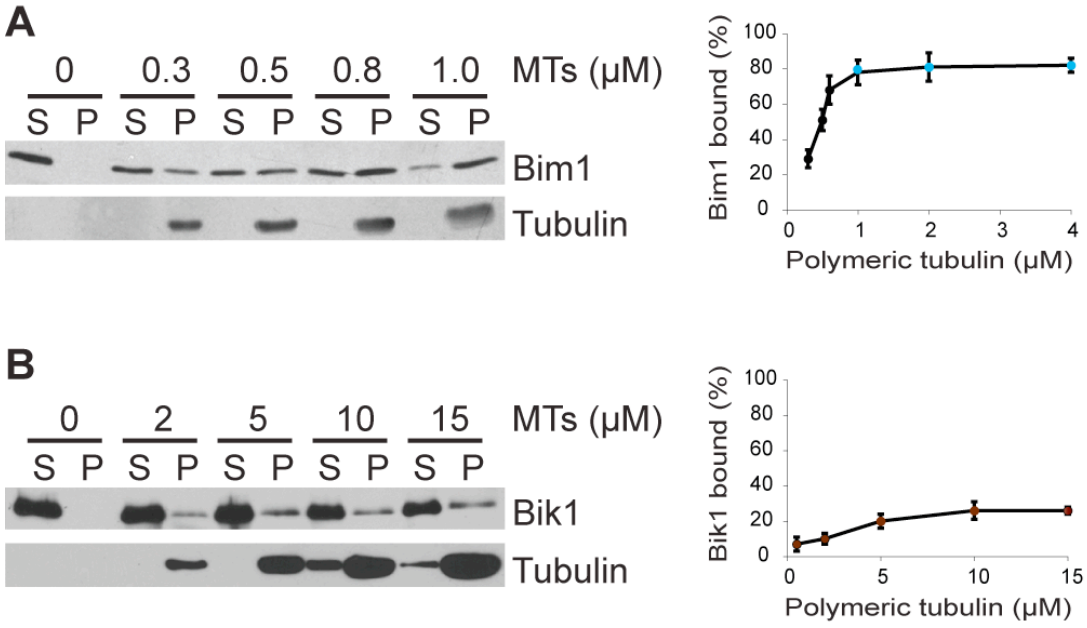

Figure 3.7 Bim1 and Bik1 cosediment with microtubules. A. 40 μM Bim1 was incubated with various concentrations of taxol stabilized microtubules. Microtubules were pelleted by centrifugation, and both the bound Bim1 (in pellets; P) and unbound Bim1 (in supernatants; S) were analyzed by SDS-PAGE and Western blotting using Bim1 and α-tubulin antibodies. Band intensities were quantified using Image J and the percentage of Bim1 bound was calculated. Error bars are +/- SD. B. Analysis of Bik1 binding to microtubules done as described in A, except that higher microtubule concentrations were used. Bik1 was visualized using Bik1 antibody.

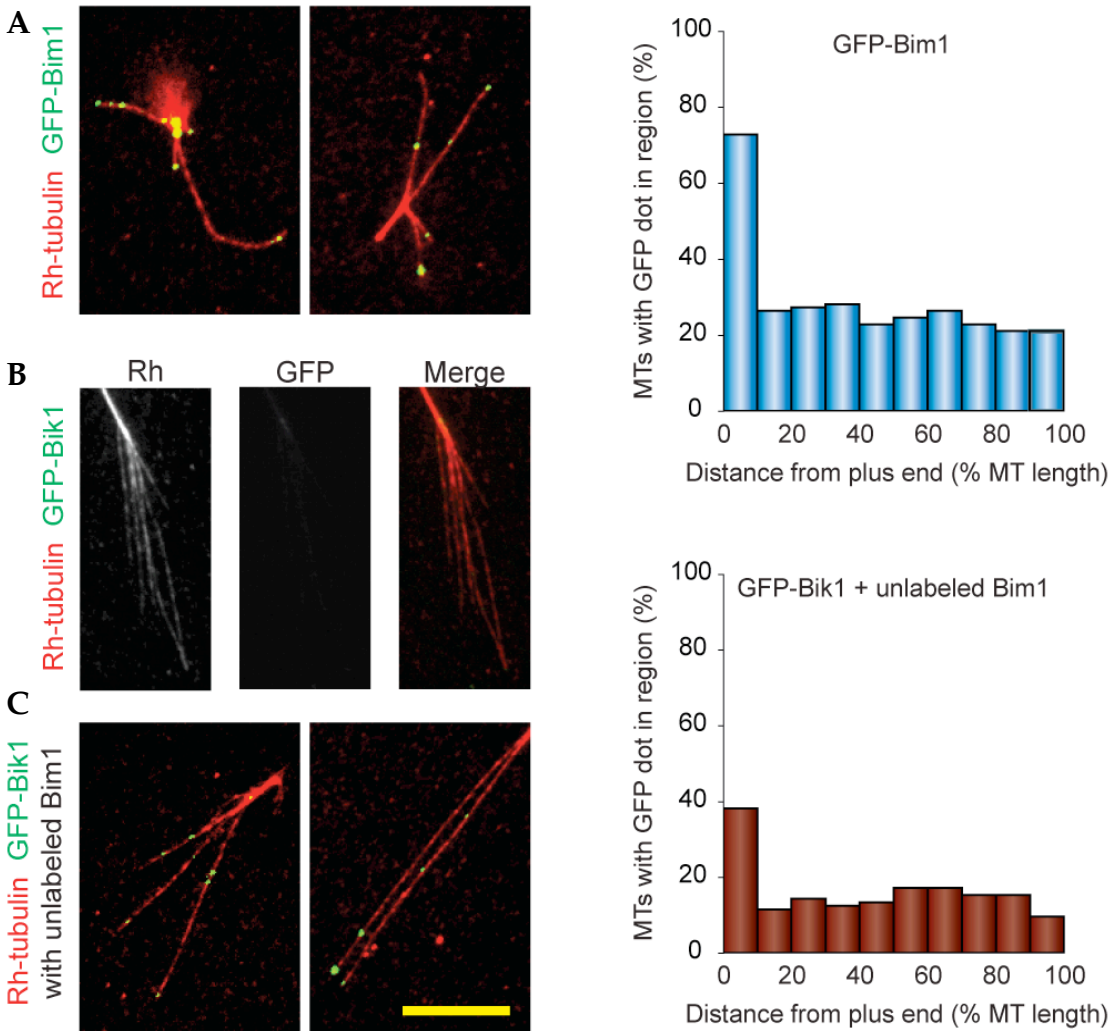

Figure 3.8 Plus-end localization of Bim1 and Bik1. A. Localization of Bim1 on microtubules. Bim1-GFP (10 nM) was incubated with MTs nucleated from sea urchin axonemes and assembled in the presence of rhodamine-labeled tubulin. MTs are shown in red and Bim1-GFP in green. Bim1-GFP is seen as discrete dots along MTs. Each MT was divided into 10 equal sections and scored for the presence of Bim1-GFP using the Image J line scan analysis. Graph shows that Bik1-GFP is enriched at MT plus ends (n=114 MTs). B. Localization of Bik1 on MTs. Bik1-GFP (100 nM) was incubated with MTs nucleated from sea urchin axonemes and assembled in the presence of rhodamine-labeled tubulin. Only a faint Bik1-GFP signal is seen along axonemes and MTs. C. Bik1-GFP was incubated with unlabeled Bim1 and then added to MTs. MTs are shown in red and Bim1-GFP in green. In the presence of Bim1, Bik1-GFP is seen as discrete dots along MTs. Graph shows that Bik1-GFP is moderately enriched at MT plus ends (n=103 MTs). Scale bar, 5 μM.

observed both along and at the MT plus tip (Figure 3.8C), similar to what I had seen with Bim1-3GFP (Figure 3.8A). The average number of Bik1-GFP dots per microtubule was 1.6 dots with 38% located at plus-end (n=103 MTs).

Assembly and Dynamics of MTs *In Vitro*

Next I examined the effects of purified Bim1 and Bik1 on MT assembly and dynamics *in vitro.* MTs were made with purified porcine brain tubulin nucleated from sea urchin axonemes and visualized using video-enhanced differential interference contrast microscopy (VE-DIC) (Walker *et al*., 1988; Vasquez *et al*., 1994). Axonemes contain parallel bundles of uniformly oriented microtubules, therefore microtubules extending from one end are plus-ended while microtubules extending from the other end are minus-ended (Figure 3.9A). Thus, it was possible to examine the assembly of plus-ended and minus-ended microtubules independently (see materials and methods).

I first examined the assembly of microtubules from axonemes using increasing concentrations of tubulin alone (8.6 μM, 11.5 μM, 13 μM and 14.4 μM tubulin). As the concentration of tubulin increased, I saw an increase in MT length and the number of microtubules nucleated from each axoneme for both plus and minus end microtubules (Figure 3.9A; Tables 3.2 and 3.3). These results were expected and agree with previous studies on microtubule assembly *in vitro* (Walker *et al.* 1988, Toso *et al.* 1993). To quantify this effect, I calculated the total microtubule length per axoneme (Figure 3.9B) by multiplying the average number of microtubules per axoneme end by the average microtubule length after 7-8 minutes of assembly.

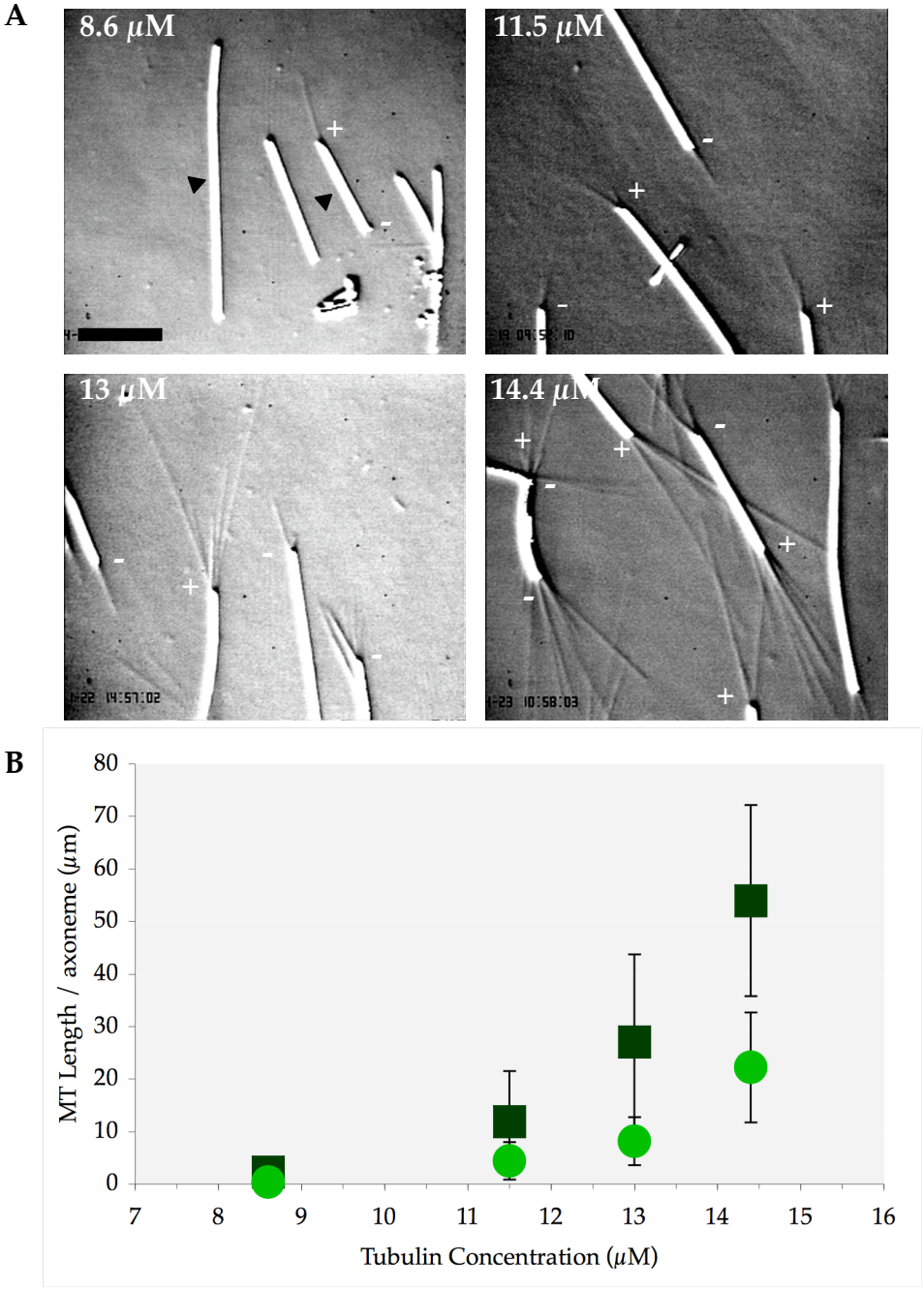

Figure 3.9 MT assembly at increasing tubulin concentrations. A. MTs were assembled from axonemes at 8.6 μM, 11.5 μM, 13 μM, and 14.4 μM tubulin and visualized using VE-DIC microscopy**.** Axonemes are the larger rod shaped structures indicated by the arrowheads in the upper left panel. Microtubules nucleated from the plus end or minus end of the axoneme are indicated by (+) and (-) symbols respectively. Scale bar, 5 μM. B. To quantify the effects of tubulin concentration on microtubule assembly, the total microtubule length per axoneme was calculated by multiplying the average length of microtubules by the average number of microtubules per axoneme.

Table 3.2. Plus-end microtubule dynamics

Plus Ends	Tubulin concentration			
	8.6 μM	11.5 μM	13.0 μM	14.4 μM
MT length / axoneme				
MT number	0.84 ± 0.57	2.18 ±1.38	3.32 ± 1.26	4.08 ± 1.26
MT length	2.85 ± 1.01 (6)	5.46 ± 2.74 (20)	8.16 ± 3.94 (18)	13.22 ± 1.81 (6)
Rates (μm / min)				
Growth	1.02 ± 0.31 (12)	1.87 ± 0.29 (59)	2.51 ± .35 (27)	3.07 ± .21 (22)
Shrinkage	42.24 ± 13.56 (4)	40.65 ± 11.18 (23)	46.63 ± 8.27 (4)	*
Frequencies (min^{-1})				
Catastrophe	0.68 ± 0.34 (5)	0.32 ± 0.06 (26)	0.13 ± 0.06 (4)	<0.03 (0)
Rescue	<4.35 (0)	<0.28 (0)	2.0 (1)	*
Total time (min)				
Growth	7.35	82.15	30.02	31.75
Shrinkage	0.23	3.53	0.5	0.00
Total MT number	16	89	47	49

Data are mean ± SD. Values in parentheses are the number of events.

* No catastrophe events were observed, so shrinkage rates and rescue frequencies could not be determined.

Table 3.3. Minus-end microtubule dynamics

mius Ends	Tubulin concentration			
	8.6 μM	11.5 μM	13.0 μM	14.4 μM
MT length/axoneme				
MT number	0.32 ± 0.23 (5)	1.79 ± 1.06	2.77 ± 1.12	3.27 ± 1.14
MT length	0.83 ± 0.48 (7)	2.46 ± 1.36 (24)	2.93 ± 1.16 (13)	6.79 ± 2.15 (8)
Rates (μm/min)				
Growth	0.45 ± 0.32 (5)	0.90 ± 0.21 (43)	1.23 ± 0.24 (24)	1.93 ± 0.12 (12)
Shrinkage	46.56 ± 13.34 (2)	49.83 ± 11.58 (12)	49.64 ± 19.62 (3)	*
Frequencies (min^{-1})				
Catastrophe	0.61 ± 0.43 (2)	0.27 ± 0.07 (14)	0.19 ± 0.1 (4)	<0.03 (0)
Rescue	<1.58 (0)	1.96 ± 1.39 (2)	<5.0 (0)	*
Total time (min)				
Growth	3.3	51.93	20.97	29.97
Shrinkage	0.63	1.17	0.2	0.00
Total MT number	7	68	38	36

Data are mean ± SD. Values in parentheses are the number of events.
* No catastrophe events were observed, so shrinkage rates and rescue frequencies could not be determined.

Microtubule dynamics are defined by four parameters: the rates of microtubule growth and shrinkage, and the frequencies of catastrophes (transitions from growing to shrinking) and rescues (transitions from shrinking to growing) (Figure 1.2). To determine how increasing the tubulin concentration affects these parameters, I observed microtubules assembled from 8.6 μM, 11.5 μM, 13 μM and 14.4 μM tubulin. over time using VE-DIC. I found that, on average, the rate of elongation at the plus end was about twice as fast the minus end (Figure 3.10A,Tables 3.2 and 3.3). As the concentration of tubulin increased, I saw an increase in both the microtubule growth rate (Figure 3.10A) and the frequency of rescues, with rescues being more frequent at minus ends (Tables 3.2 and 3.3). Conversely, as the concentrations of tubulin increased, there was decrease in the frequency of catastrophes (Figure 3.10C). Thus, higher tubulin concentrations stimulate MT growth rates and rescues while suppressing catastrophes and there is inverse relationship between catastrophe frequency and growth rate which will be examined in more detail below. The shrinkage rate, however, was independent of tubulin concentration (Figure 3.10B). These findings agree with the results of previous studies examining MT dynamics i*n vitro* (Walker *et al.,* 1988, Toso *et al*., 1993).

Bim1 promotes and Bik1 inhibits microtubule assembly *in vitro*

I next examined the effects of Bim1 and Bik1 on microtubules assembled *in vitro* (Figure 3.11, Tables 3.4-3.7). To do this, MTs were nucleated from sea urchin axonemes with 11.5 μM tubulin in the presence of 0.1 μM, 0.5 μM and 1.0 μM Bim1 or Bik1. The addition of Bim1 during MT formation at a

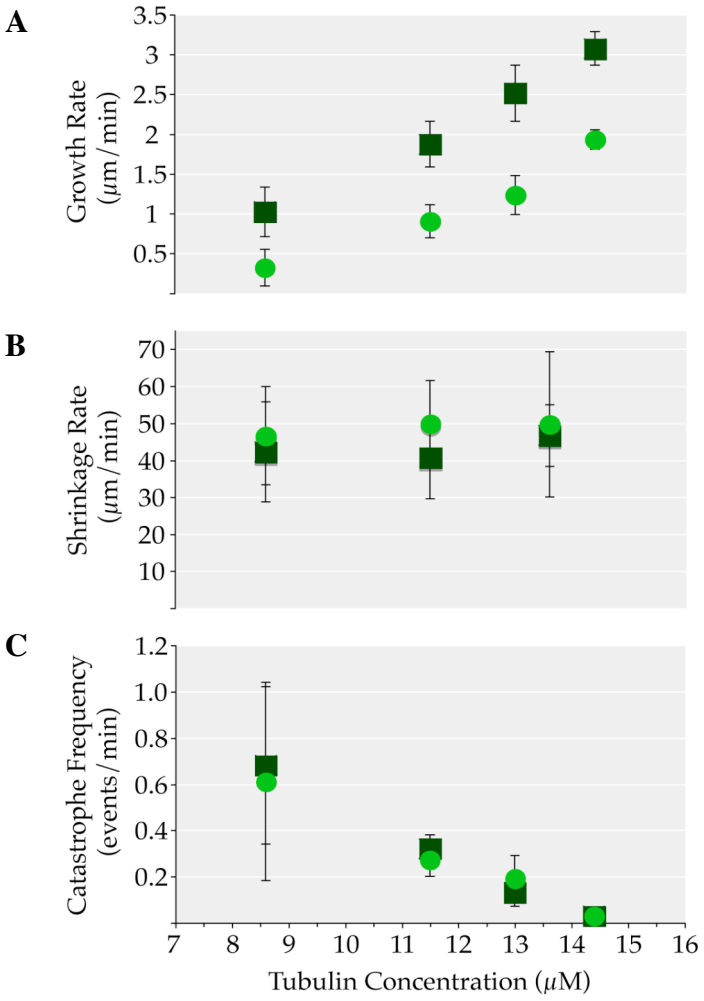

Figure 3.10 MT dynamics at increasing tubulin concentrations. A-C. MTs were assembled from axonemes at 8.6 μM, 11.5 μM, 13 μM, and 14.4 μM tubulin and visualized using VE-DIC microscopy. The length of individual microtubules were measured over time. From this data, I calculated microtubule growth (B) and shrinkage (C) rates, and catastrophe frequencies (D); rescues were rare. Plots show the effects of increasing concentrations of tubulin on these parameters. Error bars are +/- SD.

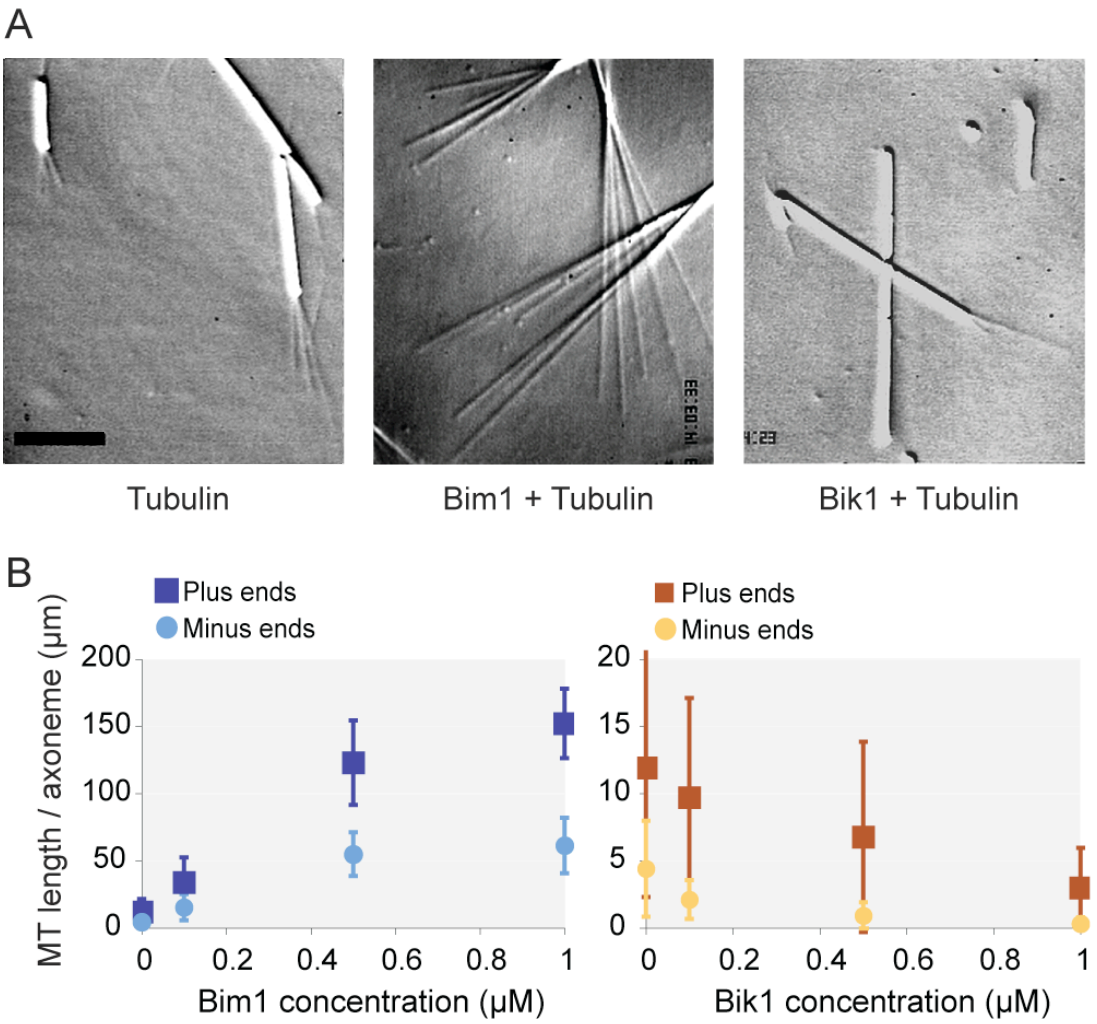

Figure 3.11. Bim1 promotes and Bik1 inhibits microtubule assembly in vitro. A. Sea urchin axonemes were incubated with 11.5 μM tubulin alone (left panel) and in the presence of 1 μM Bim1 (center panel) or 1 μM Bik1 (right panel). Microtubules were visualized using VE-DIC. Axonemes are the larger rod shaped structures indicated by the arrowheads in the left panel. Microtubules nucleated from the plus end or minus end of the axoneme are indicated by (+) and (-) symbols respectively. Scale bar, 5 μM. B. To quantify the effects of Bim1 (left panel) and Bik1 (right panel) on microtubule assembly, the total microtubule length per axoneme was calculated by multiplying the average length of microtubules by the average number of microtubules per axoneme.

Table 3.4. Effects of Bim1 on plus-end microtubule dynamics at 11.5 μM tubulin				
Plus Ends	Bim1 concentration			
	0 μM	0.1 μM	0.5 μM	1 μM
MT length/axoneme				
MT number	2.18 ±1.38	4.17 ± 1.54	8.09 ± 1.92	8.36 ± 1.08
MT length	5.46 ± 2.74 (20)	8.13 ± 3.27 (10)	15.19 ±1.46 (8)	18.19 ± 2.0 (10)
Rates (μm/min)				
Growth	1.87 ± 0.29 (59)	1.98 ± 0.25 (68)	2.56 ± 0.24 (27)	2.93 ± 0.24 (45)
Shrinkage	40.65 ± 11.18 (23)	18.65 ± 5.81 (24)	*	*
Frequencies (min^{-1})				
Catastrophe	0.32 ± 0.06 (26)	0.13 ±0.03 (24)	<0.013 (0)	<0.007 (0)
Rescue	<0.28 (0)	0.51 ± 0.25 (4)	*	*
Total time (min)				
Growth	82.15	180.98	74.47	143.80
Shrinkage	3.53	7.9	0.00	0.00
Total MT number	89	85	97	144

Data are mean ± SD. Values in parentheses are the number of events.
* No catastrophe events were observed, so shrinkage rates and rescue frequencies could not be determined.

Table 3.5. Effects of Bim1 on minus-end microtubule dynamics at 11.5 μM tubulin				
Minus Ends	Bim1 concentration			
	0 μM	0.1 μM	0.5 μM	1 μM
MT length/axoneme				
MT number	1.79 ± 1.06	3.43 ± 2.08	7.4 ± 1.4	6.36 ± 1.57
MT length	2.46 ± 1.36 (24)	4.46 ± 0.98 (10)	7.4 ± 1.7 (5)	9.64 ± 2.2 (12)
Rates (μm/min)				
Growth	0.90 ± 0.21 (43)	0.99 ± 0.21 (57)	1.51 ± 0.22 (24)	1.61 ± 0.19 (32)
Shrinkage	49.83 ± 11.58 (12)	15.55 ± 6.16 (11)	*	*
Frequencies (min^{-1})				
Catastrophe	0.27 ± 0.07 (14)	0.057 ±0.017 (11)	<0.013 (0)	<0.007 (0)
Rescue	1.96 ± 1.39 (2)	3.33 ± 1.36 (6)	*	*
Total time (min)				
Growth	51.93	193.10	74.18	140.35
Shrinkage	1.17	1.8	0.00	0.00
Total MT number	68	81	75	83
Data are mean ± SD. Values in parentheses are the number of events. * No catastrophe events were observed, so shrinkage rates and rescue frequencies could not be determined.				

Table 3.6. Effects of Bik1 on plus-end microtubule dynamics at 11.5 μM tubulin				
Plus Ends	Bik1 concentration			
	0 μM	0.1 μM	0.5 μM	1 μM
MT length/axoneme				
MT number	2.18 ±1.38	2.19 ± 0.85	1.84 ± 1.34	1.0 ± 0.88
MT length	5.46 ± 2.74 (20)	5.01 ± 1.61 (10)	3.68 ± 2.76 (11)	2.98 ± 1.42 (11)
Rates (μm/min)				
Growth	1.87 ± 0.29 (59)	1.78 ± 0.25 (41)	1.69 ± .25 (39)	1.54 ± .25 (30)
Shrinkage	40.65 ± 11.18 (23)	47.72 ± 12.25 (20)	33.65 ± 8.66 (17)	34.63 ± 12.21 (18)
Frequencies (min^{-1})				
Catastrophe	0.32 ± 0.06 (26)	0.36 ± 0.08 (20)	0.38 ± 0.09 (19)	0.44 ± 0.1 (18)
Rescue	<0.28 (0)	<0.43 (0)	<0.41 (0)	0.43 (1)
Total time (min)				
Growth	82.15	55.68	49.40	40.88
Shrinkage	3.53	2.3	2.43	2.35
Total MT number	89	46	41	36
Data are mean ± SD. Values in parentheses are the number of events.				

Table 3.7. Effects of Bik1 on minus-end microtubule dynamics at 11.5 μM tubulin				
Minus Ends	Bik1 concentration			
	0 μM	0.1 μM	0.5 μM	1 μM
MT length/axoneme				
MT number	1.79 ± 1.06	1.71 ± 0.8	0.82 ± 0.78	0.42 ± 0.64
MT length	2.46 ± 1.36 (24)	1.23± 0.61 (6)	1.12 ± 0.51 (5)	0.74 ± 0.15 (5)
Rates (μm/min)				
Growth	0.90 ± 0.21 (43)	0.84 ± 0.23 (20)	0.72 ± 0.15 (8)	0.51 ± 0.15 (7)
Shrinkage	49.83 ± 11.58 (12)	43.26 ± 9.02 (7)	35.51 ± 9.99 (4)	36.74 ± 8.62 (5)
Frequencies (min^{-1})				
Catastrophe	0.27 ± 0.07 (14)	0.32 ± 0.12 (7)	0.51 ± 0.25 (4)	0.69 ± 0.31 (5)
Rescue	1.96 ± 1.39 (2)	<1.92 (0)	<4 (0)	< 4.5 (0)
Total time (min)				
Growth	51.93	21.9	7.87	7.22
Shrinkage	1.17	0.52	0.25	0.22
Total MT number	68	24	14	10
Data are mean ± SD. Values in parentheses are the number of events.				

concentration of 11.5 μM tubulin increased MT assembly and this was again quantified by calculating the total microtubule length per axoneme end (Figure 3.11B, Tables 3.4 and 3.5). Axonemes in 11.5 μm tubulin alone contained 11.9 ± 9.6 μm of total microtubule length at their plus ends and 4.4 ± 3.6 μm of total microtubule length at their minus ends (Figure 3.9B and 3.11). Addition of 0.1 μM Bim1 increased total microtubule length 2.8-fold at plus ends and 3.5-fold at minus ends; addition of 1 μM Bim1 increased total microtubule length by 12.8-fold at plus ends and 13.9-fold minus ends. Thus, Bim1 promotes microtubule assembly. In contrast to Bim1, Bik1 decreased the length and number of both plus-ended and minus-ended microtubules (Figure 3.11B). Addition of 0.1 μM Bik1 decreased total microtubule length by 28% at plus ends and 52% at minus ends; addition of 1 μM Bik1 decreased total microtubule length by 4.0-fold at plus ends and 14.2-fold at minus ends (Figure 3.8B, Tables 3.6 and 3.7). Thus, Bik1 inhibits microtubule assembly.

Individual effects of Bim1 and Bik1 on MT dynamics

I next examined the effects of Bim1 and Bik1 on microtubule dynamics. The most substantial effect of Bim1 is on catastrophe frequency. The addition of 0.1 μM Bim1 decreased the frequency of catastrophes 2.5-fold at plus ends and 5.6-fold at minus ends (Figure 3.12A). I did not observe any catastrophes at higher Bim1 concentrations, indicating that catastrophe frequencies were reduced at both plus and minus ends >20-fold in the presence of 0.5 μM Bim1 and >40-fold in the presence of 1 μM Bim1 (Tables 3.4 and 3.5). Under the assembly conditions used, rescues are rare events, and no rescue events (<0.28

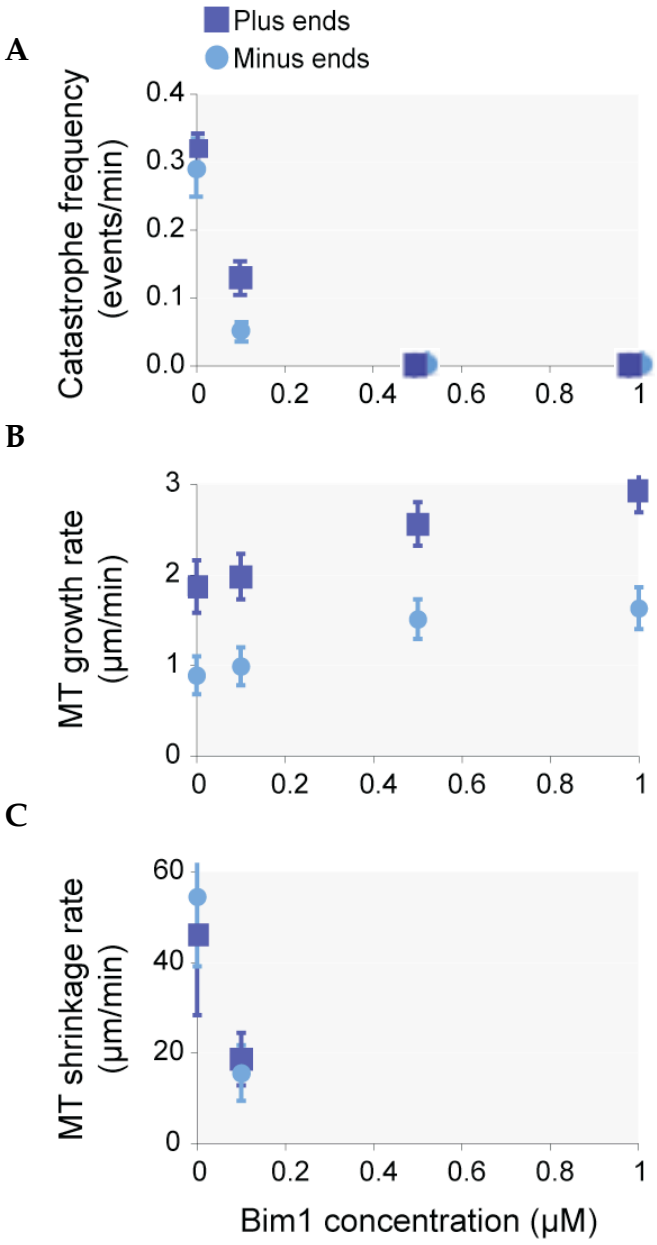

Figure 3.12 Effects of Bim1 on microtubule dynamics. A-C. Sea urchin axonemes were incubated with 11.5 μM tubulin in the presence of varying concentrations of Bim1. Individual microtubules were visualized using VE-DIC and their lengths measured over time. From this data, I calculated microtubule growth and shrinkage rates, and catastrophe frequencies; rescues were rare. Plots show the effects of increasing concentrations of Bim1 on these parameters. Error bars are +/- SD.

events/min) were observed at plus ends and only 2 rescue events (1.96 events/min) were seen at minus ends with 11.5 μM tubulin alone (Tables 3.2 and 3.3). I did observe a higher frequency of rescues in 0.1 μm Bim1 with 0.51 events/min at plus ends, and 3.33 events/min at minus ends (Tables 3.4 and 3.5), which is a 1.4 fold increase over tubulin alone for minus ends (Table 3.3) indicating that Bim1 may increase the frequency of rescues. I could not calculate a rescue frequency at higher Bim1 concentrations due to the absence of shrinking microtubules. In addition, Bim1 increased microtubule growth rates and lowered shrinkage rates (Figure 3.12B and C). 1 μM Bim1 increased plus-end and minus-end growth rates by 57% and 83%, respectively. 0.1 μM Bim1 lowered plus- end and minus-end shrinkage rates by 2.5-fold and 3.5-fold, respectively. I could not calculate shrinkage rates at higher Bim1 concentrations because shrinking microtubules were not observed. Overall, these results demonstrate that Bim1 decreases the catastrophe frequency and shrinkage rate, and increases the growth rate and rescue frequency.

Bik1 also had a substantial effect on catastrophe frequency but in the opposite direction from Bim1. In the presence of 1 μM Bik1, catastrophe frequencies rose by 38% at plus ends and 2.4-fold at minus ends (Figure 3.13A, Tables 3.6 and 3.7). Growth rates decreased by 18% at plus ends and 43% at minus ends, but there was no significant change in shrinkage rates (Figure 3.13B and C). I did not observe a significant change in the frequency of rescue events on addition of Bik1. Because Bik1 stimulated catastrophes in 11.5 μM tubulin, I also examined its effect in 14.4 μM tubulin, a tubulin concentration at which catastrophes are rarely observed. The addition of 0.1 μM Bik1 to 14.4

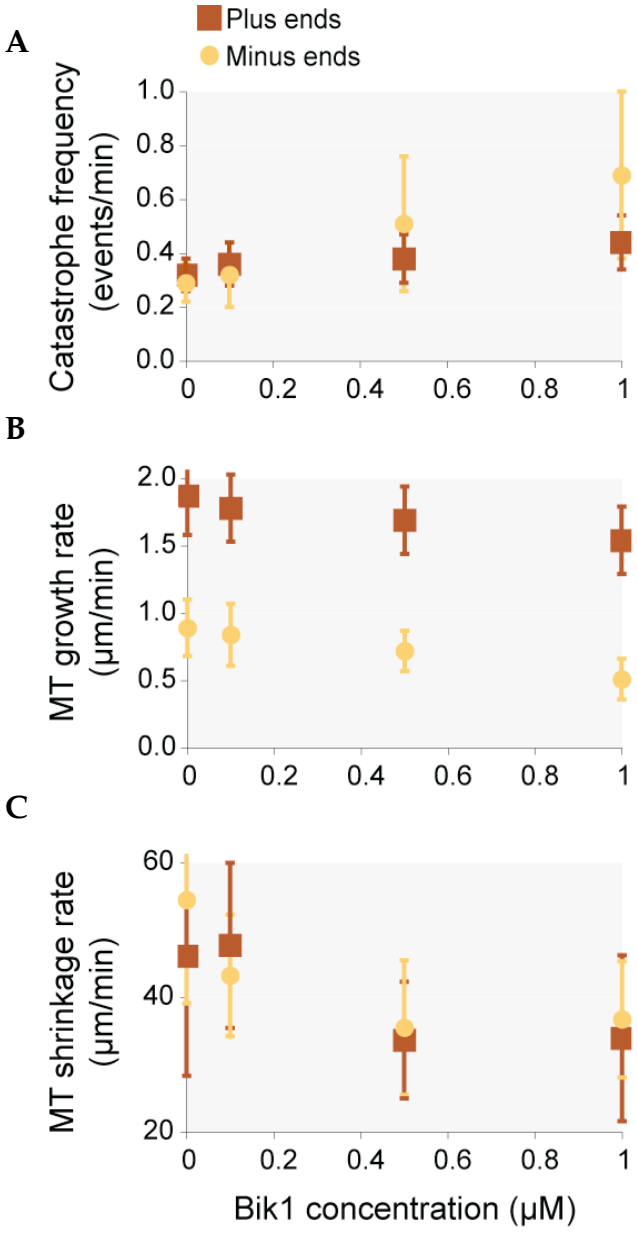

Figure 3.13 Effects of Bik1 on microtubule dynamics. A-C. Sea urchin axonemes were incubated with 11.5 μM tubulin in the presence of varying concentrations of Bim1. Individual microtubules were visualized using VE-DIC and their lengths measured over time. From this data, I calculated microtubule growth and shrinkage rates, and catastrophe frequencies; rescues were rare. Plots show the effects of increasing concentrations of Bik1 (A-C) on these parameters. Error bars are +/- SD.

Table 3.8. Effects of Bik1 on plus-end microtubule dynamics at 14.4 μM tubulin				
Plus Ends	Bik1 concentration			
	0 μM	0.1 μM	0.5 μM	1 μM
MT length/axoneme				
MT number	4.08 ± 1.26	2.73 ±1.12	2.44 ± 1.21	1.93 ± 0.92
MT length	13.22 ± 1.81 (6)	5.17 ± 1.45 (7)	3.68 ± 1.82 (8)	3.72 ± 1.56 (9)
Rates (μm/min)				
Growth	3.07 ± .21 (22)	2.18 ± 0.22 (22)	1.79 ± .1 (10)	1.53 ± .12 (19)
Shrinkage	*	61.51 ± 16.88 (7)	41.33 ± 11.26 (6)	47.45 ± 17.9 (6)
Frequencies (min^{-1})				
Catastrophe	<0.03 (0)	0.21 ± 0.07 (9)	0.26 ± 0.1 (7)	0.32 ± 0.11 (8)
Rescue	*	<1.25 (0)	<1.03 (0)	<1.72 (0)
Total time (min)				
Growth	31.75	42.02	26.88	24.88
Shrinkage	0.00	0.8	0.97	0.58
Total MT number	49	41	44	29

Data are mean ± SD. Values in parentheses are the number of events.
*No catastrophe events were observed, so shrinkage rates and rescue frequencies could not be determined.

Table 3.9. Effects of Bik1 on minus-end microtubule dynamics at 14.4 μM tubulin				
Minus Ends	Bik1 concentration			
	0 μM	0.1 μM	0.5 μM	1 μM
MT length/axoneme				
MT number	3.27 ± 1.14	1.93 ± 1.53	2.07 ± 1.22	1.88 ± 0.83
MT length	6.79 ± 2.15 (8)	1.94 ± 0.72 (7)	1.81 ± 0.81 (7)	1.24 ± 0.76 (6)
Rates (μm/min)				
Growth	1.93 ± 0.12 (12)	1.04 ± 0.18 (25)	0.79 ± 0.12 (10)	0.76 ± 0.21 (10)
Shrinkage	*	41.16 ± 10.91 (5)	40.75 ± 3.01 (4)	32.49 ± 8.39 (5)
Frequencies (min^{-1})				
Catastrophe	<0.03 (0)	0.20 ± 0.08 (6)	0.28 ± 0.13 (5)	0.37 ± 0.15 (6)
Rescue	*	<3.03 (0)	<3.03 (0)	1.36 (1)
Total time (min)				
Growth	29.97	22.05	17.82	16.03
Shrinkage	0.00	0.33	0.33	0.73
Total MT number	36	27	29	15

Data are mean ± SD. Values in parentheses are the number of events.
*No catastrophe events were observed, so shrinkage rates and rescue frequencies could not be determined.

μM tubulin increased the catastrophe frequency >8-fold at plus ends and >4-fold at minus ends, giving values similar to those observed in 11.5 μM tubulin alone (Tables 3.8 and 3.9). In summary, these results indicate that Bik1 decreases growth rates and increases catastrophes frequency.

The effect of Bim1, but not Bik1, on catastrophe frequency is independent of its effect on growth rates.

Microtubules catastrophe frequencies are known to be inversely related to microtubule growth rates (Figure 3.10A and C, Drechsel *et al*., 1992), so the effects of Bim1 and Bik1 on catastrophe frequencies could be an indirect effect of their abilities to increase and decrease growth rates, respectively. To test this possibility, I examined the relationship between microtubule growth rate and catastrophe frequency for three conditions: tubulin alone, tubulin plus Bim1, and tubulin plus Bik1. For each condition, I binned microtubules according to their growth rates and calculated the corresponding catastrophe frequencies. I then plotted the average catastrophe frequency versus the average growth rate for each binned group (Figure 3.14). As expected for tubulin alone, catastrophe frequency decreases as growth rate increases for both plus and minus ends (Figures 3.10, 3.14). In the presence of Bik1, the catastrophe frequency at each growth rate is nearly the same as for tubulin alone, indicating that Bik1 likely promotes catastrophe frequency by inhibiting growth rate. However, in the presence of Bim1, the catastrophe frequency at each growth rate is lower than for tubulin alone. Thus, Bim1 likely reduces catastrophe frequency by both its ability to increase microtubule growth rates and by a mechanism that is independent from its affect on growth rate.

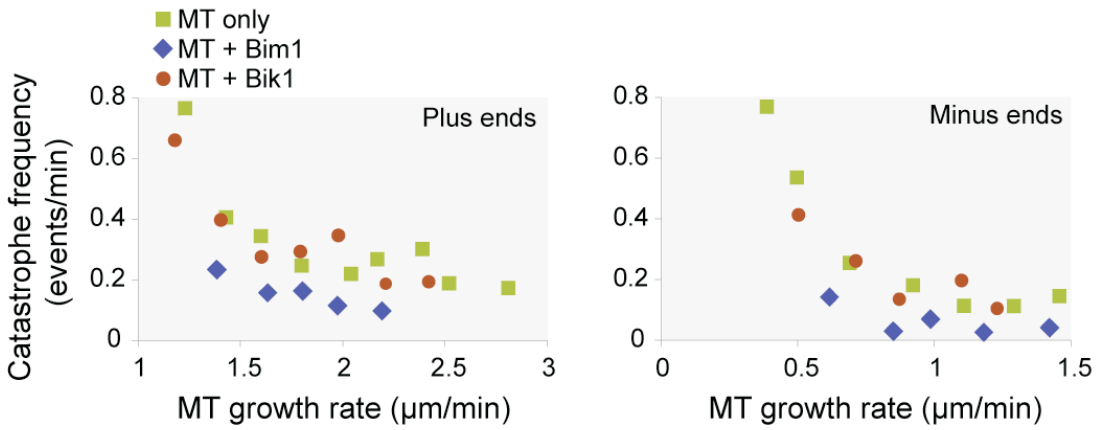

Figure 3.14 Relationship between catastrophe frequency and growth rate Catastrophe frequencies were plotted with respect to microtubule growth rates at microtubule plus ends (A) and minus ends (B). The growth rates of individual microtubules for varying concentrations of tubulin (8.6, 11.5, 13, 14.4 μM) were binned into growth rate intervals of 0.2 μm/min and the catastrophe frequency for each interval determined for tubulin alone (green), or in the presence of varying concentrations of Bim1 (blue) or Bik1 (red). For details see Materials and Methods.

The combined effects of Bim1 and Bik1 on microtubule dynamics

Combining Bim1 and Bik1 in equimolar amounts (0.1 μM and 1.0 μM each) affected microtubule assembly in nearly the same way as Bim1 alone (Figure 3.15, Tables 3.10 and 3.11). This result is more apparent at the higher concentration (1.0 μM) because the differences between the effects of the individual proteins are greater. The addition of both proteins at 1.0 μM increased total microtubule length 12.0-fold at plus ends and 12.1-fold at minus ends compared to tubulin alone (Figure 3.15A and E). I did not observe any catastrophes, indicating that catastrophe frequencies were reduced >48-fold at plus ends and >29-fold at minus ends (Figure 3.15B and F). Growth rates increased 50% at plus ends and 70% at minus ends (Figure 3.15C and G). Lack of shrinking microtubules prevented measuring shrinkage rates at 1.0 μM (Figure 3.15D and H). All of these parameters are very close to those obtained with 1.0 μM Bim1 alone and substantially different from those produced by 1.0 μM Bik1.

To see whether Bim1 maintained this dominant effect at higher Bik1:Bim1 ratios, I kept the Bik1 concentration at 1.0 μM and decreased the concentration of Bim1 to 0.5 μM and 0.1 μM. Lowering the amount of Bim1 led to a decrease in total microtubule length. However, even at a 1.0 μM Bik1 and 0.1 μM Bim1, microtubule assembly was promoted at both plus and minus ends relative to tubulin alone (Figure 3.15A and E). Catastrophe frequencies were reduced at plus ends and remained close to the values obtained for 0.1 μM Bim1 alone (Figure 3.15B), and were lowered further than 0.1 μM Bim1 at minus ends (Figure 3.15F). Growth rates were intermediate

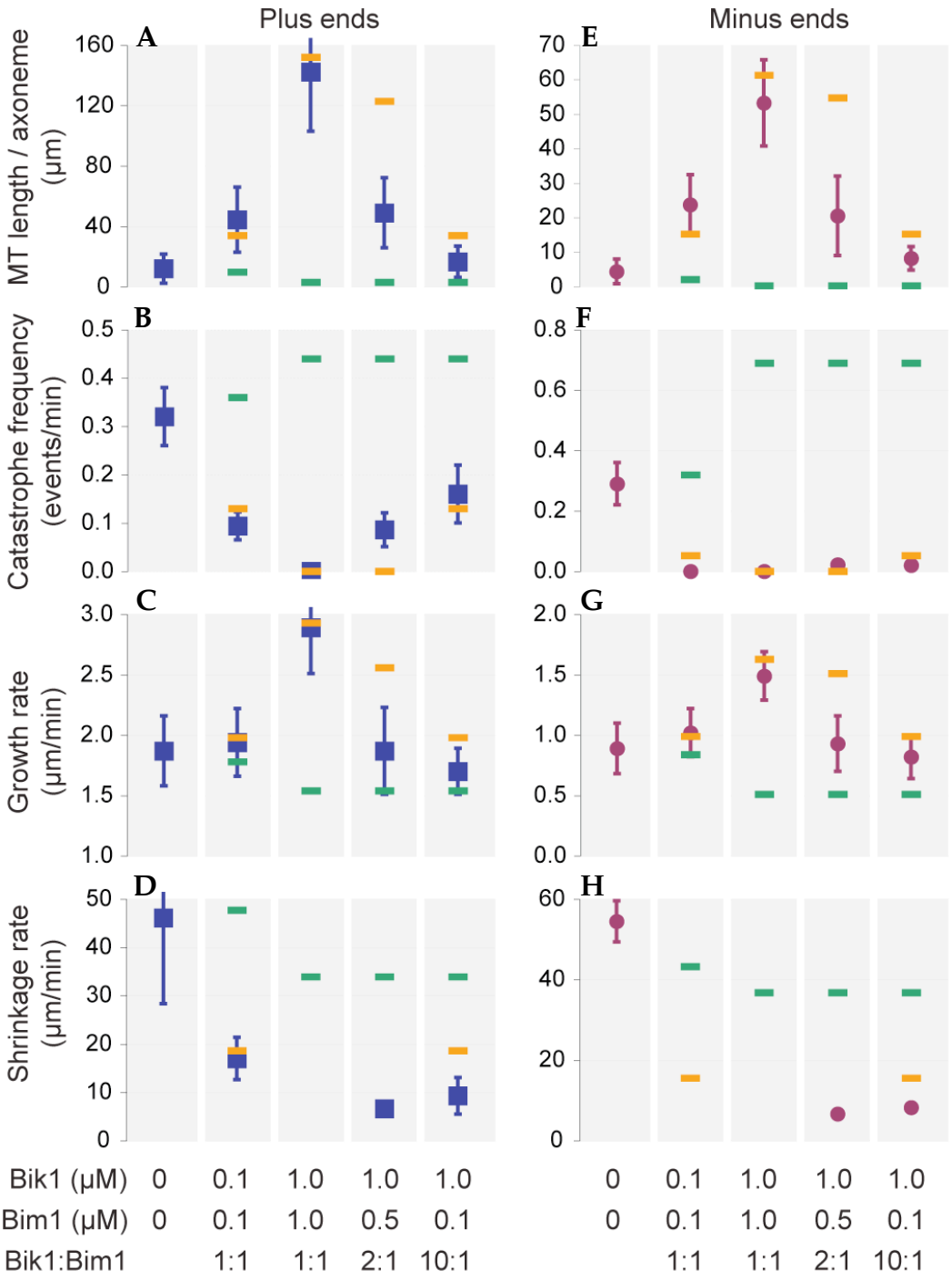

Figure 3.15 Combined effects of Bim1 and Bik1 on microtubule dynamics. Sea urchin axonemes were incubated with 11.5 μM tubulin in the presence of varying concentrations of both Bim1 and Bik1. Parameters of MT dynamic instability were determined as in Figure 3.12 and 3.12. Error bars are +/- SD. For comparison, the orange and green bars indicate the individual effects of Bim1 (orange) or Bik1 (green), as previously shown in Figures 3.12 and 3.13.

Table 3.10. Effects of Bim1 plus Bik1 on plus-end microtubule dynamics at 11.5 μM tubulin					
Bik1 Concentration	0 μM	0.1 μM	1.0 μM	1.0 μM	1.0 μM
Bim1 Concentration	0 μM	0.1 μM	1.0 μM	0.5 μM	0.1 μM
MT length/axoneme					
MT number	2.18 ±1.38	4.7 ± 1.7	8.44 ± 2.01	5.25 ± 2.12	3.00 ± 1.48
MT length	5.46 ± 2.74 (20)	9.45 ± 3.06	16.86 ± 2.38 (25)	9.32 ± 2.31 (13)	5.47 ± 2.13 (13)
Rates (μm/min)					
Growth	1.87 ± 0.29 (59)	1.94 ± 0.28 (42)	2.89 ± 0.38 (57)	1.87 ± 0.36 (34)	1.70 ± 0.19 (29)
Shrinkage	40.65 ± 11.18 (23)	16.98 ± 4.38 (10)	*	6.61 ± 1.12 (10)	9.28 ± 3.8 (7)
Frequencies (min^{-1})					
Catastrophe	0.32 ± 0.06 (26)	0.094 ± 0.029 (10)	<0.0067(0)	0.096 ± 0.035 (10)	0.16 ± 0.06 (7)
Rescue	<0.28 (0)	0.77 ± 0.55 (2)	*	0.62 ± 0.27 (5)	1.41 ± 0.71 (4)
Total time (min)					
Growth	82.15	106.82	150.18	104.08	45.05
Shrinkage	3.53	2.58	0.00	8.12	2.83
Total MT number	89	63	106	59	33

Data are mean ± SD. Values in parentheses are the number of events.
* No catastrophe events were observed, so shrinkage rates and rescue frequencies could not be determined.

Table 3.11. Effects of Bim1 plus Bik1 on minus-end microtubule dynamics at 11.5 μM tubulin					
Bik1 Concentration	0 μM	0.1 μM	1.0 μM	1.0 μM	1.0 μM
Bim1 Concentration	0 μM	0.1 μM	1.0 μM	0.5 μM	0.1 μM
MT length/axoneme					
MT number	1.79 ± 1.06	5.12 ± 1.54	6.86 ± 1.12	4.6 ± 2.1	2.82 ± 0.87
MT length	2.46 ± 1.36 (24)	4.64 ± 0.95	7.76 ± 1.31 (24)	4.46 ± 1.45 (25)	2.91 ± 0.79 (9)
Rates (μm/min)					
Growth	0.90 ± 0.21 (43)	1.02 ± 0.2 (33)	1.49 ± 0.2 (52)	0.93 ± 0.23 (35)	0.82 ± 0.18 (23)
Shrinkage	49.83 ± 11.58 (12)	*	*	6.63 ± 1.31 (3)	8.24 (1)
Frequencies (min^{-1})					
Catastrophe	0.27 ± 0.07 (14)	<0.01 (0)	<0.01 (0)	0.022± 0.012 (3)	0.02 (1)
Rescue	1.96 ± 1.39 (2)	*	*	0.95 ± 0.67 (2)	8.57 (1)
Total time (min)					
Growth	51.93	92.90	95.68	138.15	49
Shrinkage	1.17	0.00	0.00	2.12	0.12
Total MT number	68	61	80	60	35

Data are mean ± SD. Values in parentheses are the number of events.
* No catastrophe events were observed, so shrinkage rates and rescue frequencies could not be determined.

between values for 0.1 μM Bim1 and 1.0 μM Bik1 alone (Figure 3.15C and G), but 0.1 μM Bim1 alone has only a small effect on growth rates (Figure 3.12B). Thus, even though it is out-numbered by Bik1 10:1, Bim1 is still the primary influence on microtubule catastrophe frequency and growth rates.

Shrinkage rates at both ends were decreased further in the presence of Bim1 and Bik1 from the decrease seen with Bim1 alone (Figure 3.15D and H). In comparison to tubulin alone, shrinkage rates were lowered ~4.5 fold for 1 μM Bik1 plus 0.1 μM Bim1, and ~7 fold for 1 μM Bik1 plus 0.5 μM Bim1 at plus ends in comparison to the 2 fold decrease with 0.1 μM Bim1. Additionally, 0.1 μM Bim1 plus 1 μM Bik1 increased the rescue frequency at plus and minus ends, although rescues were still rare events (Tables 3.10 and 3.11). At plus ends, the rescue frequency was 0.51 ± 0.25 events/min with 0.1 μM Bim1 and 1.41± 0.71 events/min with 0.1 μM Bim1 plus 1 μM Bik1. In agreement, the percentage of microtubules which underwent a catastrophe event followed by a rescue event increased in the presence of Bim1 plus Bik1. At plus ends there were zero rescue events after catastrophes with tubulin alone, however about one quarter of catastrophe events were followed by rescues in 0.1 μM Bim1 and this increased to one-half with 0.1 μM Bim1 or 0.5 μM Bim1 with 1 μM Bik1. Thus, the combination of Bim1 and Bik1 decreases shrinkage rates and increases rescues more than the effects of Bim1 alone.

DISCUSSION

Dimerization of Bim1 and Bik1

Many +TIPs have been shown to form homodimers, including EB1 (Honnappa *et al*., 2006; Slep and Vale, 2007; Slep *et al*., 2005) and CLIP-170 (Pierre *et al*., 1992; Scheel *et al*., 1999). Previously, I had shown that Bim1 and Bik1 self-interact *in vivo* (Figure 2.4). This study confirms these interactions and expands on them by showing that these self-interactions form Bim1 and Bik1 homodimers in solution and in yeast extracts (Table 3.1). The results for Bim1 agree with a recent study that also finds Bim1 to exist as a homodimers (Zimniak *et al.,* 2009). Stu2 also self-interacts (Figure 2.4), and exists as homodimer in yeast extracts (van Breugel *et al*., 2003). These results further support the idea presented in Chapter Two, which indicated that these proteins do not exist in a larger stable plus-end complex.

The theme of dimerization among +TIPs suggests that dimerization may be important for +TIP function. Recent work has shown EB1 and CLIP-170 dimerization is not essential for plus-end tracking (Gupta *et al*., 2009; Komarova *et al*., 2009), but that dimers are more efficient than monomers in tracking (Slep and Vale, 2007; Komarova *et al*., 2009; Zimniak *et al.,* 2009). Therefore, dimerization may simply cause more efficient plus end tracking, or dimerization may be important for both plus-end tracking and for functional interactions and regulation of MT dynamics. Evidence suggests that dimerization is important for both plus-end tracking and function. First, Stu2 dimerization has been shown to be important for both its function and MT localization *in vivo* (Al-Bassam *et al*., 2006). Second, although MCAK can function as a monomer (Maney *et al*., 2001), dimerization of MCAK results in more robust and efficient MT depolymerization (Hertzer *et al*., 2006). Third,

dimerization of EB1 is needed to form the C-terminal hydrophobic pocket important for EB1 interaction with a variety of + TIPs (Honnappa *et al*., 2005). Also, the dimerization of EB1 and EB3 is required for MT stability and catastrophe suppression *in vivo* (Komarova *et al*., 2009; Hayashi *et al*., 2005; Bu and Su, 2003). However, an EB3 monomer does have the same effects on MT dynamics *in vitro* (Komarova *et al*., 2009). Additionally, the tubulin polymerizing activities of the CLIP-170 CAP-gly domain itself do not require dimerization (Gupta *et al*., 2009), but how these results fit into the context of the full-length protein, which can be autoinhibited, is unclear. As purified Bim1 and Bik1 exist primarily as homodimers in solution (Table 3.1), the effects I see of these proteins on MT dynamics *in vitro* are most likely from homodimers of these proteins, which is the predominant form *in vivo*. However, we cannot rule out that a monomer may have the same effects. Future experiments should address the importance of dimerization in protein interactions and functions.

Bik1 and Bim1 are elongated flexible molecules

Many +TIPs are elongated molecules, with N-terminal globular MT binding domains followed by a flexible linker region and C-termini which are responsible for a variety of protein-protein interactions (Akhmanova and Steinmetz, 2008). Stu2, EB1, CLIP-170, and many kinesins have all been shown to be elongated flexible molecules (Pierre *et al*., 1992; Lansbergen *et al*., 2004; Al-Bassam *et al*., 2006). The axial ratios for Bim1 (13.4) and Bik1 (23.2) indicate they are also elongated molecules. This may allow these proteins to be quite flexible and mediate their interactions with tubulin and/or MTs while still binding to other proteins with their C-terminal domains. This may be

especially important for Bim1/EB1 to recruit other proteins such as Bik1/CLIP-170, APC, and MCAK to the MT (Akhmanova and Hoogenraad, 2005; Morrison, 2007). The fact that these flexible linker regions are conserved in +TIPs from yeast to humans underscores the importance of this arrangement in function.

Bim1 acts at the plus-end to promote persistent MT growth

EB proteins have been shown to be promoters of growth in many systems (Tirnauer and Bierer, 2000). In agreement with this, we found Bim1 to promote MT polymerization *in vitro* by increasing growth rates and rescues while decreasing shortening rates and catastrophes (Figure 3.12; Tables 3.4 and 3.5). Overall, our results are in line with results from previous *in vitro* studies on EB family members (Manna *et al*., 2008; Komarova *et al*., 2009; Vitre *et al*., 2008).

How does Bim1 promote MT polymerization? Gel filtration experiments show no interaction of Bim1 with tubulin dimers (Figure 3.5), which agrees with previous work on EB1 (Niethammer *et al*., 2007; Slep and Vale, 2007). Therefore Bim1 does not act like the MT polymerase XMAP215/Stu2 family which binds tubulin dimers and incorporates them into them growing plus end (Al-Bassam *et al*., 2006; Kerssemakers *et al*., 2006; Brouhard *et al*., 2008). Rather, as our localization results show that Bim1 can directly bind MTs and has an intrinsic affinity for the plus-end structure, we hypothesize that Bim1 promotes a structural change directly at the plus tip to increase the MT growth rate and suppress catastrophes (Figure 3.16). This is in agreement with previous work indicating EBs can promote MT growth by stabilizing the lateral associations between protofilaments, which promotes

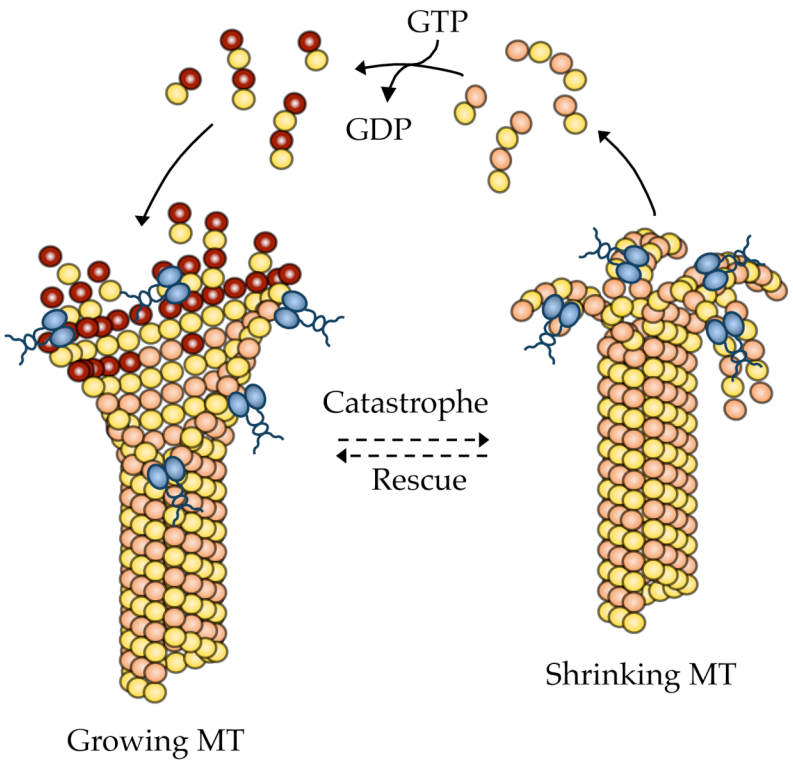

Figure 3.16 Bim1 acts at MT ends. Bim1 binds to growing MT ends and may promote growth by enhancing the lateral contacts between protofilaments, which increases growth rates and inhibits catastrophes. Additionally, Bim1 binds to the ends of shrinking MTs where it may bridge contacts between splaying protofilaments, holding together the depolymerizing MT. These contacts could slow the rate of MT shrinkage and increase the frequency of MT rescue.

sheet formation and rapid closure into tubes (Sandblad *et al,*. 2006; des Georges *et al*., 2008; Vitre *et al*., 2008).

Bim1 Suppresses Catastrophes

There are differences regarding the effect EB family members on catastrophe frequencies *in vitro*. We found Bim1 to decrease MT catastrophe rates, as did a study using EB1 (Manna *et al*., 2008), while another study using EB1 found that EB1 increases or decreases the catastrophe rate in a concentration dependent manner (Vitre *et al*., 2008). In contrast, both EB3 and mal3 increase the frequency of catastrophes (Komarova *et al*., 2009; Bieling *et al*., 2007). Although the reason for the differences in catastrophe frequencies is unclear, it has been hypothesized that lower EB1:tubulin ratios can increase catastrophes by increasing the rate of tubulin sheet closure so that it catches up with the polymerizing plus-end, while higher concentrations of EB1 decrease catastrophes by binding along the MT lattice to stabilize MTs (Vitre *et al*., 2008). However, our results show that Bim1 activity can directly suppress MT catastrophes even at low Bim1 dimer:tubulin ratios of 1:230. Manna *et al.* (2008) also found that a low concentration of EB1 (1:40) can directly suppress MT catastrophes *in vitro*. Additionally, while Mal3 and EB1 bind MTs at a ratio of ~1 mol of EB per ~10-12 moles of tubulin consistent with lattice binding (Manna *et al*., 2008; Sandblad *et al*., 2006), we find that Bim1 MT binding is saturated at a ratio of 1 mol of Bim1 per 40 moles of tubulin (Figure 3.7), indicating that Bim1 does not localize along the entire length of the lattice. The suppression of catastrophes at low Bim1:Tubulin ratios indicate that Bim1 primarily suppresses MT catastrophes by directly binding to the MT plus-end.

Bim1's effect on MT depolymerization dynamics.

Lattice binding has also been proposed for EB1's *in vitro* effects on decreasing shrinkage rates, and increasing rescues (Manna *et al*., 2008; Vitre *et al*., 2008). Unlike other EB proteins, which only bind polymerizing MTs (Dzhindzhev *et al*., 2005; Mimori-Kiyosue *et al*., 2000), Bim1 can localize to both growing and shrinking MT plus-ends (Figure 2.2). The localization to shrinking MT ends perfectly positions Bim1 to influence shrinkage rates and rescue frequencies by directly altering plus end structure, rather than by lattice binding. Bim1 may slow depolymerization by increasing the associations between protofilaments as is proposed to occur during polymerization. However, we cannot rule out that Bim1 may also bind the MT seam at low levels, and influence MTs through both lattice and plus-end interactions.

Indeed, we did see Bim1 localization along MTs as dots, although Bim1 showed a preference for the plus-end (Figure 3.8A). The plus-end localization of Bim1 may indicate it has a higher affinity for GTP-tubulin, and binds to the GTP cap, however this does not explain its ability to localize to shrinking MTs. Intriguingly, the dots of Bim1 along the MT could be Bim1 binding to GTP remnants that have recently been found to exist in the MT lattice (Dimitrov *et al*., 2008). These GTP remnants were found to be present at sites of rescue in shrinking MTs. As Bim1 also increases the frequency of rescues, it is tempting to speculate that Bim1 could interact with the GTP-tubulin remnants to promote rescues.

In budding yeast, deletion of Bim1 results in shorter cytoplasmic MTs (Tirnauer *et al.*, 1999), which agrees with our results indicating Bim1 can promote MT assembly *in vitro*. Loss of Bim1 also increases the amount of time

MTs spend in a paused state, with a decrease in MT catastrophe and rescue, indicating EBs may promote dynamics by promoting catastrophes and rescues (Wolyniak *et al*., 2006; Tirnauer *et al*., 1999). This is in disagreement with our findings that Bim1 suppresses MT catastrophes *in vitro*. However, we did find that Bim1 promotes persistent MT growth, which is consistent with Bim1's role in decreasing MT pausing. The loss of catastrophes in a *bim1*Δ background could be the result of the loss of a MT destabilizer from the plus-end if this protein was dependent on Bim1 for localization. In mammalian cells, the MT destabilizer MCAK is recruited to plus-ends by EB1 (Lee *et al*., 2008). Additionally, the major effect of Bim1 *in vivo* was to reduce the amount of MT pausing and this was not measured *in vitro* as there were very few pause events seen in any sample.

Bik1 promotes MT catastrophes in vitro

Overall, we found that Bik1 acts as a MT destabilizer *in vitro*, slowing the MT growth rate, which leads to an increase in the frequency of catastrophes (Figure 3.13; Tables 3.6-3.9). Bik1 may promote catastrophes by directly binding to the MT plus end to induce catastrophe, as has been seen for several kinesin depolymerases and Op18 (Desai *et al.*, 1999; Howell *et al.*, 1999; Sproul *et al.*, 2005; Mayr *et al.*, 2007). As Bik1 by itself was unable to target to the MT plus-end (Figure 3.8B) direct catastrophe promotion by altering the plus-end structure seems unlikely. Alternatively, Bik1 could induce MT disassembly by binding to free tubulin dimers sequestering them from polymerization, which decreases the MT growth rate. This method of depolymerization has also been seen for Op18, which can induce MT catastrophe through tubulin sequestering by binding to two tubulin dimers in

parallel (Cassimeris, 2002). We did see oligomerization of tubulin in the presence of Bik1 (Figures 3.5 and 3.6), however Bik1 does not remain stably associated with tubulin oligomers, therefore it cannot sequester tubulin dimers by stably binding to them as seen for Op18. Thus, Bik1 does not induce catastrophes by a direct end binding or by tubulin sequestering. Therefore, we concluded that the tubulin oligomers formed in the presence of Bik1 may not be competent to incorporate into the growing MT, effectively reducing the free tubulin concentration (Figure 3.17). Oligimerization has previously been seen for tubulin in the presence of the CLIP-170 MT binding domain (H2) (Arnal *et al*., 2004; Diamantopoulos *et al*., 1999), where tubulin formed curved oligomers or rings (Arnal *et al*., 2004). However, the tubulin oligomers formed in the presence of CLIP-170 readily incorporated into MTs and CLIP-170 was shown to promote MT growth and rescue (Arnal *et al*., 2004). The oligomers formed by Bik1 *in vitro* may be useful for the first step of MT nucleation from the spindle pole body rather than polymerization. These structures would not be necessary in our system as axonemes are present for MT nucleation, but could help to nucleate MTs *in vivo*. Additionally, the differences seen between our results could be due to the fact that we used full length Bik1, while the Arnal and colleagues used only the H2 MT binding domain (Arnal *et al*., 2004).

Loss of Bik1 in yeast results in many fewer and shorter aMTs (Wolyniak *et al*., 2006; Berlin *et al*., 1990) and is also important for spindle MT nucleation (Tanaka *et al*., 2005) indicating that Bik1 stabilizes MTs. The MTs in a *bik1*Δ are also less dynamic with a decrease seen in catastrophes and rescues and an increase in MT pausing, indicating that Bik1 can promote both dynamics and stability (Wolyniak *et al*., 2006). The promotion of catastrophes

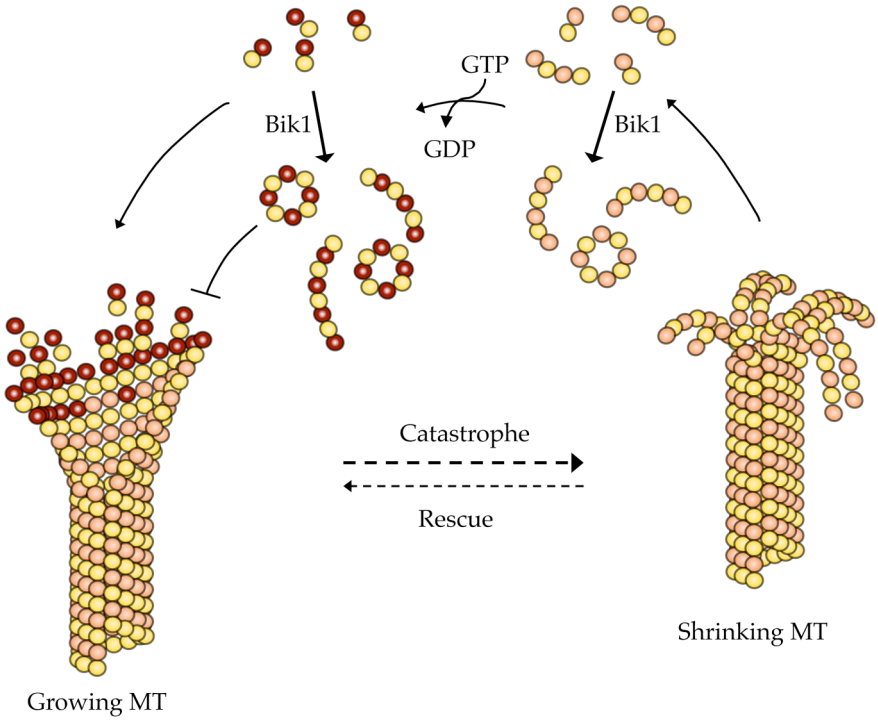

Figure 3.17 Bik1 is a MT destabilizer. Bik1 can cause oligimerization of tubulin subunits, which may be incompetent to incorporate into MTs. This lowers the concentration of polymerization competent free tubulin subunits, which slows MT growth rates. The reduction in MT growth results in an increase in the rate of MT catastrophes.

by Bik1 *in vitro* agrees with its role *in vivo* in promoting castastrophes. However, we also found that Bik1 inhibits MT assembly, which is in disagreement with its *in vivo* phenotype of promoting MT assembly.
The XMAP215/Stu2 family is another +TIP whose activity has been studied *in vitro* and *in vivo* and these proteins have been shown to be both MT stabilizers and polymerases *in vivo* (Al-Bassam *et al*., 2006; Kosco *et al*., 2001) while exhibiting depolymerizing activity *in vitro* (van Breugel *et al*., 2003). Bik1 may also have both polymerizing and depolymerizing activities, and the differences between *in vitro* and *in vivo* results may be due to the interactions of Bik1 with other molecules or posttranslational modifications *in vivo,* which influence its ability to promote polymerization or depolymerization. Bik1 could associate with other +TIPs, including Bim1 (discussed below) to regulate or suppress its catastrophe promoting activity. *In vivo*, Bik1 requires Kip2 for proper plus-end targeting, and may require Kip2 to promote MT polymerization. A Bik1-Kip2 complex may be able to incorporate the tubulin oligomers formed in the presence of Bik1 into growing MTs. Additionally, as shown in Figure 2.2, Bik1 can interact directly with Stu2, and this may also modulate Bik1's activity, although an *in vivo* double depletion study found that Bik1 and Stu2 appeared to have independent affects on MT dynamics (Wolyniak *et al.*, 2006). Phosphorylation also appears to be important in regulating Bik1's activity, as Bik1 is a target of the kinase mTOR and rapamycin inhibition of mTOR leads to a reduction MT dynamics (Choi *et al*., 2000).

Bim1 targets Bik1 to MTs and suppresses its catastrophe promoting activities

We show here that Bim1 is able to target Bik1-GFP to the MT lattice and plus-end (Figure 3.8C). This is also true in higher eukaryotes, as EB1 can target CLIP-170 to MTs *in vitro* and in Xenopus egg extracts and Drosophila S2 cells (Dzhindzhev *et al*., 2005; Bieling *et al*., 2008; Dixit *et al*., 2009). The localization pattern we saw for Bik1-GFP was similar to Bim1-GFP, indicating the Bik1-GFP dots we see may be a Bim1-Bik1 complex or Bik1-GFP may first bind Bim1 which loads it onto the MT as has been suggested for CLIP-170 and EB1 *in vivo* (Dzhindzhev *et al*., 2005). The majority of Bik1 localization to MTs *in vivo* is dependent on Kip2, however some residual Bik1 staining on MTs remains in a *kip2*Δ strain and Kip2 is not required for Bik1 targeting to polar MTs (Carvalho *et al*., 2004). The *in vitro* targeting of Bik1 to MTs in the presence of Bim1 indicates that Bim1 may be responsible for non-Kip2 dependent Bik1 MT binding *in vivo*. In agreement, Bim1 has shown to be responsible for the small amount of Bik1 binding to Glu-MTs (Caudron *et al*., 2008).

When added in combination, Bim1 was able to suppress the catastrophe activity of Bik1, as equimolar concentrations of the proteins behaved identically to Bim1 alone. The majority of Bim1 and Bik1 appeared to shift in to a stable complex when incubated in a 1:1 mixture (Figure 3.3). Therefore, Bim1-Bik1 binding may inhibit Bik1-tubulin interactions. The acidic aromatic EEF/Y C-terminal tails of EB1 and alpha tubulin both interact with the CAP-GLY domains of CLIP-170 (Honnapa 2006; Peris *et al*., 2006). Similar to their mammalian homologues, our lab has previously shown that the CAP-gly domains of Bik1 bind to the C-terminus of Bim1 (Wolyniak *et al*.,

2006) and that the final aromatic residue of alpha tubulin in important for Bik1 MT binding (Badin-Larcon *et al.*, 2004). The interaction of the Bik1 CAP-Gly domain with the C-terminal EEY/F motif of Bim1 may target Bik1 to MTs and prevent the CAP-Gly domain from interacting with alpha tubulin EEY/F C-terminal tail of free tubulin dimers, disrupting Bik's ability to induce tubulin oligimerization (Figure 3.18). Therefore, the function of the Bim1-Bik1 interaction may be to load Bik1 onto the MT and regulate Bik1's catastrophe activity.

EB1 has been shown to be autoinhibited by interactions of its C-terminal tail with its N-terminal MT binding domains (Hayashi *et al*., 2005). Binding of p150glued, another CAP-gly containing protein, to the C-terminus of EB1, or deletion of the EB1 C-terminus, strongly enhanced EB1 binding and activity at MT ends (Manna *et al*., 2008; Hayashi *et al*., 2005). Although Bik1 does bind to the Bim1 C-terminus (Wolyniak *et al*., 2006), I saw no increase of Bim1 activity in the presence of Bik1 at equimolar concentrations. However, at 2-10 fold higher concentrations of Bik1 (1μM) to Bim1 (0.5 μM, 0.1 mM), we did see a further decrease in the shrinkage rate and increase in the rescue frequency (Tables 3.0 and 3.11). These affects may be solely due to the activity of 0.5 μM Bim1, which became visible due to the appearance of catastrophes when 1 μM Bik1 was added to 0.5 μM Bim1 sample. However, the effects of shortening dynamics may also be due to a Bim1-Bik1 complex enhancing Bim1 activity or to a cooperative Bim1-Bik1 complex as the shortening rate and rescue frequency effects of 0.1 μM Bim1 are enhanced in the presence of 1 μM Bik1.

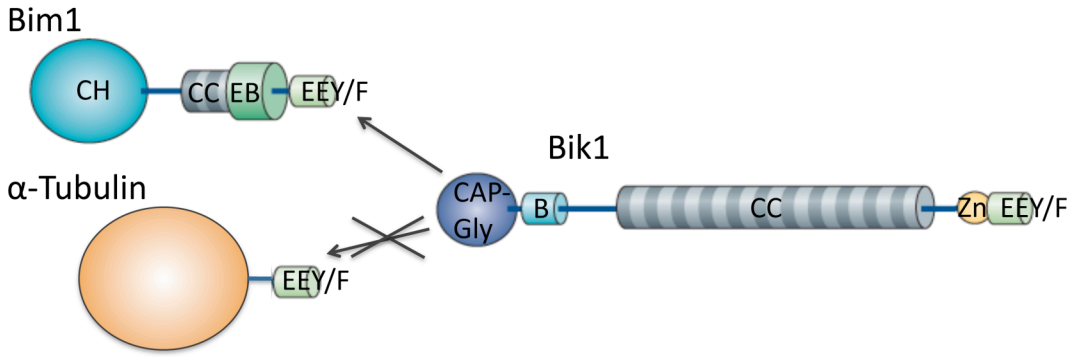

Figure 3.18 Bim1 can suppress the MT destabilizing activity of Bik1. The formation of a Bim1-Bik1 complex may disrupt Bik1-tubulin oligimerization. The Bik1 CAP-Gly domain binds the C-terminal EEY/F motifs of both Bim1 and α-tubulin, therefore when a Bim1-Bik1 complex is formed this may disrupt the interaction between Bik1 and tubulin. Proteins domains modified from Akhmanova and Steinmetz (2008).

FUTURE DIRECTIONS

This study found that *in vitro* Bim1 promotes MT assembly while Bik1 promotes MT disassembly, and that in combination, Bim1 can suppress the destabilizing activity of Bik1. These results further our understanding of how these +TIPs work to regulate MT dynamics but they also raise further questions on how these proteins work, and suggest new experiments to pursue.

I found that Bim1 can slow the MT depolymerization rate and I propose that Bim1 might slow depolymerization by increasing the associations between protofilaments as is suggested to occur during polymerization. This may be possible to visualize through a decrease in the outward splaying of protofilaments in a shrinking MT. Using cryo EM to capture images of MTs undergoing depolymerization in the presence of EBs would aid in our understanding of the mechanisms these proteins use to affect MT shrinkage dynamics.

Bim1 was also found to increase the frequency of rescues and to bind spots along the MT lattice. I proposed that this could be Bim1 binding to GTP remnants in the MT lattice (Dimitrov *et al*., 2008) and that Bim1 could interact with the GTP-tubulin remnants to promote rescues. Future experiments could examine if Bim1 shows colocalization with these remnants, and if the presence of Bim1 at these GTP-tubulin sites increases the frequency of rescues.

In this study I only examined the effect of Bim1 and Bik1 in combination. However, Bim1 interacts with several other +TIPs including Stu2, and Stu1, as well as several others. *In vivo*, Stu2 and Bim1 have been shown to work in combination to regulate MT dynamics during G1 (Wolyniak

et al., 2006) and EB1 and CLASP are thought to work together to increase rescues at the leading edge (Mimori-Kiyosue *et al*., 2005). Therefore to get a better understand of how various +TIPs are modulating Bim1's activities, we should purify each of these proteins and examine Bim1's activities with two or more proteins in combination on MT dyanmics.

Similarly, future experiments should examine the combined activities of Kip2 and Bik1 or Stu2 and Bik1, or of different Bik1 phosphorylation mutants on MT dynamics. This should yield insights into how Bik1 activity can be modulated, and perhaps help us understand the difference between the destabilizing activity I saw for Bik1 *in vitro* with its apparent stabilizing activity *in vivo.*

An examination of the tubulin oligomers I saw form in the presence of Bik1 should also yield insights into how Bik1 can slow the MT growth rate. EM should be performed to examine these structures and see if they are similar to the rings and curved oligomers formed by CLIP-170 seen by Arnal *et al.*, 2004.

REFERENCES

Akhmanova, A., and C.C. Hoogenraad. 2005. Microtubule plus-end-tracking proteins: mechanisms and functions. *Curr.Opin.Cell Biol.* 17:47-54.

Akhmanova, A., C.C. Hoogenraad, K. Drabek, T. Stepanova, B. Dortland, T. Verkerk, W. Vermeulen, B.M. Burgering, C.I. De Zeeuw, F. Grosveld, and N. Galjart. 2001. Clasps are CLIP-115 and -170 associating proteins involved in the regional regulation of microtubule dynamics in motile fibroblasts. *Cell.* 104:923-935.

Akhmanova, A., A.L. Mausset-Bonnefont, W. van Cappellen, N. Keijzer, C.C. Hoogenraad, T. Stepanova, K. Drabek, J. van der Wees, M. Mommaas, J. Onderwater, H. van der Meulen, M.E. Tanenbaum, R.H. Medema, J. Hoogerbrugge, J. Vreeburg, E.J. Uringa, J.A. Grootegoed, F. Grosveld, and N. Galjart. 2005. The microtubule plus-end-tracking protein CLIP-170 associates with the spermatid manchette and is essential for spermatogenesis. *Genes Dev.* 19:2501-2515.

Akhmanova, A., and M.O. Steinmetz. 2008. Tracking the ends: a dynamic protein network controls the fate of microtubule tips. *Nat.Rev.Mol.Cell Biol.* 9:309-322.

Akhmanova, A., and A.S. Yap. 2008. Organizing junctions at the cell-cell interface. *Cell.* 135:791-793.

Akhmanova, A., S. J. Stehbensand, and A.S. Yap. 2009. Touch, grasp, deliver and control: Functional cross-talk between microtubules and cell adhensions. *Traffic.* 10:268-274.

Al-Bassam, J., N.A. Larsen, A.A. Hyman, and S.C. Harrison. 2007. Crystal structure of a TOG domain: conserved features of XMAP215/Dis1-family TOG domains and implications for tubulin binding. *Structure.* 15:355-362.

Al-Bassam, J., M. van Breugel, S.C. Harrison, and A. Hyman. 2006. Stu2p binds tubulin and undergoes an open-to-closed conformational change. *J.Cell Biol.* 172:1009-1022.

Allingham, J.S., L.R. Sproul, I. Rayment, and S.P. Gilbert. 2007. Vik1 modulates microtubule-Kar3 interactions through a motor domain that lacks an active site. *Cell.* 128:1161-1172.

Amaro, A.I. 2010. Force-Generating Proteins Assemble and Position Mitotic Spindles in Saccharomyces cerevisiae. PhD Thesis. Cornell University

Aoki, K., Y. Nakaseko, K. Kinoshita, G. Goshima, and M. Yanagida. 2006. CDC2 phosphorylation of the fission yeast dis1 ensures accurate chromosome segregation. *Curr.Biol.* 16:1627-1635.

Arnal, I., C. Heichette, G.S. Diamantopoulos, and D. Chretien. 2004. CLIP-170/tubulin-curved oligomers coassemble at microtubule ends and promote rescues. *Curr.Biol.* 14:2086-2095.

Asbury, C.L. 2008. XMAP215: a tip tracker that really moves. *Cell.* 132:19-20.

Askham, J.M., K.T. Vaughan, H.V. Goodson, and E.E. Morrison. 2002. Evidence that an interaction between EB1 and p150(Glued) is required for the formation and maintenance of a radial microtubule array anchored at the centrosome. *Mol.Biol.Cell.* 13:3627-3645.

Baas, P.W., A. Karabay, and L. Qiang. 2005. Microtubules cut and run. *Trends Cell Biol.* 15:518-524.

Baas, P.W., C. Vidya Nadar, and K.A. Myers. 2006. Axonal transport of microtubules: the long and short of it. *Traffic.* 7:490-498.

Badin-Larcon, A.C., C. Boscheron, J.M. Soleilhac, M. Piel, C. Mann, E. Denarier, A. Fourest-Lieuvin, L. Lafanechere, M. Bornens, and D. Job. 2004. Suppression of nuclear oscillations in Saccharomyces cerevisiae expressing Glu tubulin. *Proc.Natl.Acad.Sci.U.S.A.* 101:5577-5582.

Bartolini, F., and G.G. Gundersen. 2006. Generation of noncentrosomal microtubule arrays. *J.Cell.Sci.* 119:4155-4163.

Bauer, V.W., J.C. Swaffield, S.A. Johnston, and M.T. Andrews. 1996. CADp44: a novel regulatory subunit of the 26S proteasome and the mammalian homolog of yeast Sug2p. *Gene.* 181:63-69.

Beinhauer, J.D., I.M. Hagan, J.H. Hegemann, and U. Fleig. 1997. Mal3, the fission yeast homologue of the human APC-interacting protein EB-1 is required for microtubule integrity and the maintenance of cell form. *J.Cell Biol.* 139:717-728.

Belmont, L., T. Mitchison, and H.W. Deacon. 1996. Catastrophic revelations about Op18/stathmin. *Trends Biochem.Sci.* 21:197-198.

Berlin, V., C.A. Styles, and G.R. Fink. 1990. BIK1, a protein required for microtubule function during mating and mitosis in Saccharomyces cerevisiae, colocalizes with tubulin. *J.Cell Biol.* 111:2573-2586.

Berrueta, L., S.K. Kraeft, J.S. Tirnauer, S.C. Schuyler, L.B. Chen, D.E. Hill, D. Pellman, and B.E. Bierer. 1998. The adenomatous polyposis coli-binding

protein EB1 is associated with cytoplasmic and spindle microtubules. *Proc.Natl.Acad.Sci.U.S.A.* 95:10596-10601.

Bieling, P., S. Kandels-Lewis, I.A. Telley, J. van Dijk, C. Janke, and T. Surrey. 2008. CLIP-170 tracks growing microtubule ends by dynamically recognizing composite EB1/tubulin-binding sites. *J.Cell Biol.* 183:1223-1233.

Bieling, P., L. Laan, H. Schek, E.L. Munteanu, L. Sandblad, M. Dogterom, D. Brunner, and T. Surrey. 2007. Reconstitution of a microtubule plus-end tracking system in vitro. *Nature.* 450:1100-1105.

Bieling, P., I.A. Telley, J. Piehler, and T. Surrey. 2008. Processive kinesins require loose mechanical coupling for efficient collective motility. *EMBO Rep.* 9:1121-1127.

Binker, M.G., D.Y. Zhao, S.J. Pang, and R.E. Harrison. 2007. Cytoplasmic linker protein-170 enhances spreading and phagocytosis in activated macrophages by stabilizing microtubules. *J.Immunol.* 179:3780-3791.

Bloom, G.S. 2001. The UNC-104/KIF1 family of kinesins. *Curr.Opin.Cell Biol.* 13:36-40.

Bloom, G.S., M.C. Wagner, K.K. Pfister, and S.T. Brady. 1988. Native structure and physical properties of bovine brain kinesin and identification of the ATP-binding subunit polypeptide. *Biochemistry.* 27:3409-3416.

Braun, M., D.R. Drummond, R.A. Cross, and A.D. McAinsh. 2009. The kinesin-14 Klp2 organizes microtubules into parallel bundles by an ATP-dependent sorting mechanism. *Nat.Cell Biol.* 11:724-730.

Bretscher, A. 2005. Microtubule tips redirect actin assembly. *Dev Cell.* 4:458-459.

Brittle, A.L., and H. Ohkura. 2005. Mini spindles, the XMAP215 homologue, suppresses pausing of interphase microtubules in Drosophila. *EMBO J.* 24:1387-1396.

Brouhard, G.J., J.H. Stear, T.L. Noetzel, J. Al-Bassam, K. Kinoshita, S.C. Harrison, J. Howard, and A.A. Hyman. 2008. XMAP215 is a processive microtubule polymerase. *Cell.* 132:79-88.

Browning, H., D.D. Hackney, and P. Nurse. 2003. Targeted movement of cell end factors in fission yeast. *Nat.Cell Biol.* 5:812-818.

Brunner, D., and P. Nurse. 2000. CLIP170-like tip1p spatially organizes microtubular dynamics in fission yeast. *Cell.* 102:695-704.

Brust-Mascher, I., P. Sommi, D.K. Cheerambathur, and J.M. Scholey. 2009. Kinesin-5-dependent poleward flux and spindle length control in Drosophila embryo mitosis. *Mol.Biol.Cell.* 20:1749-1762.

Bu, W., and L.K. Su. 2003. Characterization of functional domains of human EB1 family proteins. *J.Biol.Chem.* 278:49721-49731.

Buey, R.M., J.F. Diaz, and J.M. Andreu. 2006. The nucleotide switch of tubulin and microtubule assembly: a polymerization-driven structural change. *Biochemistry.* 45:5933-5938.

Burns, R.G. 1991. Alpha-, beta-, and gamma-tubulins: sequence comparisons and structural constraints. *Cell Motil.Cytoskeleton.* 20:181-189.

Busch, K.E., and D. Brunner. 2004. The microtubule plus end-tracking proteins mal3p and tip1p cooperate for cell-end targeting of interphase microtubules. *Curr.Biol.* 14:548-559.

Busch, K.E., J. Hayles, P. Nurse, and D. Brunner. 2004. Tea2p kinesin is involved in spatial microtubule organization by transporting tip1p on microtubules. *Dev.Cell.* 6:831-843.

Cai, S., L.N. Weaver, S.C. Ems-McClung, and C.E. Walczak. 2009. Kinesin-14 family proteins HSET/XCTK2 control spindle length by cross-linking and sliding microtubules. *Mol.Biol.Cell.* 20:1348-1359.

Carminati, J.L., and T. Stearns. 1997. Microtubules orient the mitotic spindle in yeast through dynein-dependent interactions with the cell cortex. *J.Cell Biol.* 138:629-641.

Carvalho, P., M.L. Gupta Jr, M.A. Hoyt, and D. Pellman. 2004. Cell cycle control of kinesin-mediated transport of Bik1 (CLIP-170) regulates microtubule stability and dynein activation. *Dev.Cell.* 6:815-829.

Carvalho, P., and D. Pellman. 2004. Mitotic spindle: laser microsurgery in yeast cells. *Curr.Biol.* 14:R748-50.

Carvalho, P., J.S. Tirnauer, and D. Pellman. 2003. Surfing on microtubule ends. *Trends Cell Biol.* 13:229-237.

Cassimeris, L. 2002. The oncoprotein 18/stathmin family of microtubule destabilizers. *Curr.Opin.Cell Biol.* 14:18-24.

Cassimeris, L. 1999. Accessory protein regulation of microtubule dynamics throughout the cell cycle. *Curr.Opin.Cell Biol.* 11:134-141.

Cassimeris, L. 1993. Regulation of microtubule dynamic instability. *Cell Motil.Cytoskeleton.* 26:275-281.

Cassimeris, L., B. Becker, and B. Carney. 2009. TOGp regulates microtubule assembly and density during mitosis and contributes to chromosome directional instability. *Cell Motil.Cytoskeleton.* 66:535-545.

Cassimeris, L., D. Gard, P.T. Tran, and H.P. Erickson. 2001. XMAP215 is a long thin molecule that does not increase microtubule stiffness. *J.Cell.Sci.* 114:3025-3033.

Cassimeris, L., and J. Morabito. 2004. TOGp, the human homolog of XMAP215/Dis1, is required for centrosome integrity, spindle pole organization, and bipolar spindle assembly. *Mol.Biol.Cell.* 15:1580-1590.

Cassimeris, L., N.K. Pryer, and E.D. Salmon. 1988. Real-time observations of microtubule dynamic instability in living cells. *J.Cell Biol.* 107:2223-2231.

Caudron, F., A. Andrieux, D. Job, and C. Boscheron. 2008. A new role for kinesin-directed transport of Bik1p (CLIP-170) in Saccharomyces cerevisiae. *J.Cell.Sci.* 121:1506-1513.

Chen, X.P. 1998. Proteins requires for microtubule function in Saccharomyces cerevisiae: from tubulin biogenesis to microtubule mediated processes. PhD Thesis. Cornell University

Chen, X.P., H. Yin, and T.C. Huffaker. 1998. The yeast spindle pole body component Spc72p interacts with Stu2p and is required for proper microtubule assembly. *J.Cell Biol.* 141:1169-1179.

Choi, J.H., N.R. Adames, T.F. Chan, C. Zeng, J.A. Cooper, and X.F. Zheng. 2000. TOR signaling regulates microtubule structure and function. *Curr.Biol.* 10:861-864.

Chretien, D., S.D. Fuller, and E. Karsenti. 1995. Structure of growing microtubule ends: two-dimensional sheets close into tubes at variable rates. *J.Cell Biol.* 129:1311-1328.

Chretien, D., J.M. Kenney, S.D. Fuller, and R.H. Wade. 1996. Determination of microtubule polarity by cryo-electron microscopy. *Structure.* 4:1031-1040.

Cottingham, F.R., L. Gheber, D.L. Miller, and M.A. Hoyt. 1999. Novel roles for saccharomyces cerevisiae mitotic spindle motors. *J.Cell Biol.* 147:335-350.

Curmi, P.A., C. Nogues, S. Lachkar, N. Carelle, M.P. Gonthier, A. Sobel, R. Lidereau, and I. Bieche. 2000. Overexpression of stathmin in breast

carcinomas points out to highly proliferative tumours. *Br.J.Cancer.* 82:142-150.

De Zeeuw, C.I., C.C. Hoogenraad, E. Goedknegt, E. Hertzberg, A. Neubauer, F. Grosveld, and N. Galjart. 1997. CLIP-115, a novel brain-specific cytoplasmic linker protein, mediates the localization of dendritic lamellar bodies. *Neuron.* 19:1187-1199.

des Georges, A., M. Katsuki, D.R. Drummond, M. Osei, R.A. Cross, and L.A. Amos. 2008. Mal3, the Schizosaccharomyces pombe homolog of EB1, changes the microtubule lattice. *Nat.Struct.Mol.Biol.* 15:1102-1108.

Desai, A., and T.J. Mitchison. 1997. Microtubule polymerization dynamics. *Annu.Rev.Cell Dev.Biol.* 13:83-117.

Desai, A., S. Verma, T.J. Mitchison, and C.E. Walczak. 1999. Kin I kinesins are microtubule-destabilizing enzymes. *Cell.* 96:69-78.

Diamantopoulos, G.S., F. Perez, H.V. Goodson, G. Batelier, R. Melki, T.E. Kreis, and J.E. Rickard. 1999. Dynamic localization of CLIP-170 to microtubule plus ends is coupled to microtubule assembly. *J.Cell Biol.* 144:99-112.

Dimitrov, A., M. Quesnoit, S. Moutel, I. Cantaloube, C. Pous, and F. Perez. 2008. Detection of GTP-tubulin conformation in vivo reveals a role for GTP remnants in microtubule rescues. *Science.* 322:1353-1356.

Dixit, R., B. Barnett, J.E. Lazarus, M. Tokito, Y.E. Goldman, and E.L. Holzbaur. 2009. Microtubule plus-end tracking by CLIP-170 requires EB1. *Proc.Natl.Acad.Sci.U.S.A.* 106:492-497.

Drabek, K., M. van Ham, T. Stepanova, K. Draegestein, R. van Horssen, C.L. Sayas, A. Akhmanova, T. Ten Hagen, R. Smits, R. Fodde, F. Grosveld, and N. Galjart. 2006. Role of CLASP2 in microtubule stabilization and the regulation of persistent motility. *Curr.Biol.* 16:2259-2264.

Dragestein, K.A., W.A. van Cappellen, J. van Haren, G.D. Tsibidis, A. Akhmanova, T.A. Knoch, F. Grosveld, and N. Galjart. 2008. Dynamic behavior of GFP-CLIP-170 reveals fast protein turnover on microtubule plus ends. *J.Cell Biol.* 180:729-737.

Drechsel, D.N., A.A. Hyman, M.H. Cobb, and M.W. Kirschner. 1992. Modulation of the dynamic instability of tubulin assembly by the microtubule-associated protein tau. *Mol.Biol.Cell.* 3:1141-1154.

Dujardin, D., U.I. Wacker, A. Moreau, T.A. Schroer, J.E. Rickard, and J.R. De Mey. 1998. Evidence for a role of CLIP-170 in the establishment of metaphase chromosome alignment. *J.Cell Biol.* 141:849-862.

Durfee, T., K. Becherer, P.L. Chen, S.H. Yeh, Y. Yang, A.E. Kilburn, W.H. Lee, and S.J. Elledge. 1993. The retinoblastoma protein associates with the protein phosphatase type 1 catalytic subunit. *Genes Dev.* 7:555-569.

Dzhindzhev, N.S., S.L. Rogers, R.D. Vale, and H. Ohkura. 2005. Distinct mechanisms govern the localisation of Drosophila CLIP-190 to unattached kinetochores and microtubule plus-ends. *J.Cell.Sci.* 118:3781-3790.

Efimov, A., A. Kharitonov, N. Efimova, J. Loncarek, P.M. Miller, N. Andreyeva, P. Gleeson, N. Galjart, A.R. Maia, I.X. McLeod, J.R. Yates 3rd, H. Maiato, A. Khodjakov, A. Akhmanova, and I. Kaverina. 2007. Asymmetric CLASP-dependent nucleation of noncentrosomal microtubules at the trans-Golgi network. *Dev.Cell.* 12:917-930.

Endow, S.A., S. Henikoff, and L. Soler-Niedziela. 1990. Mediation of meiotic and early mitotic chromosome segregation in Drosophila by a protein related to kinesin. *Nature.* 345:81-83.

Endow, S.A., S.J. Kang, L.L. Satterwhite, M.D. Rose, V.P. Skeen, and E.D. Salmon. 1994. Yeast Kar3 is a minus-end microtubule motor protein that destabilizes microtubules preferentially at the minus ends. *EMBO J.* 13:2708-2713.

Evans, L., T. Mitchison, and M. Kirschner. 1985. Influence of the centrosome on the structure of nucleated microtubules. *J.Cell Biol.* 100:1185-1191.

Feierbach, B., E. Nogales, K.H. Downing, and T. Stearns. 1999. Alf1p, a CLIP-170 domain-containing protein, is functionally and physically associated with alpha-tubulin. *J.Cell Biol.* 144:113-124.

Folker, E.S., B.M. Baker, and H.V. Goodson. 2005. Interactions between CLIP-170, tubulin, and microtubules: implications for the mechanism of Clip-170 plus-end tracking behavior. *Mol.Biol.Cell.* 16:5373-5384.

Fukata, M., T. Watanabe, J. Noritake, M. Nakagawa, M. Yamaga, S. Kuroda, Y. Matsuura, A. Iwamatsu, F. Perez, and K. Kaibuchi. 2002. Rac1 and Cdc42 capture microtubules through IQGAP1 and CLIP-170. *Cell.* 2002 7:873-85.

Galjart, N. 2005. CLIPs and CLASPs and cellular dynamics. *Nat.Rev.Mol.Cell Biol.* 6:487-498.

Ganem, N.J., K. Upton, and D.A. Compton. 2005. Efficient mitosis in human cells lacking poleward microtubule flux. *Curr.Biol.* 15:1827-1832.

Garcia, M.A., L. Vardy, N. Koonrugsa, and T. Toda. 2001. Fission yeast ch-TOG/XMAP215 homologue Alp14 connects mitotic spindles with the kinetochore and is a component of the Mad2-dependent spindle checkpoint. *EMBO J.* 20:3389-3401.

Gard, D.L., B.E. Becker, and S. Josh Romney. 2004. MAPping the eukaryotic tree of life: structure, function, and evolution of the MAP215/Dis1 family of microtubule-associated proteins. *Int.Rev.Cytol.* 239:179-272.

Gardner, M.K., D.C. Bouck, L.V. Paliulis, J.B. Meehl, E.T. O'Toole, J. Haase, A. Soubry, A.P. Joglekar, M. Winey, E.D. Salmon, K. Bloom, and D.J. Odde. 2008a. Chromosome congression by Kinesin-5 motor-mediated disassembly of longer kinetochore microtubules. *Cell.* 135:894-906.

Gardner, M.K., J. Haase, K. Mythreye, J.N. Molk, M. Anderson, A.P. Joglekar, E.T. O'Toole, M. Winey, E.D. Salmon, D.J. Odde, and K. Bloom. 2008b. The microtubule-based motor Kar3 and plus end-binding protein Bim1 provide structural support for the anaphase spindle. *J.Cell Biol.* 180:91-100.

Gardner, M.K., D.J. Odde, and K. Bloom. 2008c. Kinesin-8 molecular motors: putting the brakes on chromosome oscillations. *Trends Cell Biol.* 18:307-310.

Gergely, F., V.M. Draviam, and J.W. Raff. 2003. The ch-TOG/XMAP215 protein is essential for spindle pole organization in human somatic cells. *Genes Dev.* 17:336-341.

Goodson, H.V., S.B. Skube, R. Stalder, C. Valetti, T.E. Kreis, E.E. Morrison, and T.A. Schroer. 2003. CLIP-170 interacts with dynactin complex and the APC-binding protein EB1 by different mechanisms. *Cell Motil.Cytoskeleton.* 55:156-173.

Goshima, G., F. Nedelec, and R.D. Vale. 2005. Mechanisms for focusing mitotic spindle poles by minus end-directed motor proteins. *J.Cell Biol.* 171:229-240.

Goshima, G., and R.D. Vale. 2003. The roles of microtubule-based motor proteins in mitosis: comprehensive RNAi analysis in the Drosophila S2 cell line. *J.Cell Biol.* 162:1003-1016.

Graf, R., C. Daunderer, and M. Schliwa. 2000. Dictyostelium DdCP224 is a microtubule-associated protein and a permanent centrosomal resident involved in centrosome duplication. *J.Cell.Sci.* 113 (Pt 10):1747-1758.

Grissom, P.M., T. Fiedler, E.L. Grishchuk, D. Nicastro, R.R. West, and J.R. McIntosh. 2009. Kinesin-8 from fission yeast: a heterodimeric, plus-end-

directed motor that can couple microtubule depolymerization to cargo movement. *Mol.Biol.Cell.* 20:963-972.

Gross, S.P. 2004. Hither and yon: a review of bi-directional microtubule-based transport. *Phys.Biol.* 1:R1-11.

Gupta, K.K., B.A. Paulson, E.S. Folker, B. Charlebois, A.J. Hunt, and H.V. Goodson. 2009. Minimal plus-end tracking unit of the cytoplasmic linker protein CLIP-170. *J.Biol.Chem.* 284:6735-6742.

Hall, A. 2005. Rho GTPases and the control of cell behaviour. *Biochem. Soc. Trans*. 33: 891–895.

Hanash, S.M., J.R. Strahler, R. Kuick, E.H. Chu, and D. Nichols. 1988. Identification of a polypeptide associated with the malignant phenotype in acute leukemia. *J.Biol.Chem.* 263:12813-12815.

Harding, S.E., and H. Colfen. 1995. Inversion formulae for ellipsoid of revolution macromolecular shape functions. *Anal.Biochem.* 228:131-142.

Hayashi, I., and M. Ikura. 2003. Crystal structure of the amino-terminal microtubule-binding domain of end-binding protein 1 (EB1). *J.Biol.Chem.* 278:36430-36434.

Hayashi, I., A. Wilde, T.K. Mal, and M. Ikura. 2005. Structural basis for the activation of microtubule assembly by the EB1 and p150Glued complex. *Mol.Cell.* 19:449-460.

He, X., D.R. Rines, C.W. Espelin, and P.K. Sorger. 2001. Molecular analysis of kinetochore-microtubule attachment in budding yeast. *Cell.* 106:195-206.

Heil-Chapdelaine, R.A., N.K. Tran, and J.A. Cooper. 2000. Dynein-dependent movements of the mitotic spindle in Saccharomyces cerevisiae do not require filamentous actin. *Mol.Biol.Cell.* 11:863-872.

Helenius, J., G. Brouhard, Y. Kalaidzidis, S. Diez, and J. Howard. 2006. The depolymerizing kinesin MCAK uses lattice diffusion to rapidly target microtubule ends. *Nature.* 441:115-119.

Hertzer, K.M., S.C. Ems-McClung, S.L. Kline-Smith, T.G. Lipkin, S.P. Gilbert, and C.E. Walczak. 2006. Full-length dimeric MCAK is a more efficient microtubule depolymerase than minimal domain monomeric MCAK. *Mol.Biol.Cell.* 17:700-710.

Hildebrandt, E.R., and M.A. Hoyt. 2000. Mitotic motors in Saccharomyces cerevisiae. *Biochim.Biophys.Acta.* 1496:99-116.

Holmfeldt, P., M.E. Sellin, and M. Gullberg. 2009. Predominant regulators of tubulin monomer-polymer partitioning and their implication for cell polarization. *Cell Mol.Life Sci.*

Holmfeldt, P., S. Stenmark, and M. Gullberg. 2004. Differential functional interplay of TOGp/XMAP215 and the KinI kinesin MCAK during interphase and mitosis. *EMBO J.* 23:627-637.

Honnappa, S., S.M. Gouveia, A. Weisbrich, F.F. Damberger, N.S. Bhavesh, H. Jawhari, I. Grigoriev, F.J. van Rijssel, R.M. Buey, A. Lawera, I. Jelesarov, F.K. Winkler, K. Wuthrich, A. Akhmanova, and M.O. Steinmetz. 2009. An EB1-binding motif acts as a microtubule tip localization signal. *Cell.* 138:366-376.

Honnappa, S., C.M. John, D. Kostrewa, F.K. Winkler, and M.O. Steinmetz. 2005. Structural insights into the EB1-APC interaction. *EMBO J.* 24:261-269.

Honnappa, S., O. Okhrimenko, R. Jaussi, H. Jawhari, I. Jelesarov, F.K. Winkler, and M.O. Steinmetz. 2006. Key interaction modes of dynamic +TIP networks. *Mol.Cell.* 23:663-671.

Horio, T., and H. Hotani. 1986. Visualization of the dynamic instability of individual microtubules by dark-field microscopy. *Nature.* 321:605-607.

Howard, J., and A.A. Hyman. 2009. Growth, fluctuation and switching at microtubule plus ends. *Nat.Rev.Mol.Cell Biol.* 10:569-574.

Howard, J., and A.A. Hyman. 2007. Microtubule polymerases and depolymerases. *Curr.Opin.Cell Biol.* 19:31-35.

Howard, J., and A.A. Hyman. 2003. Dynamics and mechanics of the microtubule plus end. *Nature.* 422:753-758.

Howell, B., H. Deacon, and L. Cassimeris. 1999. Decreasing oncoprotein 18/stathmin levels reduces microtubule catastrophes and increases microtubule polymer in vivo. *J.Cell.Sci.* 112 (Pt 21):3713-3722.

Huffaker, T.C., J.H. Thomas, and D. Botstein. 1988. Diverse effects of beta-tubulin mutations on microtubule formation and function. *J.Cell Biol.* 106:1997-2010.

Hunter, A.W., M. Caplow, D.L. Coy, W.O. Hancock, S. Diez, L. Wordeman, and J. Howard. 2003. The kinesin-related protein MCAK is a microtubule depolymerase that forms an ATP-hydrolyzing complex at microtubule ends. *Mol.Cell.* 11:445-457.

Hwang, E., J. Kusch, Y. Barral, and T.C. Huffaker. 2003. Spindle orientation in Saccharomyces cerevisiae depends on the transport of microtubule ends along polarized actin cables. *J.Cell Biol.* 161:483-488.

Hyman, A.A., S. Salser, D.N. Drechsel, N. Unwin, and T.J. Mitchison. 1992. Role of GTP hydrolysis in microtubule dynamics: information from a slowly hydrolyzable analogue, GMPCPP. *Mol.Biol.Cell.* 3:1155-1167.

Inoue, S., and E.D. Salmon. 1995. Force generation by microtubule assembly/disassembly in mitosis and related movements. *Mol.Biol.Cell.* 6:1619-1640.

James, P., J. Halladay, and E.A. Craig. 1996. Genomic libraries and a host strain designed for highly efficient two-hybrid selection in yeast. *Genetics.* 144:1425-1436.

Juwana, J.P., P. Henderikx, A. Mischo, A. Wadle, N. Fadle, K. Gerlach, J.W. Arends, H. Hoogenboom, M. Pfreundschuh, and C. Renner. 1999. EB/RP gene family encodes tubulin binding proteins. *Int.J.Cancer.* 81:275-284.

Kahana, J.A., G. Schlenstedt, D.M. Evanchuk, J.R. Geiser, M.A. Hoyt, and P.A. Silver. 1998. The yeast dynactin complex is involved in partitioning the mitotic spindle between mother and daughter cells during anaphase B. *Mol.Biol.Cell.* 9:1741-1756.

Kapitein, L.C., E.J. Peterman, B.H. Kwok, J.H. Kim, T.M. Kapoor, and C.F. Schmidt. 2005. The bipolar mitotic kinesin Eg5 moves on both microtubules that it crosslinks. *Nature.* 435:114-118.

Kardon, J.R., S.L. Reck-Peterson, and R.D. Vale. 2009. Regulation of the processivity and intracellular localization of Saccharomyces cerevisiae dynein by dynactin. *Proc.Natl.Acad.Sci.U.S.A.* 106:5669-5674.

Kerssemakers, J.W., E.L. Munteanu, L. Laan, T.L. Noetzel, M.E. Janson, and M. Dogterom. 2006. Assembly dynamics of microtubules at molecular resolution. *Nature.* 442:709-712.

Kikkawa, M., T. Ishikawa, T. Nakata, T. Wakabayashi, and N. Hirokawa. 1994. Direct visualization of the microtubule lattice seam both in vitro and in vivo. *J.Cell Biol.* 127:1965-1971.

King, J.M., T.S. Hays, and R.B. Nicklas. 2000. Dynein is a transient kinetochore component whose binding is regulated by microtubule attachment, not tension. *J.Cell Biol.* 151:739-748.

King, S.J., and T.A. Schroer. 2000. Dynactin increases the processivity of the cytoplasmic dynein motor. *Nat.Cell Biol.* 2:20-24.

Kinoshita, K., I. Arnal, A. Desai, D.N. Drechsel, and A.A. Hyman. 2001. Reconstitution of physiological microtubule dynamics using purified components. *Science.* 294:1340-1343.

Kinoshita, K., T.L. Noetzel, I. Arnal, D.N. Drechsel, and A.A. Hyman. 2006. Global and local control of microtubule destabilization promoted by a catastrophe kinesin MCAK/XKCM1. *J.Muscle Res.Cell.Motil.* 27:107-114.

Kita, K., T. Wittmann, I.S. Nathke, and C.M. Waterman-Storer. 2006. Adenomatous polyposis coli on microtubule plus ends in cell extensions can promote microtubule net growth with or without EB1. *Mol.Biol.Cell.* 17:2331-2345.

Kline-Smith, S.L., A. Khodjakov, P. Hergert, and C.E. Walczak. 2004. Depletion of centromeric MCAK leads to chromosome congression and segregation defects due to improper kinetochore attachments. *Mol.Biol.Cell.* 15:1146-1159.

Kline-Smith, S.L., and C.E. Walczak. 2004. Mitotic spindle assembly and chromosome segregation: refocusing on microtubule dynamics. *Mol.Cell.* 15:317-327.

Komarova, Y., C.O. De Groot, I. Grigoriev, S.M. Gouveia, E.L. Munteanu, J.M. Schober, S. Honnappa, R.M. Buey, C.C. Hoogenraad, M. Dogterom, G.G. Borisy, M.O. Steinmetz, and A. Akhmanova. 2009. Mammalian end binding proteins control persistent microtubule growth. *J.Cell Biol.* 184:691-706.

Komarova, Y.A., A.S. Akhmanova, S. Kojima, N. Galjart, and G.G. Borisy. 2002. Cytoplasmic linker proteins promote microtubule rescue in vivo. *J.Cell Biol.* 159:589-599.

Korinek, W.S., M.J. Copeland, A. Chaudhuri, and J. Chant. 2000. Molecular linkage underlying microtubule orientation toward cortical sites in yeast. *Science.* 287:2257-2259.

Kosco, K. 2002. Characterization of Stu2: It's role in regulating microtubule dynamics and its interaction with Bik1 and Bim1 in Saccharomyces cerevisiae. PhD Thesis. Cornell University

Kosco, K.A., C.G. Pearson, P.S. Maddox, P.J. Wang, I.R. Adams, E.D. Salmon, K. Bloom, and T.C. Huffaker. 2001. Control of microtubule dynamics by Stu2p is essential for spindle orientation and metaphase chromosome alignment in yeast. *Mol.Biol.Cell.* 12:2870-2880.

Lallemand-Breitenbach, V., M. Quesnoit, V. Braun, A. El Marjou, C. Pous, B. Goud, and F. Perez. 2004. CLIPR-59 is a lipid raft-associated protein

containing a cytoskeleton-associated protein glycine-rich domain (CAP-Gly) that perturbs microtubule dynamics. *J.Biol.Chem.* 279:41168-41178.

Lan, W., X. Zhang, S.L. Kline-Smith, S.E. Rosasco, G.A. Barrett-Wilt, J. Shabanowitz, D.F. Hunt, C.E. Walczak, and P.T. Stukenberg. 2004. Aurora B phosphorylates centromeric MCAK and regulates its localization and microtubule depolymerization activity. *Curr.Biol.* 14:273-286.

Lansbergen, G., and A. Akhmanova. 2006. Microtubule plus end: a hub of cellular activities. *Traffic.* 7:499-507.

Lansbergen, G., I. Grigoriev, Y. Mimori-Kiyosue, T. Ohtsuka, S. Higa, I. Kitajima, J. Demmers, N. Galjart, A.B. Houtsmuller, F. Grosveld, and A. Akhmanova. 2006. CLASPs attach microtubule plus ends to the cell cortex through a complex with LL5beta. *Dev.Cell.* 11:21-32.

Lansbergen, G., Y. Komarova, M. Modesti, C. Wyman, C.C. Hoogenraad, H.V. Goodson, R.P. Lemaitre, D.N. Drechsel, E. van Munster, T.W. Gadella Jr, F. Grosveld, N. Galjart, G.G. Borisy, and A. Akhmanova. 2004. Conformational changes in CLIP-170 regulate its binding to microtubules and dynactin localization. *J.Cell Biol.* 166:1003-1014.

Larsson, N., B. Segerman, B. Howell, K. Fridell, L. Cassimeris, and M. Gullberg. 1999. Op18/stathmin mediates multiple region-specific tubulin and microtubule-regulating activities. *J.Cell Biol.* 146:1289-1302.

Lawrence, C.J., R.K. Dawe, K.R. Christie, D.W. Cleveland, S.C. Dawson, S.A. Endow, L.S. Goldstein, H.V. Goodson, N. Hirokawa, J. Howard, R.L. Malmberg, J.R. McIntosh, H. Miki, T.J. Mitchison, Y. Okada, A.S. Reddy, W.M. Saxton, M. Schliwa, J.M. Scholey, R.D. Vale, C.E. Walczak, and L. Wordeman. 2004. A standardized kinesin nomenclature. *J.Cell Biol.* 167:19-22.

Laycock, J.E., M.S. Savoian, and D.M. Glover. 2006. Antagonistic activities of Klp10A and Orbit regulate spindle length, bipolarity and function in vivo. *J.Cell.Sci.* 119:2354-2361.

Lee, H., U. Engel, J. Rusch, S. Scherrer, K. Sheard, and D. Van Vactor. 2004. The microtubule plus end tracking protein Orbit/MAST/CLASP acts downstream of the tyrosine kinase Abl in mediating axon guidance. *Neuron* 42: 913–926.

Lee, L., J.S. Tirnauer, J. Li, S.C. Schuyler, J.Y. Liu, and D. Pellman. 2000. Positioning of the mitotic spindle by a cortical-microtubule capture mechanism. *Science.* 287:2260-2262.

Lee, M.J., F. Gergely, K. Jeffers, S.Y. Peak-Chew, and J.W. Raff. 2001. Msps/XMAP215 interacts with the centrosomal protein D-TACC to regulate microtubule behaviour. *Nat.Cell Biol.* 3:643-649.

Lee, T., K.J. Langford, J.M. Askham, A. Bruning-Richardson, and E.E. Morrison. 2008. MCAK associates with EB1. *Oncogene.* 27:2494-2500.

Lee, W.L., J.R. Oberle, and J.A. Cooper. 2003. The role of the lissencephaly protein Pac1 during nuclear migration in budding yeast. *J.Cell Biol.* 160:355-364.

Lewkowicz, E., F. Herit, C. Le Clainche, P. Bourdoncle, F. Perez, and F. Niedergang. 2008. The microtubule-binding protein CLIP-170 coordinates mDia1 and actin reorganization during CR3-mediated phagocytosis. *J.Cell Biol.* 183:1287-1298.

Lin, H., P. de Carvalho, D. Kho, C.Y. Tai, P. Pierre, G.R. Fink, and D. Pellman. 2001. Polyploids require Bik1 for kinetochore-microtubule attachment. *J.Cell Biol.* 155:1173-1184.

Longtine, M.S., A. McKenzie 3rd, D.J. Demarini, N.G. Shah, A. Wach, A. Brachat, P. Philippsen, and J.R. Pringle. 1998. Additional modules for versatile and economical PCR-based gene deletion and modification in Saccharomyces cerevisiae. *Yeast.* 14:953-961.

Louie, R.K., S. Bahmanyar, K.A. Siemers, V. Votin, P. Chang, T. Stearns, W.J. Nelson, and A.I. Barth. 2004. Adenomatous polyposis coli and EB1 localize in close proximity of the mother centriole and EB1 is a functional component of centrosomes. *J.Cell.Sci.* 117:1117-1128.

Luders, J., and T. Stearns. 2007. Microtubule-organizing centres: a re-evaluation. *Nat.Rev.Mol.Cell Biol.* 8:161-167.

Maddox, P.S., J.K. Stemple, L. Satterwhite, E.D. Salmon, and K. Bloom. 2003. The minus end-directed motor Kar3 is required for coupling dynamic microtubule plus ends to the cortical shmoo tip in budding yeast. *Curr.Biol.* 13:1423-1428.

Maiato, H., E.A. Fairley, C.L. Rieder, J.R. Swedlow, C.E. Sunkel, and W.C. Earnshaw. 2003. Human CLASP1 is an outer kinetochore component that regulates spindle microtubule dynamics. *Cell.* 113:891-904.

Maiato, H., A. Khodjakov, and C.L. Rieder. 2005. Drosophila CLASP is required for the incorporation of microtubule subunits into fluxing kinetochore fibres. *Nat.Cell Biol.* 7:42-47.

Mandelkow, E.M., E. Mandelkow, and R.A. Milligan. 1991. Microtubule dynamics and microtubule caps: a time-resolved cryo-electron microscopy study. *J.Cell Biol.* 114:977-991.

Maney, T., M. Wagenbach, and L. Wordeman. 2001. Molecular dissection of the microtubule depolymerizing activity of mitotic centromere-associated kinesin. *J.Biol.Chem.* 276:34753-34758.

Manna, T., S. Honnappa, M.O. Steinmetz, and L. Wilson. 2008. Suppression of microtubule dynamic instability by the +TIP protein EB1 and its modulation by the CAP-Gly domain of p150glued. *Biochemistry.* 47:779-786.

Manna, T., D. Thrower, H.P. Miller, P. Curmi, and L. Wilson. 2006. Stathmin strongly increases the minus end catastrophe frequency and induces rapid treadmilling of bovine brain microtubules at steady state in vitro. *J.Biol.Chem.* 281:2071-2078.

Manna, T., D.A. Thrower, S. Honnappa, M.O. Steinmetz, and L. Wilson. 2009. Regulation of microtubule dynamic instability in vitro by differentially phosphorylated stathmin. *J.Biol.Chem.* 284:15640-15649.

Manning, B.D., J.G. Barrett, J.A. Wallace, H. Granok, and M. Snyder. 1999. Differential regulation of the Kar3p kinesin-related protein by two associated proteins, Cik1p and Vik1p. *J.Cell Biol.* 144:1219-1233.

Matthews, L.R., P. Carter, D. Thierry-Mieg, and K. Kemphues. 1998. ZYG-9, a Caenorhabditis elegans protein required for microtubule organization and function, is a component of meiotic and mitotic spindle poles. *J.Cell Biol.* 141:1159-1168.

Mayr, M.I., S. Hummer, J. Bormann, T. Gruner, S. Adio, G. Woehlke, and T.U. Mayer. 2007. The human kinesin Kif18A is a motile microtubule depolymerase essential for chromosome congression. *Curr.Biol.* 17:488-498.

McDonald, H.B., R.J. Stewart, and L.S. Goldstein. 1990. The kinesin-like ncd protein of Drosophila is a minus end-directed microtubule motor. *Cell.* 63:1159-1165.

Mennella, V., G.C. Rogers, S.L. Rogers, D.W. Buster, R.D. Vale, and D.J. Sharp. 2005. Functionally distinct kinesin-13 family members cooperate to regulate microtubule dynamics during interphase. *Nat.Cell Biol.* 7:235-245.

Miller, R.K., S.C. Cheng, and M.D. Rose. 2000. Bim1p/Yeb1p mediates the Kar9p-dependent cortical attachment of cytoplasmic microtubules. *Mol.Biol.Cell.* 11:2949-2959.

Miller, R.K., S. D'Silva, J.K. Moore, and H.V. Goodson. 2006. The CLIP-170 orthologue Bik1p and positioning the mitotic spindle in yeast. *Curr.Top.Dev.Biol.* 76:49-87.

Mimori-Kiyosue, Y., I. Grigoriev, G. Lansbergen, H. Sasaki, C. Matsui, F. Severin, N. Galjart, F. Grosveld, I. Vorobjev, S. Tsukita, and A. Akhmanova. 2005. CLASP1 and CLASP2 bind to EB1 and regulate microtubule plus-end dynamics at the cell cortex. *J.Cell Biol.* 168:141-153.

Mimori-Kiyosue, Y., N. Shiina, and S. Tsukita. 2000. The dynamic behavior of the APC-binding protein EB1 on the distal ends of microtubules. *Curr.Biol.* 10:865-868.

Mimori-Kiyosue, Y., and S. Tsukita. 2003. "Search-and-capture" of microtubules through plus-end-binding proteins (+TIPs). *J.Biochem.* 134:321-326.

Mishima, M., R. Maesaki, M. Kasa, T. Watanabe, M. Fukata, K. Kaibuchi, and T. Hakoshima. 2007. Structural basis for tubulin recognition by cytoplasmic linker protein 170 and its autoinhibition. *Proc.Natl.Acad.Sci.U.S.A.* 104:10346-10351.

Mitchison, T., and M. Kirschner. 1984. Dynamic instability of microtubule growth. *Nature.* 312:237-242.

Mitchison, T.J., P. Maddox, J. Gaetz, A. Groen, M. Shirasu, A. Desai, E.D. Salmon, and T.M. Kapoor. 2005. Roles of polymerization dynamics, opposed motors, and a tensile element in governing the length of Xenopus extract meiotic spindles. *Mol.Biol.Cell.* 16:3064-3076.

Moore, A., and L. Wordeman. 2004. The mechanism, function and regulation of depolymerizing kinesins during mitosis. *Trends Cell Biol.* 14:537-546.

Moores, C.A., and R.A. Milligan. 2006. Lucky 13-microtubule depolymerisation by kinesin-13 motors. *J.Cell.Sci.* 119:3905-3913.

Morrison, E.E. 2007. Action and interactions at microtubule ends. *Cell Mol.Life Sci.* 64:307-317.

Moseley, J.B., I. Sagot, A.L. Manning, Y. Xu, M.J. Eck, D. Pellman, and B.L. Goode. 2004. A conserved mechanism for Bni1- and mDia1-induced actin assembly and dual regulation of Bni1 by Bud6 and profilin. *Mol.Biol.Cell.* 15:896-907.

Nakamura, M., X.Z. Zhou, and K.P. Lu. 2001. Critical role for the EB1 and APC interaction in the regulation of microtubule polymerization. *Curr.Biol.* 11:1062-1067.

Nakaseko, Y., G. Goshima, J. Morishita, and M. Yanagida. 2001. M phase-specific kinetochore proteins in fission yeast: microtubule-associating Dis1 and Mtc1 display rapid separation and segregation during anaphase. *Curr.Biol.* 11:537-549.

Nguyen-Ngoc, T., K. Afshar, and P. Gonczy. 2007. Coupling of cortical dynein and G alpha proteins mediates spindle positioning in Caenorhabditis elegans. *Nat.Cell Biol.* 9:1294-1302.

Niethammer, P., I. Kronja, S. Kandels-Lewis, S. Rybina, P. Bastiaens, and E. Karsenti. 2007. Discrete states of a protein interaction network govern interphase and mitotic microtubule dynamics. *PLoS Biol.* 5:e29.

O'Connell, C.B., and Y.L. Wang. 2000. Mammalian spindle orientation and position respond to changes in cell shape in a dynein-dependent fashion. *Mol.Biol.Cell.* 11:1765-1774.

Ohkura, H., M.A. Garcia, and T. Toda. 2001. Dis1/TOG universal microtubule adaptors - one MAP for all? *J.Cell.Sci.* 114:3805-3812.

Olmsted, J.B. 1986. Microtubule-associated proteins. *Annu.Rev.Cell Biol.* 2:421-457.

Palmer, R.E., D.S. Sullivan, T. Huffaker, and D. Koshland. 1992. Role of astral microtubules and actin in spindle orientation and migration in the budding yeast, Saccharomyces cerevisiae. *J.Cell Biol.* 119:583-593.

Pellman, D., M. Bagget, Y.H. Tu, G.R. Fink, and H. Tu. 1995. Two microtubule-associated proteins required for anaphase spindle movement in Saccharomyces cerevisiae. *J.Cell Biol.* 130:1373-1385.

Perez, F., G.S. Diamantopoulos, R. Stalder, and T.E. Kreis. 1999. CLIP-170 highlights growing microtubule ends in vivo. *Cell.* 96:517-527.

Peris, L., M. Thery, J. Faure, Y. Saoudi, L. Lafanechere, J.K. Chilton, P. Gordon-Weeks, N. Galjart, M. Bornens, L. Wordeman, J. Wehland, A. Andrieux, and D. Job. 2006. Tubulin tyrosination is a major factor affecting the recruitment of CAP-Gly proteins at microtubule plus ends. *J.Cell Biol.* 174:839-849.

Peris, L., M. Wagenbach, L. Lafanechere, J. Brocard, A.T. Moore, F. Kozielski, D. Job, L. Wordeman, and A. Andrieux. 2009. Motor-dependent

microtubule disassembly driven by tubulin tyrosination. *J.Cell Biol.* 185:1159-1166.

Pierre, P., J. Scheel, J.E. Rickard, and T.E. Kreis. 1992. CLIP-170 links endocytic vesicles to microtubules. *Cell.* 70:887-900.

Popov, A.V., and E. Karsenti. 2003. Stu2p and XMAP215: turncoat microtubule-associated proteins? *Trends Cell Biol.* 13:547-550.

Popov, A.V., A. Pozniakovsky, I. Arnal, C. Antony, A.J. Ashford, K. Kinoshita, R. Tournebize, A.A. Hyman, and E. Karsenti. 2001. XMAP215 regulates microtubule dynamics through two distinct domains. *EMBO J.* 20:397-410.

Popov, A.V., F. Severin, and E. Karsenti. 2002. XMAP215 is required for the microtubule-nucleating activity of centrosomes. *Curr.Biol.* 12:1326-1330.

Price, D.K., J.R. Ball, Z. Bahrani-Mostafavi, J.C. Vachris, J.S. Kaufman, R.W. Naumann, R.V. Higgins, and J.B. Hall. 2000. The phosphoprotein Op18/stathmin is differentially expressed in ovarian cancer. *Cancer Invest.* 18:722-730.

Rehberg, M., and R. Graf. 2002. Dictyostelium EB1 is a genuine centrosomal component required for proper spindle formation. *Mol.Biol.Cell.* 13:2301-2310.

Rice, L.M., E.A. Montabana, and D.A. Agard. 2008. The lattice as allosteric effector: structural studies of alphabeta- and gamma-tubulin clarify the role of GTP in microtubule assembly. *Proc.Natl.Acad.Sci.U.S.A.* 105:5378-5383.

Riedel-Kruse, I.H., A. Hilfinger, J. Howard, and F. Julicher. 2007. How molecular motors shape the flagellar beat. *HFSP J.* 1:192-208.

Rieder, C.L., and A. Khodjakov. 2003. Mitosis through the microscope: advances in seeing inside live dividing cells. *Science.* 300:91-96.

Ringhoff, D.N., and L. Cassimeris. 2009. Stathmin regulates centrosomal nucleation of microtubules and tubulin dimer/polymer partitioning. *Mol.Biol.Cell.* 20:3451-3458.

Rogers, G.C., S.L. Rogers, T.A. Schwimmer, S.C. Ems-McClung, C.E. Walczak, R.D. Vale, J.M. Scholey, and D.J. Sharp. 2004. Two mitotic kinesins cooperate to drive sister chromatid separation during anaphase. *Nature.* 427:364-370.

Rogers, G.C., S.L. Rogers, and D.J. Sharp. 2005. Spindle microtubules in flux. *J.Cell.Sci.* 118:1105-1116.

Rogers, G.C., N.M. Rusan, M. Peifer, and S.L. Rogers. 2008. A multicomponent assembly pathway contributes to the formation of acentrosomal microtubule arrays in interphase Drosophila cells. *Mol.Biol.Cell.* 19:3163-3178.

Rogers, S.L., G.C. Rogers, D.J. Sharp, and R.D. Vale. 2002. Drosophila EB1 is important for proper assembly, dynamics, and positioning of the mitotic spindle. *J.Cell Biol.* 158:873-884.

Sammak, P.J., and G.G. Borisy. 1988. Direct observation of microtubule dynamics in living cells. *Nature.* 332:724-726.

Sandblad, L., K.E. Busch, P. Tittmann, H. Gross, D. Brunner, and A. Hoenger. 2006. The Schizosaccharomyces pombe EB1 homolog Mal3p binds and stabilizes the microtubule lattice seam. *Cell.* 127:1415-1424.

Sawin, K.E. and H.A. Snaith. 2004. Role of microtubules and tea1p in establishment and maintenance of fission yeast cell polarity. *J. Cell Sci*. 117: 689–700.

Scheel, J., P. Pierre, J.E. Rickard, G.S. Diamantopoulos, C. Valetti, F.G. van der Goot, M. Haner, U. Aebi, and T.E. Kreis. 1999. Purification and analysis of authentic CLIP-170 and recombinant fragments. *J.Biol.Chem.* 274:25883-25891.

Schek, H.T.,3rd, M.K. Gardner, J. Cheng, D.J. Odde, and A.J. Hunt. 2007. Microtubule assembly dynamics at the nanoscale. *Curr.Biol.* 17:1445-1455.

Schmidt, D.J., D.J. Rose, W.M. Saxton, and S. Strome. 2005. Functional analysis of cytoplasmic dynein heavy chain in Caenorhabditis elegans with fast-acting temperature-sensitive mutations. *Mol.Biol.Cell.* 16:1200-1212.

Schulze, E., and M. Kirschner. 1988. New features of microtubule behaviour observed in vivo. *Nature.* 334:356-359.

Schuyler, S.C., and D. Pellman. 2001. Microtubule "plus-end-tracking proteins": The end is just the beginning. *Cell.* 105:421-424.

Severin, F., B. Habermann, T. Huffaker, and T. Hyman. 2001. Stu2 promotes mitotic spindle elongation in anaphase. *J.Cell Biol.* 153:435-442.

Sheeman, B., P. Carvalho, I. Sagot, J. Geiser, D. Kho, M.A. Hoyt, and D. Pellman. 2003. Determinants of S. cerevisiae dynein localization and activation: implications for the mechanism of spindle positioning. *Curr.Biol.* 13:364-372.

Shirasu-Hiza, M., P. Coughlin, and T. Mitchison. 2003. Identification of XMAP215 as a microtubule-destabilizing factor in Xenopus egg extract by biochemical purification. *J.Cell Biol.* 161:349-358.

Siegel, L.M., and K.J. Monty. 1966. Determination of molecular weights and frictional ratios of proteins in impure systems by use of gel filtration and density gradient centrifugation. Application to crude preparations of sulfite and hydroxylamine reductases. *Biochim.Biophys.Acta.* 112:346-362.

Slep, K.C., S.L. Rogers, S.L. Elliott, H. Ohkura, P.A. Kolodziej, and R.D. Vale. 2005. Structural determinants for EB1-mediated recruitment of APC and spectraplakins to the microtubule plus end. *J.Cell Biol.* 168:587-598.

Slep, K.C., and R.D. Vale. 2007. Structural basis of microtubule plus end tracking by XMAP215, CLIP-170, and EB1. *Mol.Cell.* 27:976-991.

Sorger, P.K., F.F. Severin, and A.A. Hyman. 1994. Factors required for the binding of reassembled yeast kinetochores to microtubules in vitro. *J.Cell Biol.* 127:995-1008.

Sousa, A., R. Reis, P. Sampaio, and C.E. Sunkel. 2007. The Drosophila CLASP homologue, Mast/Orbit regulates the dynamic behaviour of interphase microtubules by promoting the pause state. *Cell Motil.Cytoskeleton.* 64:605-620.

Sproul, L.R., D.J. Anderson, A.T. Mackey, W.S. Saunders, and S.P. Gilbert. 2005. Cik1 targets the minus-end kinesin depolymerase kar3 to microtubule plus ends. *Curr.Biol.* 15:1420-1427.

Steinmetz, M.O., R.A. Kammerer, W. Jahnke, K.N. Goldie, A. Lustig, and J. van Oostrum. 2000. Op18/stathmin caps a kinked protofilament-like tubulin tetramer. *EMBO J.* 19:572-580.

Stumpff, J., G. von Dassow, M. Wagenbach, C. Asbury, and L. Wordeman. 2008. The kinesin-8 motor Kif18A suppresses kinetochore movements to control mitotic chromosome alignment. *Dev.Cell.* 14:252-262.

Stumpff, J., and L. Wordeman. 2007. Chromosome congression: the kinesin-8-step path to alignment. *Curr.Biol.* 17:R326-8.

Tan, D., A.B. Asenjo, V. Mennella, D.J. Sharp, and H. Sosa. 2006. Kinesin-13s form rings around microtubules. *J.Cell Biol.* 175:25-31.

Tanaka, K., N. Mukae, H. Dewar, M. van Breugel, E.K. James, A.R. Prescott, C. Antony, and T.U. Tanaka. 2005. Molecular mechanisms of kinetochore capture by spindle microtubules. *Nature.* 434:987-994.

Tanaka, T.U. 2005. Chromosome bi-orientation on the mitotic spindle. *Philos.Trans.R.Soc.Lond.B.Biol.Sci.* 360:581-589.

Tanaka, T.U., M.J. Stark, and K. Tanaka. 2005. Kinetochore capture and bi-orientation on the mitotic spindle. *Nat.Rev.Mol.Cell Biol.* 6:929-942.

Tanenbaum, M.E., N. Galjart, M.A. van Vugt, and R.H. Medema. 2006. CLIP-170 facilitates the formation of kinetochore-microtubule attachments. *EMBO J.* 25:45-57.

Tilney, L.G., J. Bryan, D.J. Bush, K. Fujiwara, M.S. Mooseker, D.B. Murphy, and D.H. Snyder. 1973. Microtubules: evidence for 13 protofilaments. *J.Cell Biol.* 59:267-275.

Tirnauer, J.S., and B.E. Bierer. 2000. EB1 proteins regulate microtubule dynamics, cell polarity, and chromosome stability. *J.Cell Biol.* 149:761-766.

Tirnauer, J.S., J.C. Canman, E.D. Salmon, and T.J. Mitchison. 2002a. EB1 targets to kinetochores with attached, polymerizing microtubules. *Mol.Biol.Cell.* 13:4308-4316.

Tirnauer, J.S., S. Grego, E.D. Salmon, and T.J. Mitchison. 2002b. EB1-microtubule interactions in Xenopus egg extracts: role of EB1 in microtubule stabilization and mechanisms of targeting to microtubules. *Mol.Biol.Cell.* 13:3614-3626.

Tirnauer, J.S., E. O'Toole, L. Berrueta, B.E. Bierer, and D. Pellman. 1999. Yeast Bim1p promotes the G1-specific dynamics of microtubules. *J.Cell Biol.* 145:993-1007.

Toso, R.J., M.A. Jordan, K.W. Farrell, B. Matsumoto, and L. Wilson. 1993. Kinetic stabilization of microtubule dynamic instability in vitro by vinblastine. *Biochemistry.* 32:1285-1293.

Tournebize, R., A. Popov, K. Kinoshita, A.J. Ashford, S. Rybina, A. Pozniakovsky, T.U. Mayer, C.E. Walczak, E. Karsenti, and A.A. Hyman. 2000. Control of microtubule dynamics by the antagonistic activities of XMAP215 and XKCM1 in Xenopus egg extracts. *Nat.Cell Biol.* 2:13-19.

Tran, P.T., E.D. Salmon, and S. Inoue. 1997. UV cutting of MAPs-bound microtubules. *Biol.Bull.* 193:218-219.

Tytell, J.D., and P.K. Sorger. 2006. Analysis of kinesin motor function at budding yeast kinetochores. *J.Cell Biol.* 172:861-874.

Usui, T., H. Maekawa, G. Pereira, and E. Schiebel. 2003. The XMAP215 homologue Stu2 at yeast spindle pole bodies regulates microtubule dynamics and anchorage. *EMBO J.* 22:4779-4793.

Vale, R.D., F. Malik, and D. Brown. 1992. Directional instability of microtubule transport in the presence of kinesin and dynein, two opposite polarity motor proteins. *J.Cell Biol.* 119:1589-1596.

Vallee, R.B., J.C. Williams, D. Varma, and L.E. Barnhart. 2004. Dynein: An ancient motor protein involved in multiple modes of transport. *J.Neurobiol.* 58:189-200.

van Breugel, M., D. Drechsel, and A. Hyman. 2003. Stu2p, the budding yeast member of the conserved Dis1/XMAP215 family of microtubule-associated proteins is a plus end-binding microtubule destabilizer. *J.Cell Biol.* 161:359-369.

Varga, V., J. Helenius, K. Tanaka, A.A. Hyman, T.U. Tanaka, and J. Howard. 2006. Yeast kinesin-8 depolymerizes microtubules in a length-dependent manner. *Nat.Cell Biol.* 8:957-962.

Vasquez, R.J., D.L. Gard, and L. Cassimeris. 1994. XMAP from Xenopus eggs promotes rapid plus end assembly of microtubules and rapid microtubule polymer turnover. *J.Cell Biol.* 127:985-993.

Vasquez, R.J., B. Howell, A.M. Yvon, P. Wadsworth, and L. Cassimeris. 1997. Nanomolar concentrations of nocodazole alter microtubule dynamic instability in vivo and in vitro. *Mol.Biol.Cell.* 8:973-985.

Vaughan, K.T. 2005. TIP maker and TIP marker; EB1 as a master controller of microtubule plus ends. *J.Cell Biol.* 171:197-200.

Vaughan, K.T, 2005. Microtubule plus ends, motors, and traffic of Golgi membranes. *Biochim Biophys Acta*. 3:316-24.

Vaughan, P.S., P. Miura, M. Henderson, B. Byrne, and K.T. Vaughan. 2002. A role for regulated binding of p150(Glued) to microtubule plus ends in organelle transport. *J.Cell Biol.* 158:305-319.

Vitre, B., F.M. Coquelle, C. Heichette, C. Garnier, D. Chretien, and I. Arnal. 2008. EB1 regulates microtubule dynamics and tubulin sheet closure in vitro. *Nat.Cell Biol.* 10:415-421.

Walczak, C.E., and R. Heald. 2008. Mechanisms of mitotic spindle assembly and function. *Int.Rev.Cytol.* 265:111-158.

Walczak, C.E., and T.J. Mitchison. 1996. Kinesin-related proteins at mitotic spindle poles: function and regulation. *Cell.* 85:943-946.

Walker, R.A., S. Inoue, and E.D. Salmon. 1989. Asymmetric behavior of severed microtubule ends after ultraviolet-microbeam irradiation of individual microtubules in vitro. *J.Cell Biol.* 108:931-937.

Walker, R.A., E.T. O'Brien, N.K. Pryer, M.F. Soboeiro, W.A. Voter, H.P. Erickson, and E.D. Salmon. 1988. Dynamic instability of individual microtubules analyzed by video light microscopy: rate constants and transition frequencies. *J.Cell Biol.* 107:1437-1448.

Wang, H.W., and E. Nogales. 2005. Nucleotide-dependent bending flexibility of tubulin regulates microtubule assembly. *Nature.* 435:911-915.

Wang, P.J., and T.C. Huffaker. 1997. Stu2p: A microtubule-binding protein that is an essential component of the yeast spindle pole body. *J.Cell Biol.* 139:1271-1280.

Watanabe, T., S. Wang, J. Noritake, K. Sato, M. Fukata, M. Takefuji, M. Nakagawa, N. Izumi, T. Akiyama, and K. Kaibuchi. 2004. Interaction with IQGAP1 links APC to Rac1, Cdc42, and actin filaments during cell polarization and migration. *Dev. Cell* 7: 871–883.

Weisbrich, A., S. Honnappa, R. Jaussi, O. Okhrimenko, D. Frey, I. Jelesarov, A. Akhmanova, and M.O. Steinmetz. 2007. Structure-function relationship of CAP-Gly domains. *Nat.Struct.Mol.Biol.* 14:959-967.

Weisenberg, R.C. 1972. Microtubule formation in vitro in solutions containing low calcium concentrations. *Science.* 177:1104-1105.

Wen, Y., C.H. Eng, J. Schmoranzer, N. Cabrera-Poch, E.J. Morris, M. Chen, B.J. Wallar, A.S. Alberts, and G.G. Gundersen. 2004. EB1 and APC bind to mDia to stabilize microtubules downstream of Rho and promote cell migration. *Nat.Cell Biol.* 6:820-830.

Wieland, G., S. Orthaus, S. Ohndorf, S. Diekmann, and P. Hemmerich. 2004. Functional complementation of human centromere protein A (CENP-A) by Cse4p from Saccharomyces cerevisiae. *Mol.Cell.Biol.* 24:6620-6630.

Wittmann, T., and C.M. Waterman-Storer. 2005. Spatial regulation of CLASP affinity for microtubules by Rac1 and GSK3beta in migrating epithelial cells. *J.Cell Biol.* 169:929-939.

Wolyniak, M.J., K. Blake-Hodek, K. Kosco, E. Hwang, L. You, and T.C. Huffaker. 2006. The regulation of microtubule dynamics in Saccharomyces

cerevisiae by three interacting plus-end tracking proteins. *Mol.Biol.Cell.* 17:2789-2798.

Wu, X., X. Xiang, and J.A. Hammer 3rd. 2006. Motor proteins at the microtubule plus-end. *Trends Cell Biol.* 16:135-143.

Yan, X., R. Habedanck, and E.A. Nigg. 2006. A complex of two centrosomal proteins, CAP350 and FOP, cooperates with EB1 in microtubule anchoring. *Mol.Biol.Cell.* 17:634-644.

Yin, H., D. Pruyne, T.C. Huffaker, and A. Bretscher. 2000. Myosin V orientates the mitotic spindle in yeast. *Nature.* 406:1013-1015.

Yin, H., L. You, D. Pasqualone, K.M. Kopski, and T.C. Huffaker. 2002. Stu1p is physically associated with beta-tubulin and is required for structural integrity of the mitotic spindle. *Mol.Biol.Cell.* 13:1881-1892.

Zhou, F.-Q., Zhou, J., Dedhar, S., Wu, Y.-H., and Snider, W.D. 2004. NGF-induced axon growth is mediated by localized inactivation of GSK-3beta and functions of the microtubule plus end binding protein APC. *Neuron* 42:897–912.

Zimniak, T., K. Stengl, K. Mechtler, S. Westermann. 2009. Phosphoregulation of the budding yeast EB1 homologue Bim1p by Aurora/Ipl1p. *J Cell Biol.* 186:379-91.